5-2020

Comparative Geochemical Analysis of Ordovician and Mississippian Cherts in Relation to the Northern Arkansas and the Tri-State Mississippi Valley-type Ore Districts

Jonathan T. Chick
University of Arkansas, Fayetteville

Comparative Geochemical Analysis of Ordovician and Mississippian Cherts in Relation to the Northern Arkansas and the Tri-State Mississippi Valley-type Ore Districts

A thesis presented in partial fulfillment
of the requirements for the degree of
Master of Science in Geology

by

Jonathan Chick
University of Arkansas
Bachelor of Science in Geology, 2013

May 2020
University of Arkansas

This thesis is approved for recommendation to the Graduate Council

_____
Walter L. Manger, Ph.D.
Thesis Director

_____
Adriana Potra, Ph.D.
Committee Member

_____
Phillip D. Hays, Ph.D.
Committee Member

_____
Erik Pollock, M.S.
Committee Member

ABSTRACT

It has been hypothesized that Ordovician, Mississippian, and younger carbonate and clastic formations found within the Ouachita Basin of west-central Arkansas and northward onto the Ozark Dome have experienced interaction with hydrothermal fluids due to tectonic forces produced by the Ouachita Orogeny. Lead (Pb) isotope analyses and resulting values produced through previous and concurrent geochemical studies of several formations indicate that the Mississippi Valley-type (MVT) ores were produced from a mixing and cooling of these sedimentary basinal brines by meteoric or connate waters. Reduction of sulfate to sulfide is one of the possible mechanisms by which MVT ore precipitation may be recognized. Organics sequestered in shales result in general enrichment of uranium (U) through their decay, as evidenced by the U-enriched Devonian Chattanooga Shale. The Chattanooga Shale and early Pennsylvanian Jackfork Sandstone of the Ouachitas have been shown to be prominent source rocks through metal source evaluations (Bottoms *et al.*, 2019 and Simbo *et al.*, 2019). The linear trend defined by the Pb isotope ratios of the MVT ores suggests that two end-members were involved in the formation of the MVT ores. Of particular interest is the identity of source rocks that contributed the enriched radiogenic Pb component to the MVT ores. A highly radiogenic end-member appears to exist, as evidenced by the Pb isotope values of the Cotter Dolomite analyzed in this study. The Bigfork Chert, Boone tripolitic chert, and Hatton Tuff appear to be related through elemental concentration analyses, confirming volcanic ash contributions. Other studies cited herein suggest that metasomatic fluid pulses produced by Reelfoot Rift tectonics may have contributed genetically related, metalliferous fluids to these brines. Meteoric waters originally confined to the Ozark Aquifer may have also interacted with initial and subsequent pulses through fracturing and faulting following the uplift produced by the Ouachita Orogeny. Close stratigraphic position to Pre-Cambrian basement rocks may have also resulted in

Pb enrichment by fluid-rock interactions. In addition, the briny Western Interior Plains Aquifer is in close proximity to the Tri-State MVT ore district and may have also supplied elemental additions to the fluids that resulted in deposition of these MVT ore deposits. Other chert formations, such as the Grand Falls, Penters, and Short Creek, or cherty dolomites, including the Jefferson City, Roubidoux, Gasconade, Eminence, and Potosi of southern Missouri could be sampled for Pb isotope values in future studies in order to further constrain the linear two end-member components that contributed Pb to the ores. Clastic formations, including the Blaylock and Hartshorne Sandstones within the Ouachita Mountains and Arkoma Basin of Arkansas may also have enriched radiogenic Pb signatures. The Upper Cambrian Davis Formation, as well as the Lamotte, Mt, Simon, and Reagan Sandstones, in southern Missouri may have also contributed elemental Pb to the MVT ore fluids through dissolution of potassium feldspars, exclusive of any primary U and Th or accumulation of lead through radiogenic decay.

ACKNOWLEDGEMENTS

I would like to extend a very special thanks to my advisor, Dr. Walt Manger, whose idea this project was and who has been an instrumental source of knowledge and support in many aspects through my years with the Geoscience Department at the University of Arkansas. Thanks to Dr. Adriana Potra for her considerate effort, support, kind patience, and guidance in seeing the Geochemistry aspect of this project to its completion. This project would not have been possible without their enthusiasm and backing.

Secondly, to my Thesis Committee: Dr. Phil Hays, Eric Pollock, and Dr. Adriana Potra for their invaluable advice and critiques in the culmination of this project. Many other faculty and staff have also played a role in my education and success through this journey.

I would like to thank my fellow Lower Mississippian Research Group members Julie Cains, Forrest McFarlin, Sydney McKim, and John Philbrick, as well as Bryan Bottoms and Christophe Simbo for their friendship and work that made the comparisons in this study possible. Also, David Baylor, Joshua Blackstock, Noah Morris, and John Samuelsen along with countless other graduate students for their input and encouragement throughout this project.

I would also like to thank the USGS for allowing and motivating me to complete this thesis while working towards a career as a Pathways Hydrologic Technician Intern.

Last but certainly not least, I would like to truly thank my parents for many opportunities in life and my sister for their continued support and inspiration to complete this task. Without all of these individuals, this milestone in my academic career and life would not have been possible.

TABLE OF CONTENTS

1. INTRODUCTION

The purpose of this study is to compare the Pb isotopic signatures and elemental concentrations of cherts found associated with Ordovician and Mississippian carbonates (specifically the Lower Ordovician Cotter Dolomite and the Lower Mississippian tripolitic chert of the Boone Formation) to those of the Middle-Upper Ordovician Bigfork Chert and other Ordovician and Mississippian clastic lithologies found within the Ouachita Mountains. These formations were chosen for sampling for their stratigraphic positions along hypothesized hydrothermal fluid flow paths in relation to the tripolitic chert. Extensive geochemical studies of the Ordovician clastics of the Ouachitas, the Devonian-Lower Mississippian Arkansas Novaculite, and various cherts from the Lower Mississippian Boone Formation have been carried out by Cains *et al.*, (2016), Philbrick *et al.*, (2016), Chick *et al.*, (2017), McKim *et al.*, (2017), Cains, (2019), and Simbo *et al.*, (2019). Philbrick *et al.*, (2016) used energy-dispersive X-ray spectroscopy (EDX) and inductively coupled plasma mass-spectrometer analysis (ICP-MS) to determine the concentration of trace elements of the Arkansas Novaculite. Cains *et al.*, (2016) also used ICP-MS to examine the trace element assemblages of the Boone chert. Those two studies identified significant concentrations of potassium in the various cherts. A biogenic versus volcanic silica source has long been debated for the cherts and novaculite within the Ozark region (see reviews in Cains, 2019 and McKim, 2018). The elemental concentrations reported in the studies cited herein seem to favor a volcanic silica source for the sampled region, possibly related to an island arc system produced during the Ouachita Orogeny as Laurasia collided with Gondwana (Philbrick *et al.*, 2016).

The ultimate goal of this study is to further define the geochemistry of Phanerozoic chert formations on the North American craton and attempt to constrain the flow paths and fluid-rock

interaction of hydrothermal basinal brines suggested to have emplaced many large MVT ore deposits. It is known that sedimentary basinal brine fluids have undergone up-ramp flow from the Ouachitas. Fluid flow through confined aquifers, such as the tripolitic chert of the basal upper Boone Limestone in northwest Arkansas, or Elsey Formation, as it is known in Missouri, is very likely (McKim, 2018).

Extensive previous investigations of mid-continent and related southern Ozark MVT Pb and zinc (Zn) mineralization have been conducted, resulting in both a large amount of geological and geochemical data as well as numerous theories as to the origin of the MVT ore metals and mineralizing fluids. The Pb isotope signature of the MVT ores in the southern Ozark region suggests that mixing of metals from two end-member components generated the MVT ores. One end-member must be highly radiogenic with Pb isotope ratios equal or higher than the highest measured value in the ores. The other end-member must be less radiogenic, with Pb isotopes equal or lowest than the lowest measured value. While the less radiogenic component has been generally attributed to various shale units, the more radiogenic component is still a matter of debate. Previous research (Goldhaber *et al.*, 1995) suggested the basement rocks as a possible radiogenic end-member.

Trace and rare-earth element (REE) chemistry, as well as Pb isotope analyses conducted in this study, may help better constrain the more radiogenic component and determine genetic relations and potential flow paths for the saline basinal ore fluids that formed the Tri-State MVT ore district and other coeval deposits, providing a more comprehensive understanding of MVT ore deposits. Available Pb isotope data for samples of sphalerite ore from the Northern Arkansas and Tri-State Mining Districts (Bottoms *et al.*, 2019), the Ozark Plateau Chattanooga and Fayetteville shales (Bottoms *et al*., 2019), the Ouachita shales and sandstones (Simbo *et al.*,

2019) and the northern Arkansas and southern Missouri tripolitic chert (McKim *et al.*, 2018), have been incorporated into this study.

While 32 Pb isotopes exist, only five are stable isotopes. Three of those five -- ^{206}Pb, ^{207}Pb, and ^{208}Pb -- are radiogenic, *i.e.* the stable end products result from the decay of uranium (^{235}U and ^{238}U) and thorium (^{232}Th). Pb isotopes are reported as a ratio with respect to the non-radiogenic isotope - ^{204}Pb. U-Pb, Th-Pb, and Pb-Pb isotopic ratios may be used for age dating and petrogenetic tracing of igneous, metamorphic, and hydrothermal rocks. Due to a divergence in chemical behavior among the radioactive parents U and Th and their radiogenic daughter element Pb, geological processes can produce broad fractionation of the various isotopes by controlling the amount of U and Th present (Arizona Board of Regents, 2005). Thus, Pb isotopes are a useful tool for understanding the nature and timing of these geological processes. Since the isotopic Pb composition of geologic material is a function of three independent decay chains, great potential exists for isotopic variability in minerals. These complex and distinctive patterns provide understanding of rock histories (ABR, 2005). Comparative Pb isotope research will generate a better picture of the environmental, depositional, and hydrothermal dynamics of bedded and nodular cherts of Mississippian and older Ordovician age found on the Burlington Shelf and within the Ozark Dome.

2. GEOLOGIC SETTING

2.1 OZARK DOME

The Ozark Dome is asymmetrical and composed of three plateaus on the Burlington Shelf of southern Missouri and northern Arkansas. The Salem, Springfield, and Boston Mountains plateaus surround Pre-Cambrian granite of the St. Francois Mountains at its core. The Osage Plains are located to the northwest. The Ordovician Period is the second period of the Paleozoic Era recognized by the International Commission on Stratigraphy, bounded by the Cambrian below and Silurian above. It began 485.4 million years ago, following the Cambrian-Ordovician boundary extinction event, and includes the greatest global sea level high-stand occurring during the Phanerozoic Eon, probably as the result of rapid sea-floor spreading along ocean ridges (Holland, 2018). In the southern midcontinent, most of the Paleozoic section reflects eustatic cycles of transgression and regression by epeiric seas in a cratonic setting (McKim *et al.*, 2017). This pattern resulted in the deposition of thin lithostratigraphic units of a variety of sedimentary lithologies that dip radially away from the central Ozark Dome, a broad cratonic uplift cored by Precambrian granite and rhyolite basement centered in southeastern Missouri (Chinn and Konig, 1973; Philbrick *et al.*, 2016), Figures 1 and 2.

Lower Ordovician strata in northwestern Arkansas accumulated in a warm, shallow, epeiric sea on a broad, cratonic, and fully-aggraded platform (He, 1995), with the Ozark region covering most of the Laurentian continent between 10° and 25° S latitude during Ordovician time (Overstreet *et al.*, 2003), Figures 3 and 4. Ancient carbonate platforms and passive margin environments mainly consisted of sediment produced by, and resulting from, calcareous green algae, in addition to stromatolites, and possibly sea-floor precipitates (Grotzinger and James, 2000).

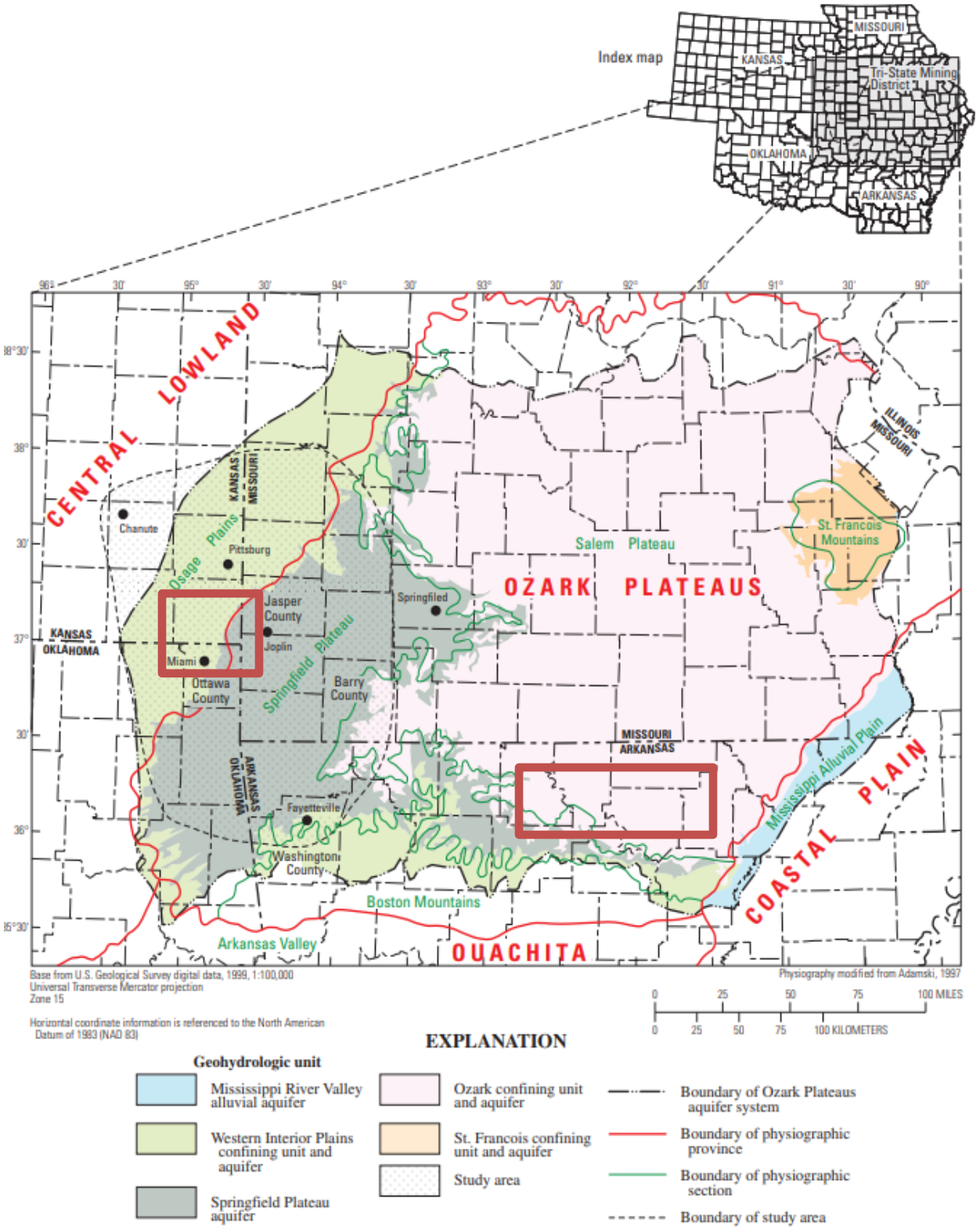

Figure 1. Geographic location of Ozark Dome, and its aquifers, surficial extent of geohydrologic units, physiographic areas, and water-quality study area of the Ozarks Plateau aquifer in parts of Arkansas, Kansas, Missouri, and Oklahoma (Pope *et al.*, 2009). Red rectangles are ore districts.

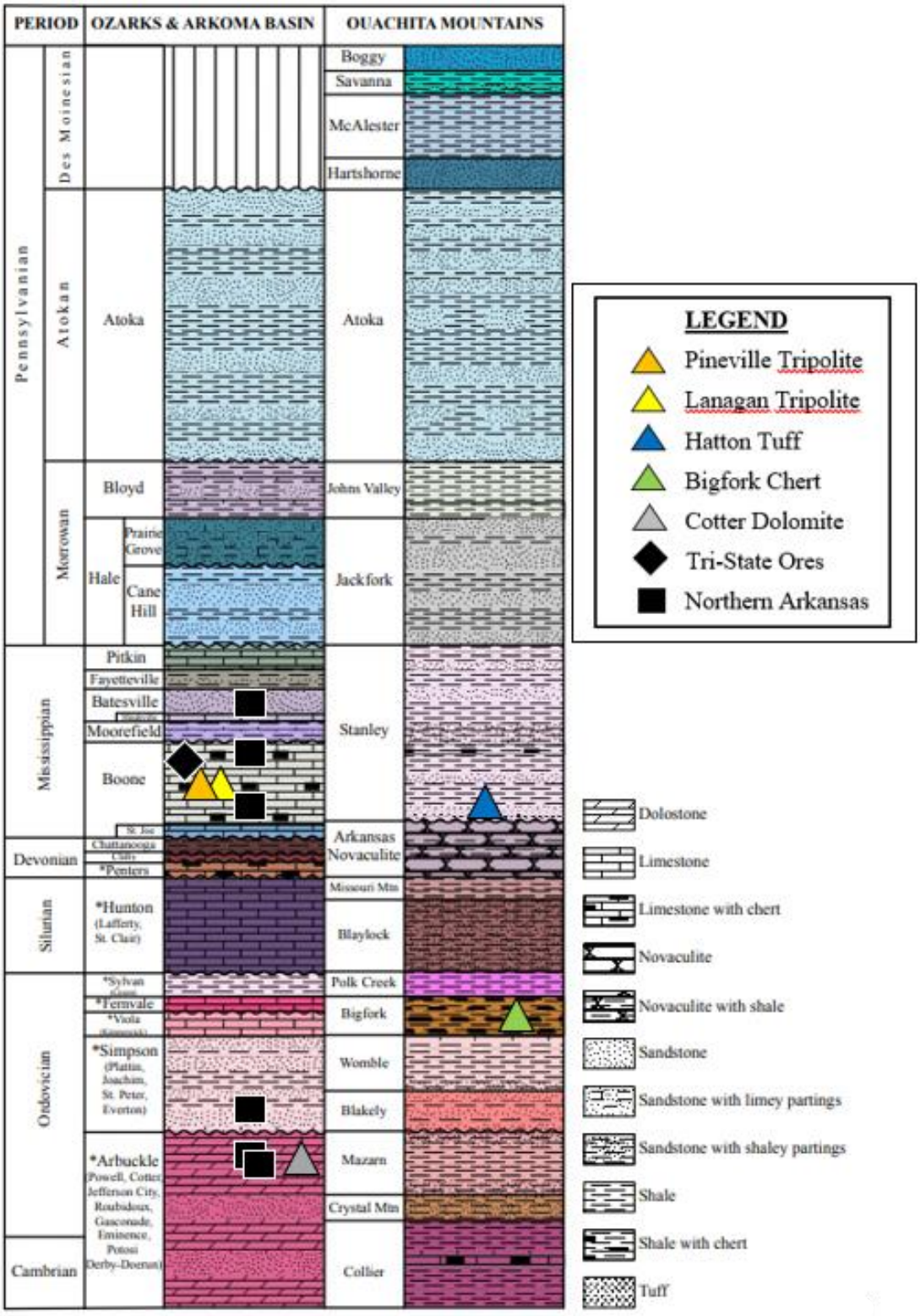

Figure 2. Paleozoic stratigraphic column of Arkansas from Figure 1, Godo, Ted, Li, Peng, Ratchford, M. E. (2014) Structural and Stratigraphic Analysis of the Shell International Paper No. 1-21 Well, Southern Ouachita Fold and Thrust Belt, Hot Spring County, Arkansas. Arkansas Geological Survey Information Circular 39C, p. 2.

The carbonate sediments that make up the Lower Mississippian Boone Formation were produced on a broad, shallow carbonate platform, designated the Burlington Shelf (Lane, 1978). It occupied much of the central southern mid-continent and rests on the Cambrian to Ordovician Salem Plateau. Those sediments were transported down-ramp, where they accumulated. Thus, the interval reflects a single, third order, transgressive-regressive cycle, bounded by regional unconformities and designated the Springfield Plateau (McKim *et al.*, 2017). The Salem Plateau is the largest and second-oldest (Upper Cambrian to Lower Ordovician) physiographic feature of the Ozark Dome, extending across northeastern Oklahoma, northern Arkansas, and northeastward into southeastern Missouri surrounding the exposed Precambrian granites of the St. Francois Mountains at its core (Figure 1). The Salem Plateau contains many significant and important groundwater aquifers that may have potentially served as flow paths for MVT sedimentary brine fluid migration in response to forces generated by the Ouachita Orogeny or other tectonic activities such as those of the Reelfoot rift.

The early Ordovician Upper Knox/Beekmantown Group of the Appalachians is composed of five third-order, transgressive-regressive sequences of peritidal cyclic tidal flat carbonates deposited on a pericratonic platform that have been pervasively dolomitized. Knox mud-rich facies were selectively dolomitized by “early” dolomite, making up 75% of all matrix dolomite. “Late” replacement-dolomite occurs in all Knox facies and is typically fabric-obliterative. These cements occur in secondary solution voids and fractures associated with anhydrite, authigenic pyrite, fluorite, calcite, quartz, and MVT minerals (Montañez, 1989).

Having formed in a related way, the tripolite found within the basal layers of the upper Boone Limestone Formation (Mississippian) has been found to contain microcrystalline quartz druse (Figure 3 from Minor, 2013). These mineral assemblages indicate at least two periods of

hydrothermal activity culminating in the formation of the tripolitic chert and associated gangue minerals of ‘cotton rock’ (McKnight and Fischer, 1970) and the MVT ore deposits (McKim *et al.*, 2017).

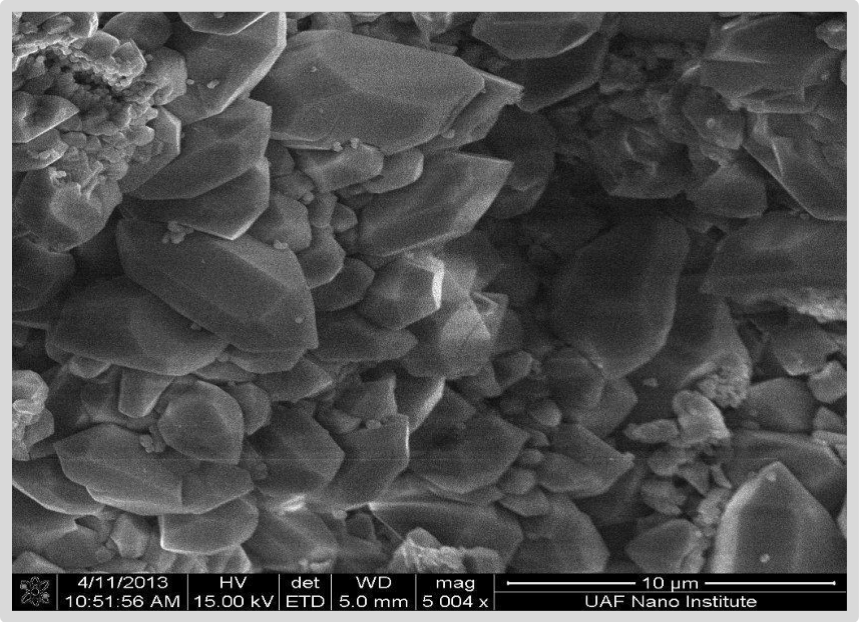

Figure 3. Well-developed euhedral quartz crystals in tripolitic chert void, 5000x magnification (Minor, 2013).

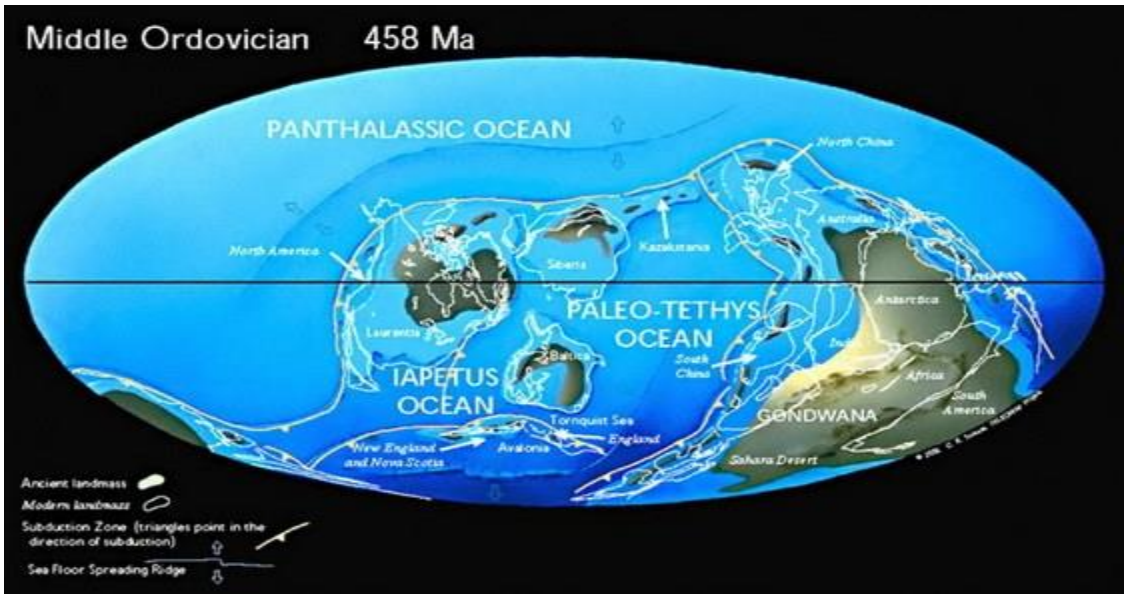

Figure 4. Middle Ordovician global reconstruction, showing North America largely inundated and positioned along the Equator (Scotese, 2001).

2.2 Ouachita Mountains

The Ouachita Mountains are true fold-belt mountains formed from strata deposited in deep-water settings and deformation by compressional events associated with plate collision along the southern border of North America during Late Pennsylvanian and Permian time in what has been called the Geosynclinal Cycle. The Ouachita Fold Belt apparently extends across the southern midcontinent from the Mississippi-Alabama border into the Big Bend Region of west Texas. Oddly, the bulk of the belt is confined to the subsurface, and the only exposed portions are the Ouachita Mountains in central Arkansas and eastern Oklahoma, and the Marathon Uplift in west Texas (Denison, 1989). The general structure of the Ouachita Mountains is a broad anticlinorium and synclinorium modified by numerous thrust faults (Miser, 1959).

The Ouachita Mountains comprise complexly folded and faulted Paleozoic sedimentary rocks originally formed in primarily deep marine environments. The Late Paleozoic continental collision that deformed this region created an east-west trending structural fabric. Intricate folding of Ouachita strata at all scale levels resulted in rotation and several overturned partial and complete local sequences of the succession (Figure 5). Compressional faulting is expressed throughout the area. The Ouachita Province can be recognized as an anticlinorium with Late Cambrian to Early Ordovician age deposits exposed in its center, and mostly Mississippian and Pennsylvanian age strata exposed around its margins (McFarland, 2004). Down-faulting against the Gulf Coastal Plain and Mississippi Embayment encouraged cover of this region to the east.

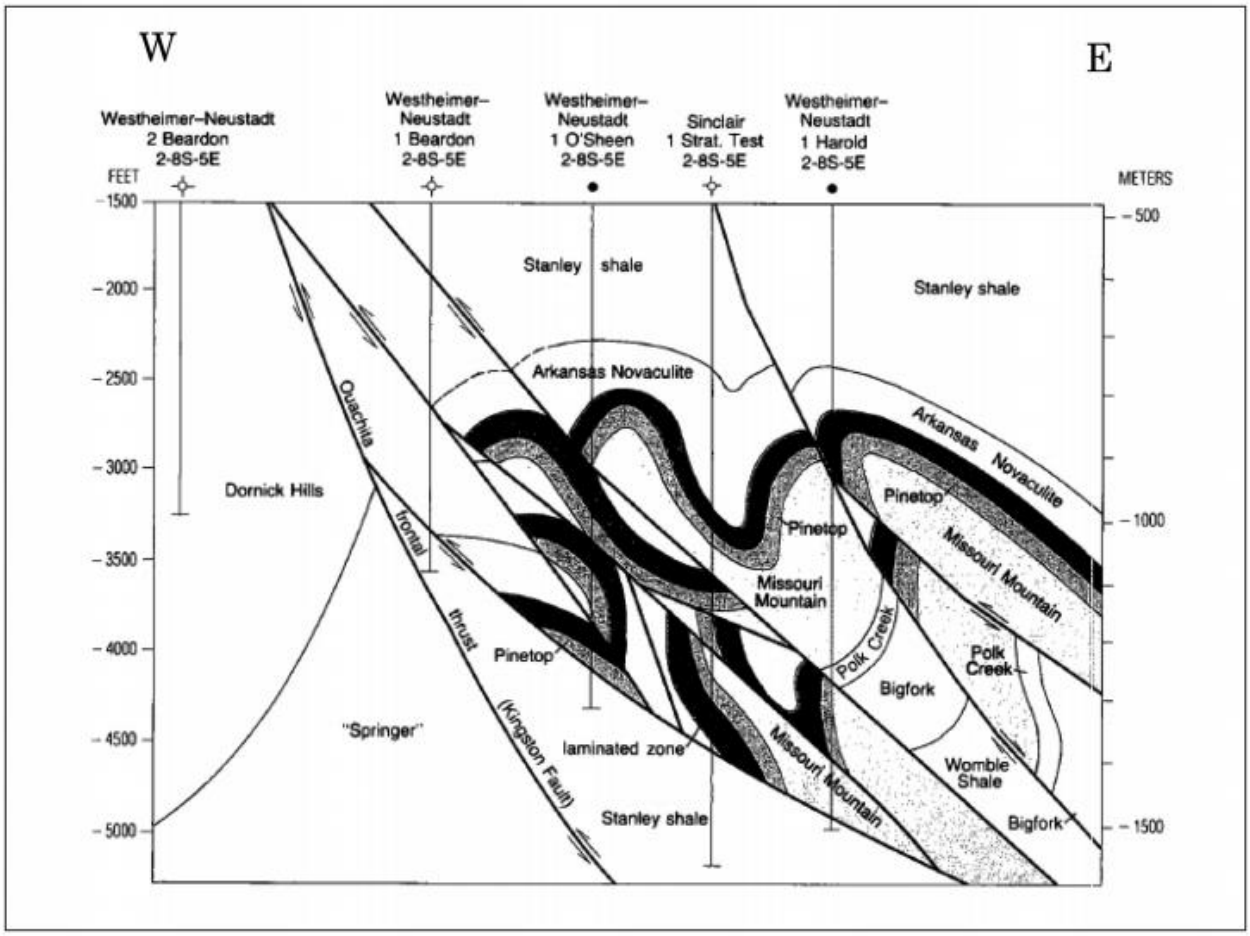

Figure 5. East-west cross section through Isom Springs Field showing complex structure, thrust faults, and overturned folds. West end of cross section approximately C SW¼ NW¼ sec. 2, T. 8 S., R. 5 E.; east end of cross section approximately C NW¼ NW¼ sec. 1, T. 8 S., R. 5 E. From Suneson, Neil H., Shale Shaker, July-August 2012 Issue.

3. LITHOSTRATIGRAPHIC SUCCESSION AND CHARACTER

3.1 LITHOLOGY

Lower Ordovician strata in the Ozark Aquifer are primarily composed of three main lithologies: dolomite, chert, and quartz sandstone. The less permeable Jefferson City and Cotter Formations of the Arbuckle group and Middle Ozark Aquifer (Nottmeier, 2015) are predominately cherty dolomite with minor quartz sand beds compared to the older Roubidoux and Gasconade Formations, and the Gunter Sandstone Member of the Gasconade below. The Jefferson City and Cotter dolomites contain an increased occurrence of chalcedonic chert nodules found in very similar shape and texture to the gypsum and anhydrite nodules common on modern sabkha supratidal flats. Casts of halite and ghosts of gypsum laths can also be found in the Jefferson City and Cotter, but seldomly in underlying units (Overstreet *et al.*, 2003). Wackestone-laminite cycles mainly occur in the Jefferson City and Cotter dolomites. These comprise a thin unit of wavy, peloidal, wackestone that is overlain by mechanical, tidal flat, laminites. Mechanical laminites are intertidal to supratidal and are fine grained with mm-scale horizontal laminae. Examples include mudcracks, replaced evaporite molds and casts, and solution-collapse breccias. Thin beds of mechanical laminites commonly cap meter-scale cycles in the Ozarks. Wackestone cycles are most common in the upper Jefferson City as well as throughout the Cotter dolomite, and the main component of this cycle subtype is massively bedded, wavy, peloidal wackestone (Overstreet *et al.*, 2003). Chalcedonic chert nodules are prominent in peloidal wackestones, and laminate Type I cycles occurring within the Jefferson City and Cotter. In some horizons, these nodules are somewhat common, but only account for about 1%, a very small segment of the volume of these formations (Overstreet *et al.*, 2003).

The tripolitic chert is located within the basal upper Boone Limestone. The lower Boone Limestone, known as the Reeds Spring Formation in southern Missouri, reflects the Lower Mississippian maximum flooding interval on the Burlington Shelf (Manger and Shelby, 2000). The lower Boone comprises calcisiltites and contains dark, nodular, penecontemporaneous chert exhibiting dessication and compaction fractures that indicate deposition prior to lithification of the surrounding limestone (Manger and Thompson, 1982). In turn, the upper Boone marks the high-stand and regressive intervals and consists of sand to gravel size bioclastic grains (Shelby 1986), usually crinozoan detritus (McFarland, 2004; McKim *et al.*, 2017).

The Bigfork Chert is stratigraphically equivalent to the Late Ordovician Fernvale and Viola Formations in the Ozarks and Arkoma Basin province (Godo *et al.*, 2014). In Arkansas, the Bigfork Chert ranges in thickness from "about 450 feet thick in the northern Ouachitas to about 750 feet thick in the southern Ouachitas" (McFarland, 2004). The Bigfork consists of thinly bedded, dark gray, cryptocrystalline chert interbedded with differing amounts of siliceous black shale, calcareous siltstone, and dense bluish gray limestone. Cherts in this formation are normally highly fractured and "occur in thin to medium beds." (Arkansas Geological Survey, 2018). Interbedded siliceous shales are found in "thin to thick sequences" and are often pyritic. Limestones mainly occur as interbeds with the cherts and are more common in the northwestern exposures. Fossils are rare, but fragments of marine organisms have been reported. The Bigfork Chert is known to include planerite, turquoise, variscite, and wavellite as accessory minerals (McFarland, 2004).

The Middle-Late Ordovician Bigfork Chert was deposited in a sediment-starved basin on the margin of a continental shelf (Overstreet *et al.*, 2003; McFarland, 2004). The Bigfork Chert spans the Upper (Middle-Late) Ordovician age and is approximately dated 471-444 Ma. While

complete fossils are rare, fragments of brachiopods, conodonts, crinoids, sponges, and graptolites have been reported (Arkansas Geological Survey, 2018). Thin to thickening bed sequences are common in the Bigfork Chert, and often include pyritic, siliceous shales. Limestones weather to a soft brown, and are found mostly interbedded with the chert. These attributes suggest that this formation developed in deep water, distant from the cratonic shelf margin. Basinal and shelf environments promote precipitation of the Middle and Upper Ordovician bedded and nodular cherts found in chert-bearing formations (Figure 6, Kidder and Tomescu, 2016).

No primary reference section for the Middle-Late Ordovician Bigfork Chert is currently recognized. The Bigfork Chert was described in 1892, but not named until 1909 by A. H. Purdue, who designated a type locality, but not a stratotype for the formation (McFarland, 2004), which remains unassigned to present day. The chert, which is typically black and laminated, is interbedded with siliceous shale, limestone, and sandstone. The shale occurs in intervals ranging from 1 in to 3 ft (3 cm to 1 m) in thickness. The bluish-black limestone is dense and finely crystalline with thicknesses reported between 1 to 12 in (3 to 30 cm). Interbedded sandstone exposures in the Zig Zag Mountains are fine-grained, gray, and thin-bedded (Godo *et al.*, 2014). The Bigfork was deposited in a basinal setting, and then folded, and subsequently faulted, by the Ouachita Orogeny.

The Womble Shale (Middle Ordovician) conformably underlies the Bigfork, while it is succeeded by the Polk Creek Shale (Late Ordovician). The Hatton and Chickasaw Creek Tuffs occur near the bottom, and the top of the Stanley Shale in the Ouachita Mountains, respectively (Figure 2). Rb and Sr isotopic analysis of the Hatton Tuff yielded an isochron age of 310 +/- 15 mya (Mose, 1969).

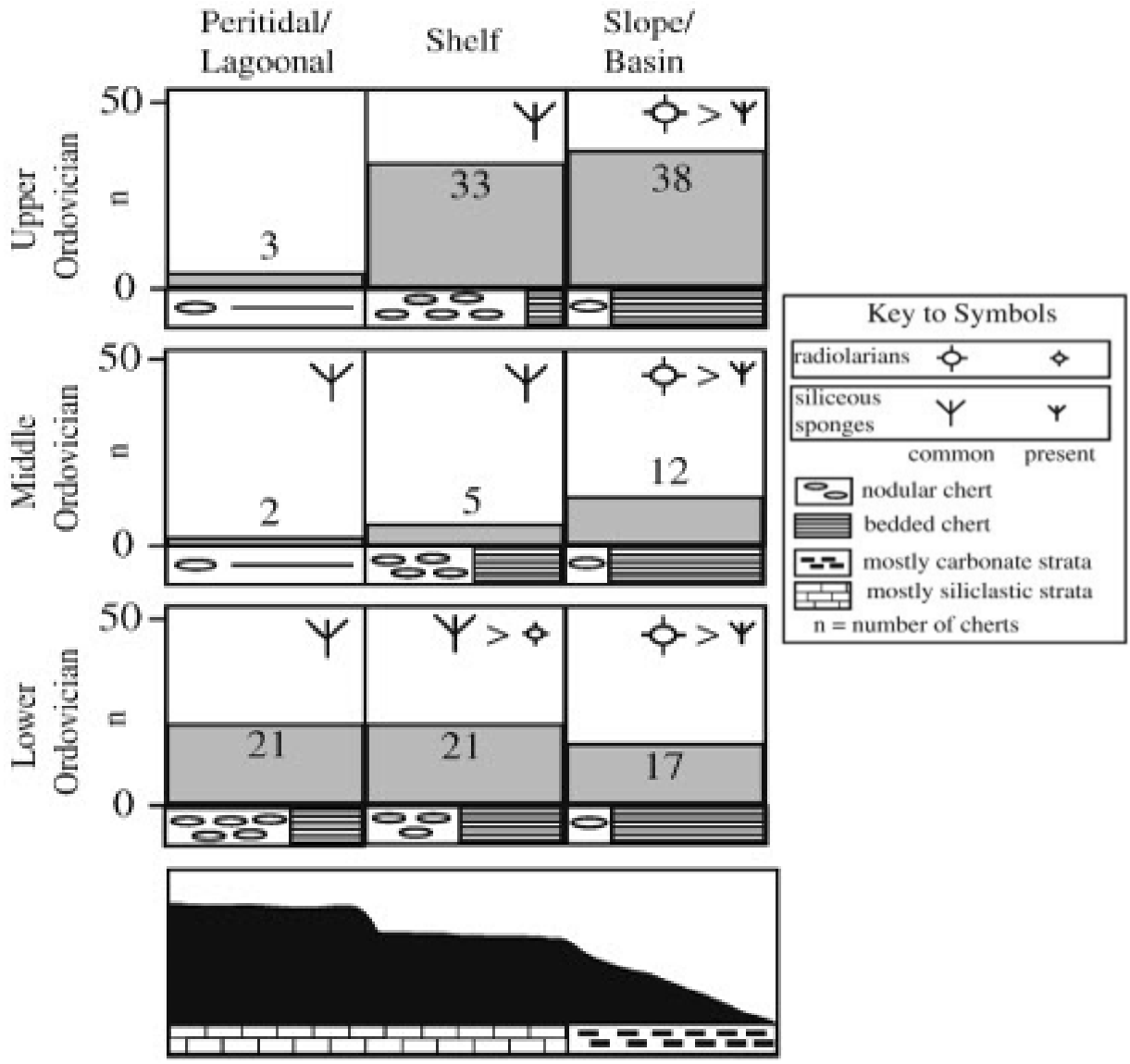

Figure 6. Numbers of chert-bearing formations in peritidal/lagoonal, shelf, and slope/basin facies through the Ordovician. The relative size of the radiolarian and sponge symbols reflects the dominance of the corresponding type of organisms in the cherts in a particular environment. Symbols below boxes show the relative abundance of the nodular chert (ovals) and bedded chert (horizontal lines) so as to illustrate the dominance of the chert type in a particular environment (Kidder and Tomescu, 2016). Note: Samples for this study are from the Lower Ordovician peritidal/lagoonal setting (nodular Cotter Dolomite) and Middle Ordovician slope/basin setting (bedded Bigfork Chert). Radiolarians and sponge spicules are not the source of the silica, as they are included remnants in these cherts.

3.2 STRUCTURE

The region of present-day southern Missouri and northern Arkansas comprises generally flat-lying Paleozoic strata divisible into three plateau surfaces (Figure 7). The lowest and northern-most of these plateaus is the Salem, comprising a succession typically of dolostones, sandstones, and limestones of early through late Ordovician age (McFarland, 2004). The Springfield Plateau succeeds the Salem with younger strata of Devonian through Mississippian age, capped with Pennsylvanian strata, designated the Boston Mountains Plateau. Each of these intervals preserves unconformity surfaces marking transgressive-regressive sea level changes as part of this Paleozoic record. In the subsurface, the succession of Jefferson City (Early-Middle Ordovician) through Upper Derby-Doerun and earlier Upper Cambrian carbonates of the Arbuckle Group (descending order) is encountered above the Lamotte Sandstone, which rests unconformably on Precambrian igneous rocks (Overstreet *et al.*, 2003) (Figure 2).

Faulting in the Ozarks, most of which rises to the surface, is generally normal with the majority of faults exhibiting downthrown blocks on their southeastern sides. A few strike-slip faults trending NE-SW were also developed (Hudson, 2000). The depositional environment of most rocks present in the Ozarks of Arkansas is one of a relatively shallow cratonic continental shelf, generally sloping toward deeper water oceanic settings to the South. Several transgressive-regressive cycles covered and uncovered the shelf during the Paleozoic Era, producing numerous unconformities throughout the sequence (McFarland, 2004).

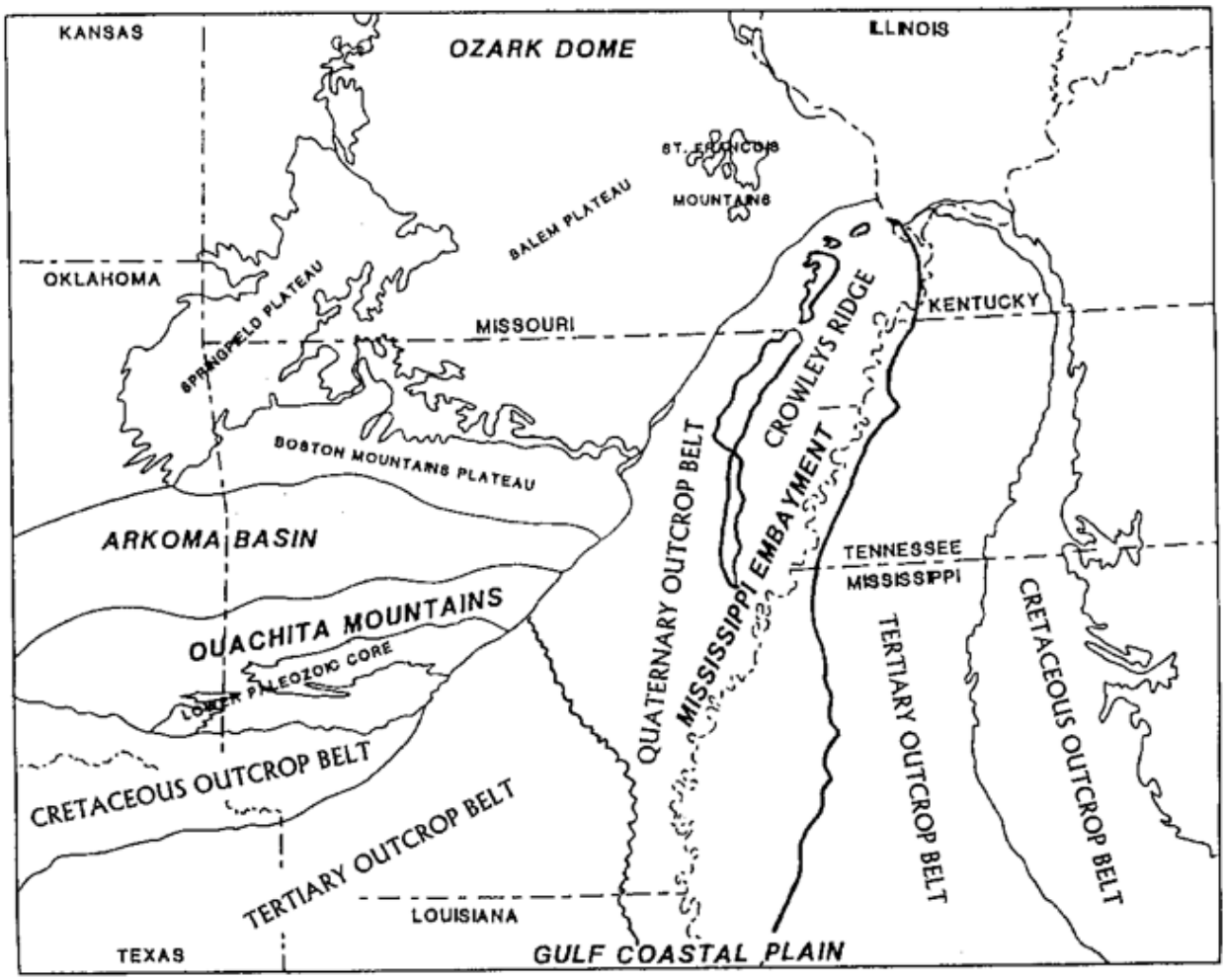

Figure 7. General geographic relationships of physiographic provinces of Arkansas and surrounding states (Manger, Zachry, and Garrigan, 1988).

To the south, two shallow basins occupied the Arkansas Valley at least as early as Everton time, one lying east and the other west of a Pope-Conway County high and separated in effect by a nose trending southeastward through Pope, Conway, and Faulkner counties. The boundary appeared to migrate westward by Pitkin or Morrowan time. These basins are thought to be considerably older than the Everton and possibly date back to pre-Cambrian time. Uplift appears to have initiated at the end of Powell time (Caplan, 1957: Figure 8). Renewed uplift of the Ozarks caused by the Ouachita Orogeny in the middle Pennsylvanian exposed the region to faulting and fracturing, followed by broad and extensive weathering and erosion. All but a few outliers of the Pennsylvanian deposits have been removed from the Ozark Plateaus.

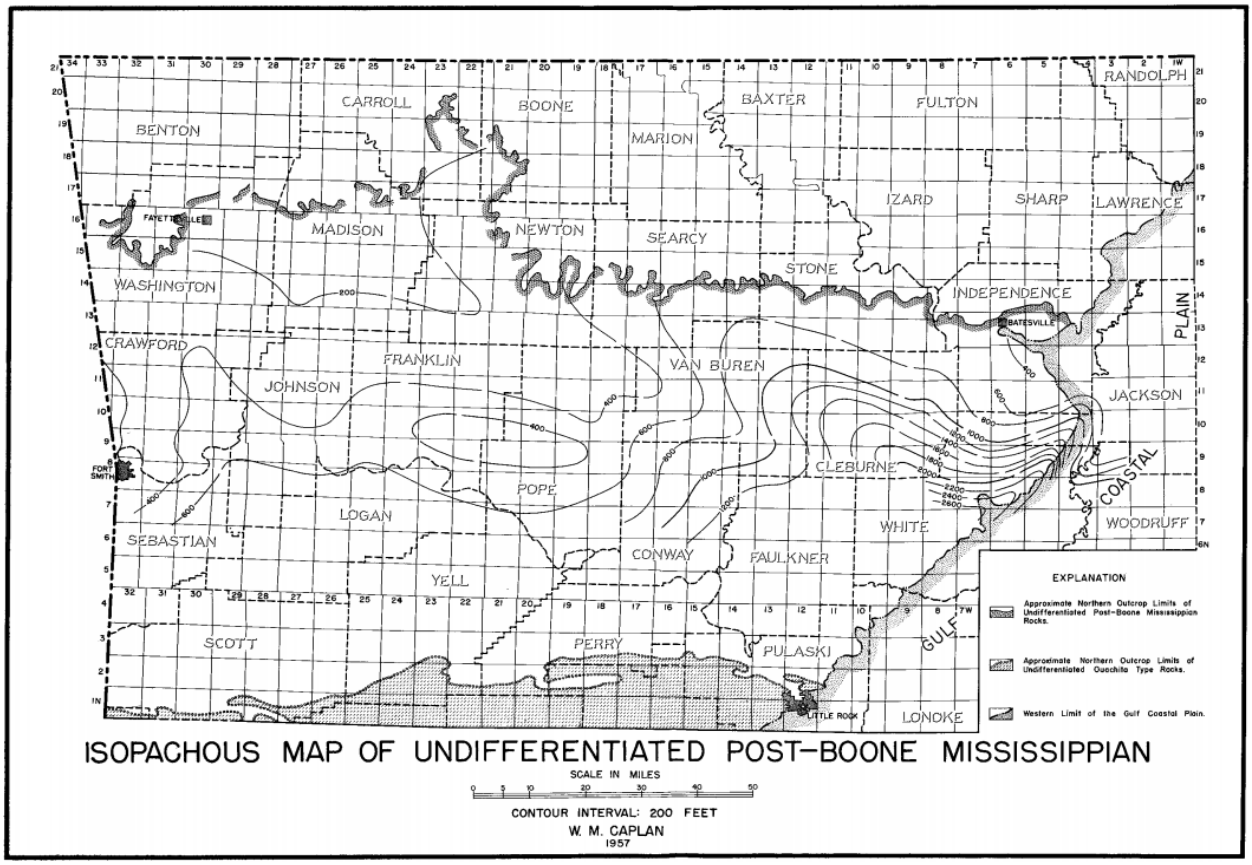

Figure 8. Caplan, William M. (1957). Plate IX. Post-Boone Mississippian Isopach. Subsurface Geology of Northwestern Arkansas, Arkansas Geological and Conservation Commission, Info. Circular 19. 14 p. Note inferred topographic high above Pope County dividing the two basins.

3.3 DEPOSITIONAL DYNAMICS

The main stratigraphic and sedimentary components of the Roubidoux, Jefferson City Dolomite, and Cotter Dolomite (Early Ordovician – ascending order) Type I cycles include algal stromatolites, tidal-flat laminites (mechanical and algal), ooid grainstones, wavy peloidal wackestones, and quartz sandstones described as peritidal facies. Shown in Figure 9, Type I cycles are thinner and represent highstand systems tracts, compared to thicker Type II cycles that reflect transgressive systems tracts and are dominant in earlier formations, such as the Gasconade Dolomite (also Early Ordovician) (Overstreet *et al.*, 2003).

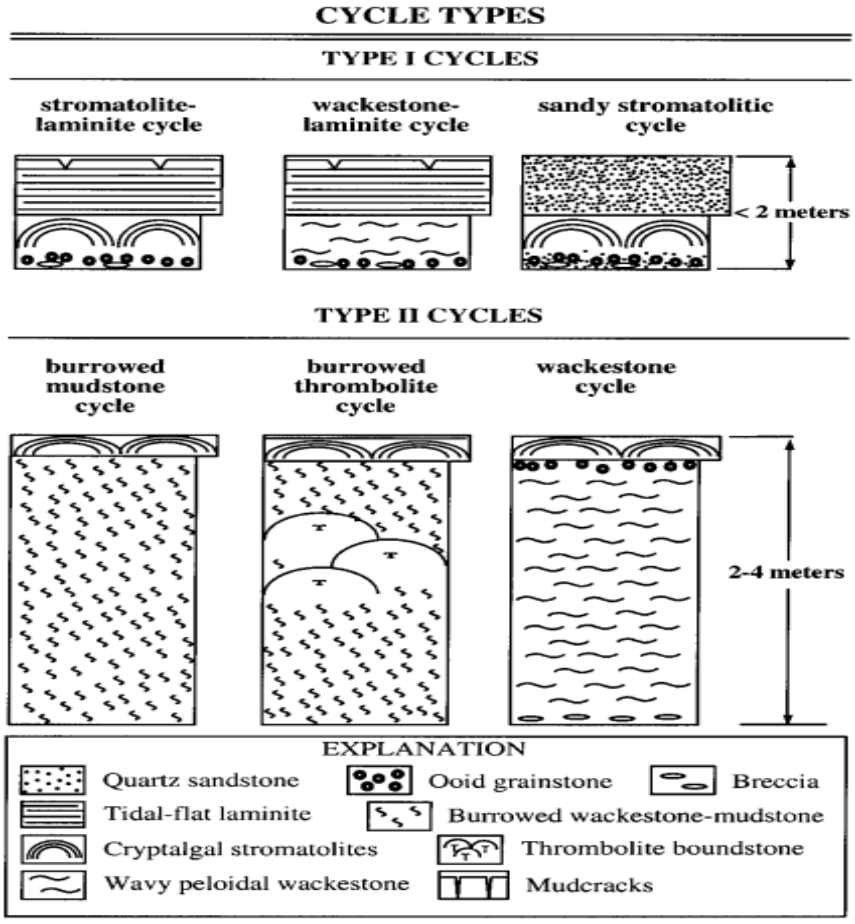

Figure 9. Meter-scale cycle types in the Lower Ordovician of the Ozarks. Two general types are based on the relative thickness of the subtidal and peritidal facies. In addition, Type I cycles have a relatively thick peritidal portion, whereas Type II cycles have a relatively thick subtidal portion. Six common variations of the two cycle types are illustrated (Overstreet *et al.*, 2003).

Two major theories on the origin of the Bigfork Chert, proposed by Miser and Purdue (1929), and Honess (1923), were summarized by Goldstein and Hendricks (1953), p. 436. The seawater was initially relatively clear, but during late Bigfork deposition mud was brought in from the adjacent land area, and intermittently deposited with silica forming chert (Miser and Purdue, 1929, p. 129). Earlier, Honess (1923, pp. 79-80), concluded that the Bigfork Chert is a marine deposit, much of it is secondary, and component limestone was originally more abundant in the Bigfork than now.

The Mississippian Hatton and later Chickasaw Creek Tuffs, both Late Mississippian, occur below and above the Stanley Shale in the Ouachita Mountains along the AR-OK border (Mose, 1969). Petrographic analysis by C. W. Honess (1923) states that the Hatton Tuff is massive, homogenous, and mostly devitrified, with inclusions of basalt, sandstone, slate, limestone, and fossils, but predominately resembles a porphyritic (2 to 7 mm phenocrysts) igneous rock. The Chickasaw Tuff is petrographically described as a partially devitrified tuff with many large calcite crystals in and around glass shards (Mose, 1969).

From Alan Niem (1977),

> "Two pumiceous vitric-crystal tuffs, the Hatton Tuff Lentil and Beavers Bend tuff, occur in the deep-marine Mississippian Stanley Group. These widespread rhyodacitic tuffs range in thickness from 7 to 40 m and are separated by tens of metres of non-tuffaceous quartzose and feldspathic turbidite sandstone and shale. The tuffs consist of varying proportions of ash-sized embayed quartz crystals, plagioclase crystals (oligoclase to andesine), relict shards, volcanic dust, and altered flattened pumice fragments.
>
> Each pyroclastic unit consists of two or more tuff lithologies, including a thick lower unstratified pumiceous vitric-crystal tuff with a density-graded crystal-rich base overlain by thin-bedded pumiceous tuff and an upper massive fine-grained siliceous vitric tuff.
>
> These tuffs were probably formed by highly explosive eruptions of vesiculating acidic magma from a vent or fissure that produced incandescent avalanches of pyroclastic debris and accompanying ash clouds. The hot turbulent suspensions were rapidly quenched by sea water to form steam-inflated density slurries that flowed into the Ouachita basin. Pyroclastic flows created thick, density-graded, pumiceous vitric-crystal tuff. Numerous smaller density slurries following the main flow in rapid succession deposited the overlying bedded pumiceous tuff. Toward the end of each volcanic eruption, continuous settling of fine ash formed thick, fine-grained upper vitric tuff.
>
> Isopach maps of tuff thicknesses, an isopleth map of pumice sizes, logarithmic plots of crystal size versus distance, paleocurrent indicators, and Late Mississippian paleogeography suggest a southern volcanic source that may have been part of a magmatic arc formed at a continental margin during plate convergence between the North American plate and a southern continental plate."

3.4 SEQUENCE HISTORY

The Jefferson City and Cotter Dolomites are early Ordovician (Ibexian: Morris, 2017; Ross *et al.,* 1993), and were deposited as Type I cycles, which are relatively thin and built up from peritidal facies. Localized fossil assemblages found in the early Ordovician suggest that much of the sequence reflects a hypersaline nearshore environment, particularly in association with abundant evaporite casts of halite and gypsum (He, 1995). Similarly, the Lower Ordovician Knox Group of the Appalachian Basin constitutes shallowing-upward, peritidal cyles extensively dolomitized to form massive dolomite (Montañez and Read, 1992).

The Mississippian limestone succession of the Ozark region hosts a number of different types of chert. Penecontemporaneous chert is dark and nodular and is shown to have been emplaced before the surrounding limestone was lithified. In later diagenetic periods of groundwater replacement, carbonate grains with silica are evident and tend to have favored finer-grained intervals due to a greater surface area (Manger and Shelby, 2000). These dynamics are found in the Pennsylvanian later diagenetic and tripolitic cherts. The tripolite is confined stratigraphically to the basal portion of the upper Boone and characterized by massive, white, very fine-grained chert with interbedded carbonate between the St. Joe Limestone and upper Boone (McKim *et al.,* 2017). The tripolitic chert has been found to contain microscopic euhedral quartz druse (Figure 3), evidencing a minimum of a second hydrothermal fluid pulse through the previously dissolved basal Upper Boone Limestone. Furthermore, the topographic head and hydrological gradient critical to fluid migration in the formation of MVT deposits is activated by collisional/compressional orogeny resulting in thrust faulting and uplift (Leach and Rowan, 1986; Garven *et al.,* 1993), such as in the case of the Ouachita Orogeny.

3.5 TYPE AREAS

3.5.1 Ozark Region

The Cotter Dolomite (Lower Ordovician) of the Ozark region was named by E.O. Ulrich (1911) from exposures at Cotter, Baxter County, Arkansas. The Jefferson City Dolomite unconformably overlies the Roubidoux Formation and may be succeeded by the Cotter either conformably or unconformably. The Powell Limestone may overlie the Cotter unconformably with an occasional basal conglomerate (McFarland, 2014).

In the geographic area of the Picher Field, northeastern Oklahoma, the Cotter Dolomite is unconformably overlain by the Chattanooga Shale of Late Devonian and Early Mississippian (Kinderhook) age (McKnight and Fischer, 1970). One of the great and historic mining districts of the world, the Picher Field has yielded more than a billion dollars' worth of lead and zinc, since the first ore was marketed in 1904 (McKnight and Fischer, 1970). The main mining area encompasses about 8 by 9 miles, overlain by a rather thin interval of nearly flat lying Mississippian and Pennsylvanian strata. Precambrian granite basement and perhaps igneous flow rocks have been encountered by at least 11 drill holes in and adjacent to the mining operation at depths ranging from 291 to 1,942 feet (McKnight and Fischer, 1970).

The Devonian Chattanooga Shale is overlain disconformably by the Boone Limestone Formation of Mississippian age, composed of fossiliferous limestone, 'cotton rock', and chert. The Boone is 350-400 feet thick in the Picher Field, where it hosts most of the MVT ore deposits. In a report by McKnight and Fischer (1970), the Boone within the Picher Field is sub-divided into seven members; the St. Joe Limestone, Reeds Spring, Grand Falls Chert, Joplin, Short Creek Oolite, Baxter Springs, and Moccasin Bend Members (McKnight and Fischer,

1970). The tripolitic chert, also known as the 'cotton rock', is found within the basal Upper Boone in the Picher area.

3.5.2 Ouachita Region

The Bigfork Chert (Middle-Late Ordovician) of the Ouachita Mountains was named for its development over a large area surrounding Bigfork P.O., Montgomery County, Arkansas (Purdue, 1909). Currently, there is no listed type or primary reference section for the Bigfork Chert.

4. The Mississippi Valley-type Deposits

The Middle Cambrian through Lower Ordovician carbonate rocks of North America (Figure 10) host several of the largest economic MVT base-metal sulfide deposits in the world (Gregg *et al.*, 2012). Most MVT deposits are recognized as having a temporal and spatial connection with orogenic forelands, such as produced by the Ouachita orogeny (Leach *et al.*, 2010). Many MVT deposits formed during Devonian to Permian time in response to a series of intense tectonic events during the assembling of Pangaea. This process resulted in approximately 61 percent of the Pb and Zn content in dated MVT deposits (Leach *et al.*, 2010). More than 80 percent of MVT deposits are hosted by Phanerozoic rocks, with 20 percent present in Precambrian rocks. Phanerozoic MVTs also comprise 94 percent of total MVT ore and 93 percent of total MVT Pb + Zn metal (Leach *et al.*, 2010).

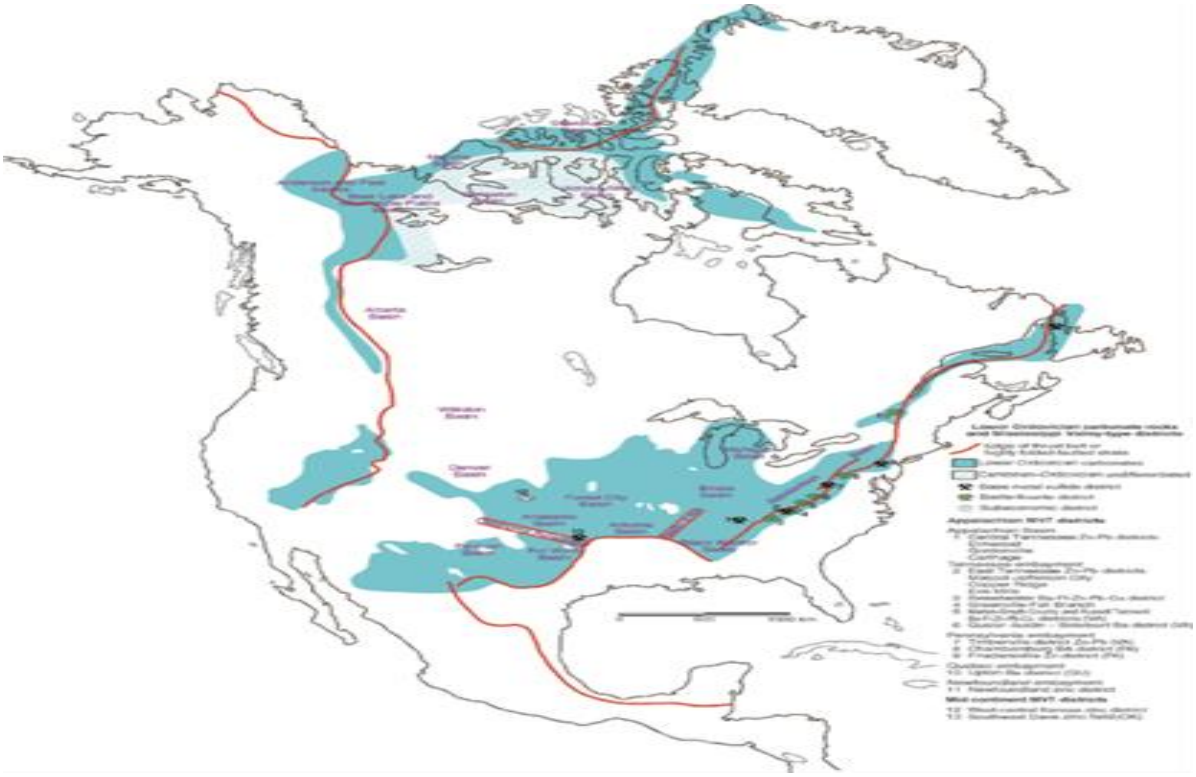

Figure 10. The distribution of the Cambrian-Ordovician (Sauk megasequence) carbonate rocks on the North American continent and major Mississippi Valley-type (MVT) districts hosted in super-Sauk meqasequence strata. The distribution of the Lower Ordovician strata of the Great American carbonate bank is shown. 1000 km (621 mi) (From Gregg *et al.*, 2012).

MVT deposits are strata-bound, carbonate-hosted, sulfide bodies, predominantly composed of the dominant ores of sphalerite (zinc sulfide) and galena (lead sulfide) with minor amounts of iron sulfides and the presence of carbonate, barite, and/or fluorite as gangue minerals, respectively (Simbo *et al.*, 2019, p. 1). The deposits occur principally in dolostones as open-space fillings, collapse breccias and/or as replacement of the carbonate host rock. Less often, sulfide and gangue minerals fill primary carbonate porosity. The deposits are epigenetic, having been emplaced after lithification of the host rock (Paradis *et al.*, 2007).

The Alleghanian-Ouachita Orogeny (Pennsylvanian–Permian) is responsible for the mineralization in the Appalachian and midcontinent regions (Gregg *et al.*, 2012). The Ouachita Orogeny began in the Mississippian and continued into the Pennsylvanian (Aber, 2003). In the Tri-State, Northern Arkansas, and Central Tennessee districts, mineralization occurred in association with an orogenic foreland-bulge, as a low-amplitude (few hundred meter), long-wavelength (100-200 km) swell formed by vertical loading of the forebulge plate (Bradley and Leach, 2003). In the Tri-State District, mineralization occurred above this orogenic foreland-bulge; six major deposits trending southwest-northeast are primarily hosted by cherty limestones of the Lower Mississippian Boone Formation (Figure 9). The ore deposition in this district is controlled by the Miami Fault, a "trough" or graben averaging 1000 ft deep with a maximum fault displacement of 300 feet (McKnight and Fischer, 1970). Some MVT deposits occur immediately below unconformities that originated at the forebulge and along syn-collisional, flexure-induced, normal and strike-slip faults in collisional forelands (Bradley and Leach, 2003).

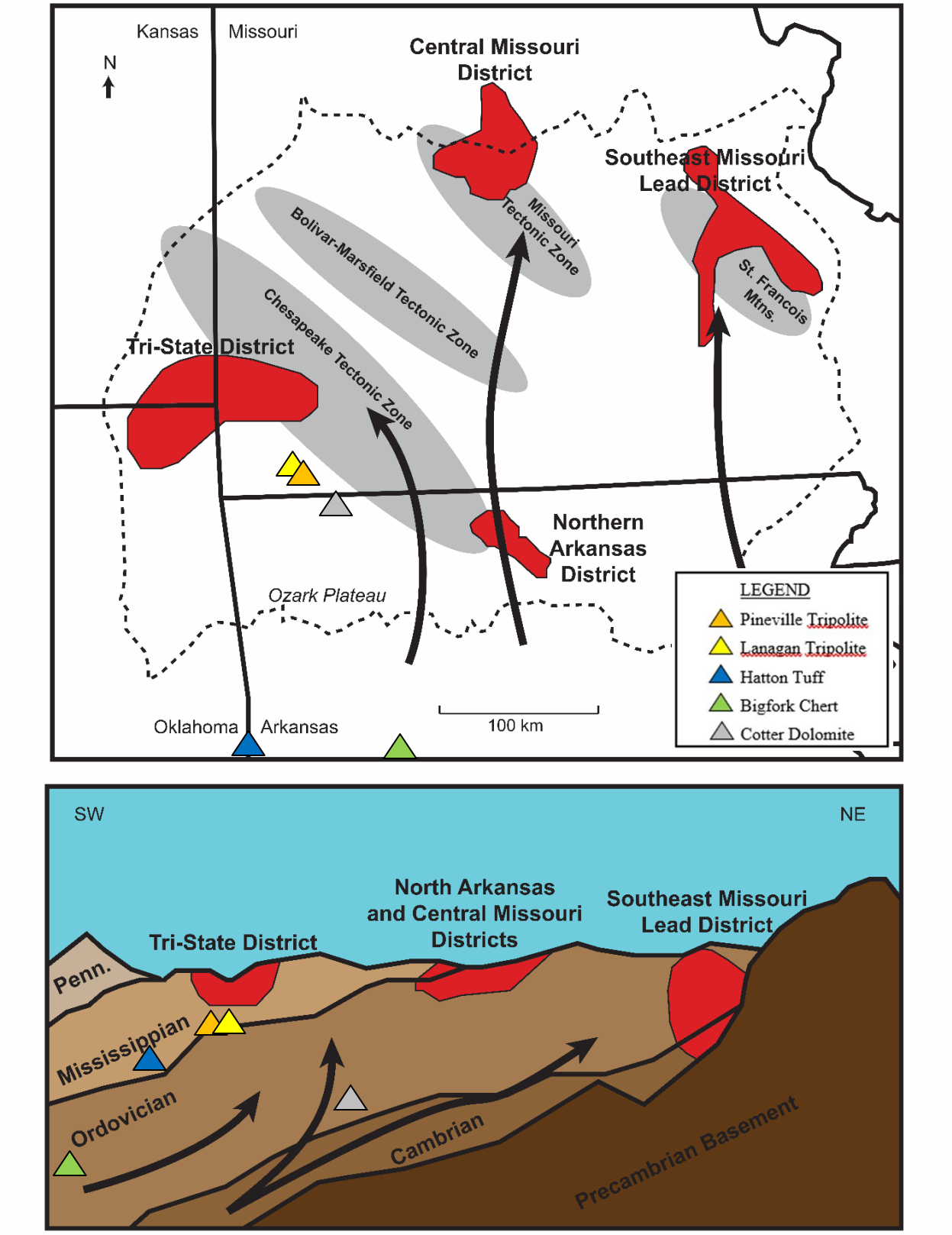

Figure 11. Regional MVT ore districts are shown in red; formations sampled for this study are indicated by colored triangles described in the legend (modified from Lee, 2000).

The MVT deposits are of predominately Phanerozoic age (more than 80 percent) and thought to have been emplaced during Devonian through Permian time, coincident with a series of intense tectonic events during the assembly of Pangaea (Leach *et al.*, 2010). The MVTs are a partial result of the Cambrian-Ordovician, Sauk megasequence of Laurentia (Gregg *et al.*, 2012). Abundant evidence has shown that ore fluids were mainly derived from evaporated seawater and driven into platform carbonates by large-scale tectonic events (Leach *et al.*, 2010). According to Leach *et al.*, Mississippi Valley-Type (MVT) lead-zinc deposits occur throughout the world, but the largest and more intensely researched deposits are found in North America, where the deposit type was first recognized approximately 80 years ago (Bastin, 1939). "The most important characteristics of MVT ore deposits include that they are hosted mainly by dolostone and limestone in platform carbonate sequences and usually located at the flanks of basins, orogenic forelands, or foreland thrust belts inboard of the clastic-rock dominated passive margin sequences" (Leach *et al.*, 2010).

In addition to sulfate and sulfide mineralization, common characteristics of MVT deposits include large-scale dissolution and brecciation of carbonate host rocks, precipitation of large volumes of dolomite and calcite cements, epigenetic (hydrothermal) dolomitization, and recrystallization of pre-existing dolomite. Mineralizing fluids have the effects of 1) both increasing the original porosity through dissolution, and 2) brecciation, and occlusion of porosity due to the precipitation of cements (Gregg *et al.*, 2012).

The most important characteristics of MVT deposits, (Leach and others, 2005) are: (1) they are epigenetic; (2) they are not normally associated with igneous activity; (3) they are hosted mainly by dolostone and limestone, rarely in sandstone; (4) the dominant minerals are sphalerite, galena, pyrite, marcasite, dolomite, and calcite, whereas barite is typically minor to

absent, and fluorite is rare; (5) they occur in platform carbonate sequences commonly at the flanks of basins or foreland thrust belts; (6) they are commonly strata-bound, but may be locally stratiform; (7) they typically occur in large districts; (8) the ore fluids were basinal brines with ~10 to 30 wt. percent salts; (9) they have crustal sources for metals and sulfur; (10) temperatures of ore deposition are typically 75°C to about 200°C; (11) the most important ore controls are faults and fractures, dissolution collapse breccias, and lithological transitions; (12) sulfide-mineral texture varies broadly from coarsely crystalline to fine grained, massive to disseminated; (13) the sulfides occur mainly as replacement of carbonate rocks and to a lesser extent, open-space fill; and (14) host-rock alteration consists mainly of dolomitization, dissolution, and hydrothermal brecciation (Corbella *et al.*, 2004; Leach *et al.*, 2010, p. 3). The Middle Cambrian through Lower Ordovician rocks also host plentiful, but sub-economic MVT deposits, minor and trace element occurrences, and hydrocarbon reservoirs. Mississippi Valley-type deposits commonly contain bitumen, pyrobitumen, and/or liquid petroleum (Gregg *et al.*, 2012).

From Gregg *et al.*, (2012) and others, Mississippi Valley-type mineralization is thought to result from complex mixing and/or cooling of saline fluids expelled from sedimentary basins. According to Gregg *et al.*, (2012), MVT fluids retain temperatures ranging from 60 to 250°C, while another reported formation temperature range is that "MVT deposits originate from basinal saline metalliferous fluids at temperatures in the range of 75°-200°C" (Paradis *et al.*, 2007). Hydrothermal dolomite cement commonly associated with trace amounts of sulfides results from hydrothermal alteration and dissolution followed by recrystallization through acid-producing reactions caused by fluid mixing (Anderson, 1983; Leach, 2010) within host carbonate rocks, such as gray, coarse-grained, early dolomite halos in the Tri-State district (McKnight and Fischer, 1970; Leach, 2010). Alteration halos and dolomite and/or calcite cement may extend

for hundreds of kilometers beyond the ore deposits (Leach and Rowan, 1986; Leach *et al.*, 2010). Minor silicification may be present as microcrystalline quartz in small, discontinuous zones both within and peripheral to sulfide ore (Paradis *et al.*, 2007). As sedimentary (shale) and basement rocks interact with hydrothermal fluids, sulfuric acid produced from oxidation of iron sulfides (predominantly pyrite) attacks other sulfide minerals releasing Zn and Pb as the major metals and associated trace elements (TEs) into solution. In the Tri-State district (1800 km^2), major ore sulfides include sphalerite and galena, while chalcopyrite and galena comprise the minor sulfides (Leach *et al.*, 2010). In the Dobson mine of the Tri-State MVT ore deposits, "The sparse barite is later than marcasite, and earlier than the botryoidal calcite with which it is associated. It was severely leached before deposition of the calcite." (McKnight and Fischer, 1970). This statement indicates different periods of mineral formation likely resulting from multiple pulses of hydrothermal fluids within the MVT deposits. According to Banner *et al.*, (1988a), a detailed diagenetic history of the Burlington-Keokuk Formation includes five episodes of dolomitization, two major generations of calcite cementation (early non-ferroan and late ferroan), dedolomitization, chertification, and mechanical and chemical compaction.

Gregg *et al.*, (2012) states that "Most of the fluids originate from evaporated seawater or water that has dissolved halite, and that has interacted with sedimentary rocks and, possibly, basement rocks." While several geochemical and hydrogeological mechanisms have been introduced for MVT deposits, the precise mechanisms and dynamics driving fluid flow and deposition are not completely understood (Gregg *et al.*, 2012). While found in a variety of carbonate facies, the most favorable rocks and their depositional environments are the Phanerozoic passive margin sequences with dolomitized carbonate platform sequences, particularly those deposited in arid belts (Leach *et al.*, 2010).

5. PREVIOUS INVESTIGATIONS

By the Middle Ordovician, the shallow water, bio-siliceous facies that were common in the Lower Ordovician had mostly withdrawn from peritidal-lagoonal depositional settings and shifted basinward. Evidently low relative sea level in the Middle Ordovician likely curbed the formation and/or preservation of shallow-water cherts by reducing the area of available shelf to host such deposits. Bio-silicification induced variation into the global silica cycle through geologic time (Kidder and Tomescu, 2016). Some researchers hypothesize that biological processes have influenced oceanic dissolved silica (DSi) concentrations, since the dawn of oxygenic photosynthesis (Figure 12, Conley, 2017). Silicon is usually not ionized when dissolved; it is present as ortho silicic acid H_4SiO_4 or $Si(OH)_4$. These compounds are the result of slow dissolution of silica in ancient seawater (Swain and Rout, 2017). A significant, but unknown, silica source seemingly must have been present to increase dissolved silica concentrations, allowing siliceous organisms to thrive. The use and depletion of DSi by radiolarians may have begun in the Middle Ordovician as radiolarians appeared and radiolarite deposition commenced. With the rise of radiolaria to ecological and biogeochemical prominence during the Ordovician, accumulating tests became a principal sink for dissolved oceanic silica (Maliva, 1989). These effects on shallow-water DSi may have also caused siliceous sponges to migrate toward deeper waters due to a lack of needed skeletal silica. The rebound of shelf chert in the Upper (Late) Ordovician, while peritidal cherts are effectively absent, suggests that biological activity was critical to driving a basinward shift of cherty facies (Kidder and Tomescu, 2016).

Widespread deposition of cherts and ultimate control of DSi concentrations in the oceans has been attributed to the Pre-Cambrian silica cycle that was dominated by inorganic reactions

and diagenetic silicification (Conley, 2017), as well as shown by Figure 13 (Scholle, 1978). The abundance of sedimentary chert is a signature of the early Archean geological record that is believed to indicate the absence of biological controls on the early silica cycle (Stefurak *et al.*, 2014).

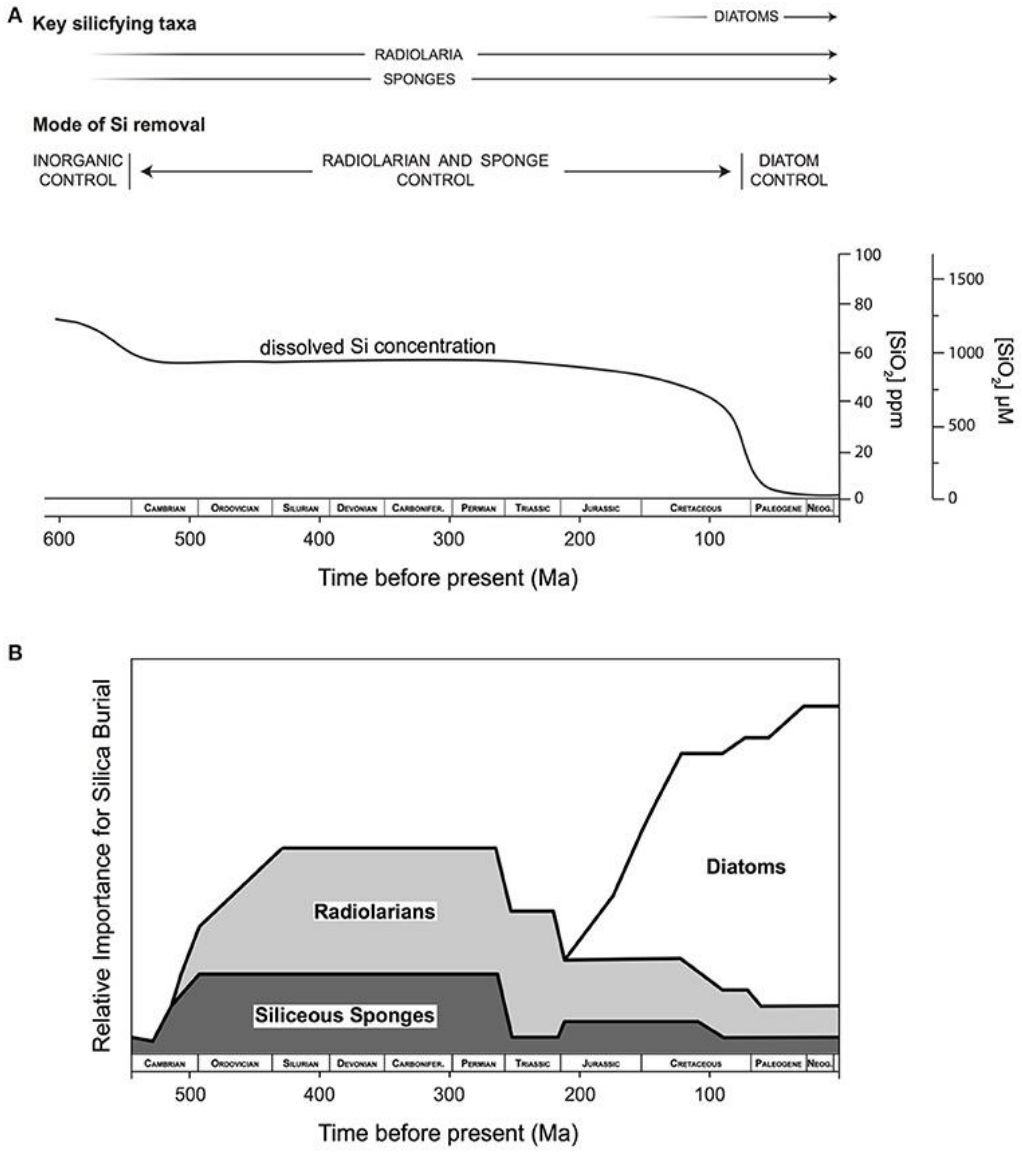

Figure 12. Siever, 1991, evolution of oceanic Si cycle in geologic record, latest Pre-Cambrian - present (Conley, 2017).

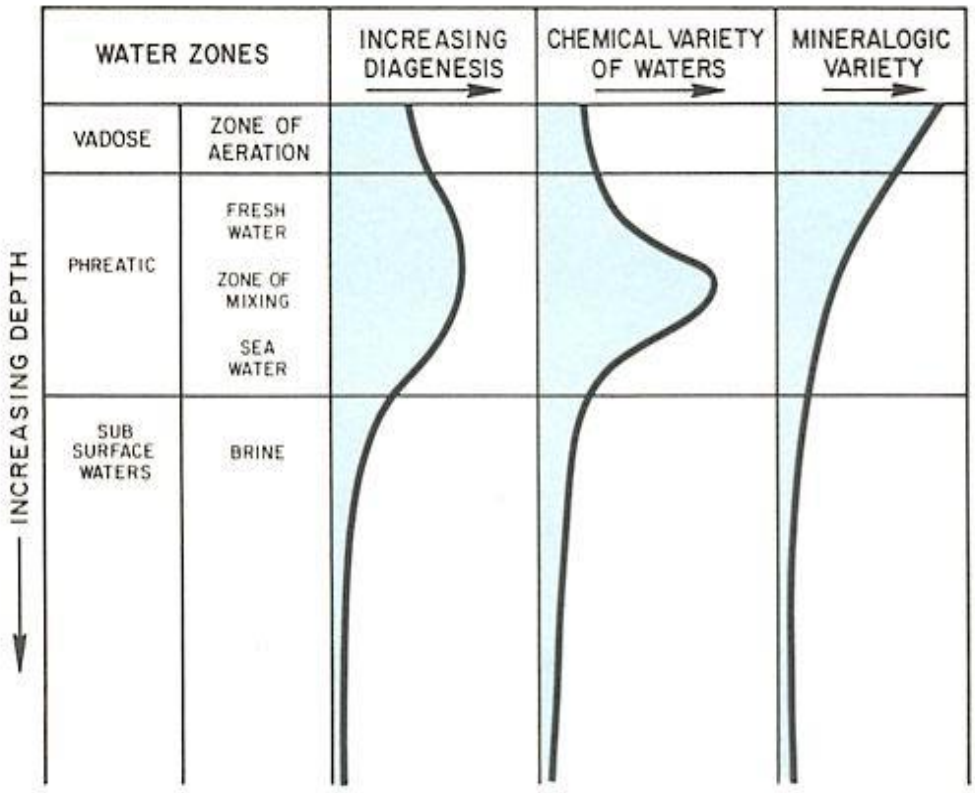

Figure 13. Diagenesis dynamics and control parameters on diagenetic processes (Scholle, 1978).

With knowledge of Si isotope fractionations of processes, including polymerization, co-precipitation and adsorption processes in the formation of amorphous quartz and other secondary minerals, net Si isotope fractionation during chert forming processes can be quantitatively calculated. Furthermore, it is possible to link Si isotope chert composition to that of seawater from present back to the early Archean (Liu, 2016). Precipitated minerals will strongly assimilate heavy isotopes relative to aqueous H_4SiO_4, due to shorter Si-O bonds. Conversely, fractionation between quartz and solution appears to favor the solution becoming enriched with heavier isotopic Si in contrast to quartz, although quartz has much shorter Si-O bonds than aqueous H_4SiO_4 (Liu, 2016). In addition, the silicon isotope budget is hypothesized to be balanced by the coetaneous (coeval) deposition of Si-enriched cherts and Si-depleted, iron formational lithologies (Stefurak *et al.*, 2014).

6. SAMPLING AREA

6.1 Ozark Region

A series of 18 chert samples (Tables 1a-1d and Figure 14) were analyzed for Pb isotopes from the Ordovician Bigfork Chert and Cotter Dolomite, as well as the Mississippian Hatton Tuff and Pennsylvanian tripolitic chert. Samples of the tripolite of the Boone Formation were collected in pairs near Pineville and Lanagan, MO (Figure 14). Another series of six field hand specimens of Lower Ordovician Cotter Dolomite chert nodules were collected in large chunks from the Bourbon Arch along I-49 in southern Missouri and northern Arkansas as well as the east Beaver Dam roadcut (Figure 14).

6.2 Ouachita Region

Seven more samples were collected from the bedded Middle-Upper Ordovician Bigfork Chert in west-central Arkansas, east of Hot Springs as well as near Little Rock along I-430 at Colonel Glenn Road (Figure 14). Two more from the Hatton Tuff (HT 4 = J 22 and HT 5 = J 23) were provided by Julie Cains (at the time an Arkansas graduate student). These formations were chosen in order to draw further conclusions about the flow paths of hydrothermal and basinal brine fluids related to the Mississippi Valley-type ore deposits via Pb isotope relationships through analysis of chert inclusions found within each.

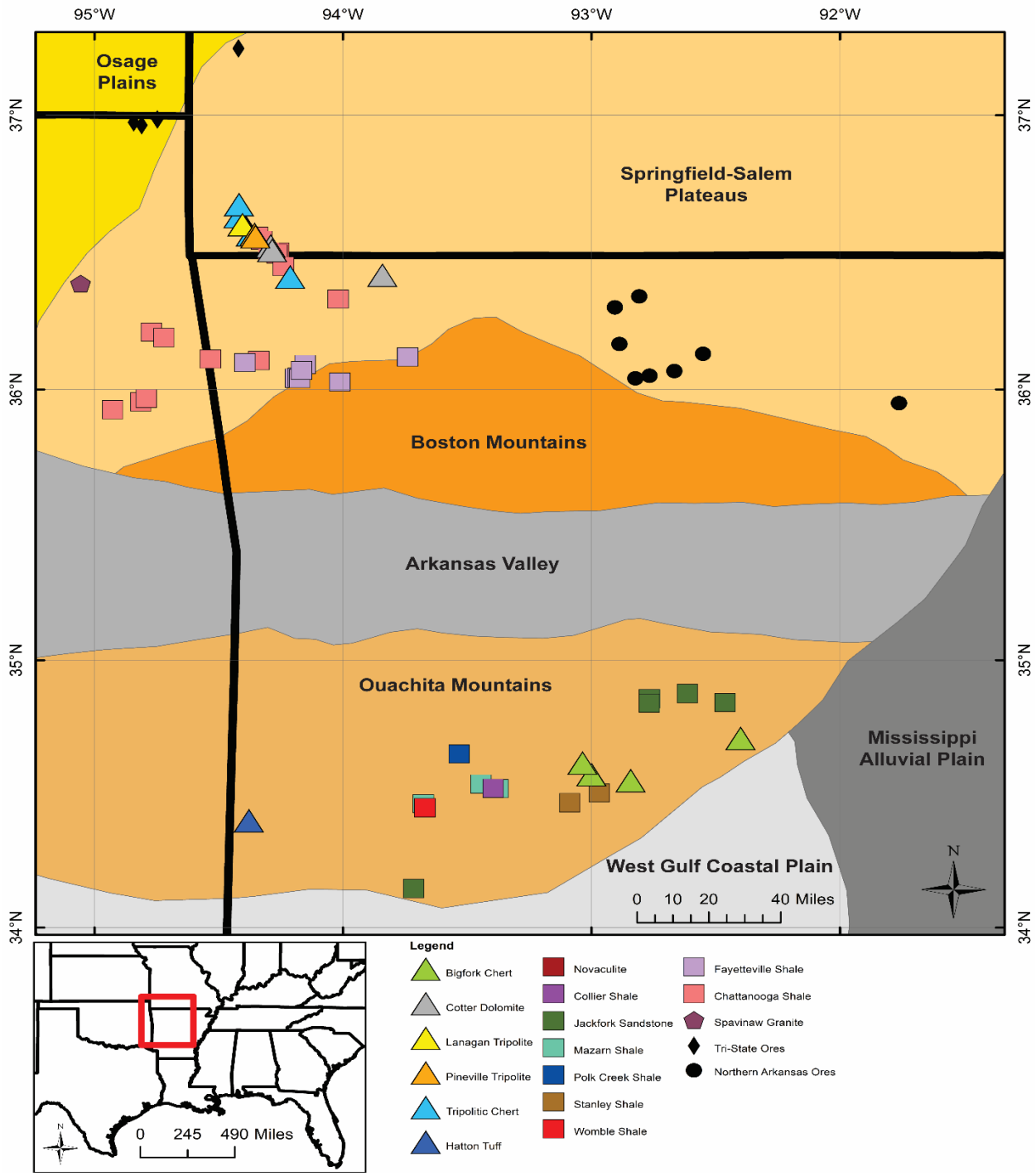

Figure 14. Location of sampled rocks in this study, along with samples previously collected and analyzed by Bottoms *et al.*, 2019 (Fayetteville and Chattanooga Shales and Tri-State and Northern Arkansas ores), Cains, 2019 (Novaculite), McKim, 2018 (tripolitic chert), and Simbo *et al.*, 2019 (Ouachita Shales). The rocks in this study include the Bigfork Chert (green) near bottom center, Hatton Tuff (blue) near Oklahoma border, with the Cotter Dolomite (grey) and tripolitic chert (orange and yellow) in northwest Arkansas and southwestern Missouri. Locations of formations from previous studies and ore districts are also indicated as shown in legend. Image courtesy of John Samuelsen.

Table 1a. Northwest Arkansas Samples, collected 10/28/2017

Sample Name	Location	Latitude	Longitude	Sample Type
CD 1	Upper Chert 6.5 ft above base, west of I-49	36°31'50.39" N	94°17'48.36" W	Cotter Dolomite, gray and white chert in discrete bodies
CD 2	4.5 ft above base of roadcut, west of I-49	36°31'50.39" N	94°17'48.36" W	Cotter Dolomite, oolitic chert
CD 4	18” above base, west of I-49	36°31'50.39" N	94°17'48.36" W	Cotter Dolomite, gray and white chert as discrete bodies
CD 6	Shaddox Slip Roadcut, 62” above base	36°30'53.52" N	94°17'11.67" W	Cotter Dolomite, gray banded chert
CD 7	Shaddox Slip Roadcut, 6’ below CD 6II	36°30'54.33" N	94°17'13.10" W	Cotter Dolomite, dolomite and gray banded chert
CD 8 (Beaver Lake)	Lower chert, ~9.84 ft below Powell Dolomite contact	36°25'11.37" N	93°50'51.93" W	Cotter Dolomite

Table 1b. Southwestern Missouri Tripolite, collected on 03/15/2017 and 01/24/2018

Sample Name	Location	Latitude	Longitude	Sample Type
PT 2	Pineville, MO	36° 34' 2.84" N	94° 21' 35.43" W	Tripolitic Chert
PT 6	Pineville, MO	36° 33' 56.99" N	94° 21' 17.46" W	Tripolitic Chert
LT 1	Lanagan, MO	36° 36' 14.86" N	94° 24' 29.61" W	Tripolitic Chert
LT 1 Duplicate	Lanagan, MO	36° 36' 14.86" N	94° 24' 29.61" W	Tripolitic Chert
LT 2	Lanagan, MO	36° 36' 16.15" N	94° 24' 30.15" W	Tripolitic Chert

Table 1c. Hatton Tuff, collected and provided by Julie Cains

Sample Name	Location	Latitude	Longitude	Sample Type
HT 4 (J 22)	AR/OK Border	34° 21' 3.22" N	94° 22' 16.60" W	Tuff
HT 5 (J 23)	AR/OK Border	34° 21' 3.22" N	94° 22' 16.60" W	Tuff

Table 1d. Bigfork Chert Samples, Collected 01/05/2019

Sample	Location	Latitude	Longitude	Sample Type
BF 1, Lower	Malvern Minerals Company “Ten Mile Pit”	34° 33' 6.43" N	92° 50' 56.78" W	Chert with calcite veins
BF 2, Upper	Malvern Minerals Company “Ten Mile Pit”	34° 33' 8.70" N	92° 50' 58.52" W	Chert with small black inclusions
BF 3, Lower	Fox Pass Cutoff Quarry, north of Hot Springs	34° 34' 39.71" N	93° 0' 1.25" W	Chert with red/black inclusions, numerous black veins
BF 4, Upper	Fox Pass Cutoff Quarry, north of Hot Springs	34° 34' 41.41" N	93° 0' 4.50" W	Chert with numerous black stains
BF 5, Upper	Hwy 7, adjacent to Mexican Restaurant, 40’ from top of cut	34° 37' 0.67" N	93° 2' 21.48" W	Chert
BF 6	I-430 at Colonel Glenn	34° 42' 54.46" N	92° 24' 3.33" W	Chert with rhombohedral calcite voids

7. METHODS

7.1 Sample Preparation

The samples were cut into 1/4” to 3/8” thick slabs using a MK modified water tile saw. The saw blade was first self-contaminated for each sample by cutting a series of slabs from the outer perimeters of the larger specimens to help eliminate the possibility of cross-contamination between samples. The slabs were described, photographed, and recorded according to collection location and stored in Ziplock bags in the Radiogenic Isotope Class 100 Clean Laboratory at the University of Arkansas. These slabs were then rinsed 3 times with de-ionized water and allowed to dry. They were then wrapped in 2 layers of aluminum foil followed by another 2 layers of paper towel and placed in a ziplock bag. Slabs were then smashed with a sledgehammer to crush them into small chips with fresh surfaces. For powdering, the innermost chert slab samples were selected in order to produce results with the least amount of error or outside contamination, although altered from their original depositional petrography themselves by diagenetic processes. Two series of the innermost chert chips were then collected and powdered in a centrifugal Spex SamplePrep Shatterbox unit in order to self-contaminate the centrifuge vessel, the remnants of which were then discarded. A third and final round of the chert chips was then powdered and stored in previously leached plastic containers. The centrifuge vessel was wiped with Kimwipes© in order to remove remaining residue, rinsed with DI water and allowed to dry, filled and powdered with orthoquartzitic sand in between cleaning and rinse cycles, and then washed again with DI and Double-DI water. The vessel was rinsed with alcohol to speed the drying process and allowed to dry completely before the process was repeated again with the next subsequent sample.

7.2 Chemical Processing

The polypropylene specimen storage containers were leached by boiling in HNO_3 (nitric acid) and rinsing three times with a series of DI, double DI, and triple distilled (Savillex) water, respectively.

For sample digestion, 0.3 grams (300 mg) of each powdered sample was selected by shaking the specimen container to target the lightest and blended portion of each respective sample. The precise weights of each individual sample were recorded for later calculation of concentrations. The suite of 18 samples was processed through a series of heated acid treatments to digest silica and purify the samples of organics and other impurities. All of the Bigfork Chert samples contained considerable amounts of organics, evidenced by dark coloration and particulate matter in some samples after digestion. Particulate matter was separated from effected samples through use of a centrifuge for both trace element concentrations and Pb isotope samples. Organic matter was less apparent in the lightly colored samples BF1 and BF2, collected from the Malvern Minerals Company Ten Mile Pit, east of Hot Springs, Arkansas. A detailed description of the chemical processing is presented in the Appendix.

7.3 Sample Analysis

For trace element concentration analysis, the 18 samples, one duplicate (LT1), and one blank were processed. Six USGS rock standards (AGV-2, BHVO-2, BIR-1, DNC-1, QLO-1, and W-2: Table 3 of Appendix) were treated identically and measured along with the samples in order to build calibration curves and define the accuracy and reproducibility of the individual sample measurements. Elemental concentration samples were run on a Thermo Scientific iCap Q Quadrupole ICP-MS with a kinetic energy collision cell (Bremen, Germany) using external

quantification from a commercially available multi-element standard (USGS high purity standards 68a in 1, 5, 10, 50, and 100 ppb dilutions). Calculations of theoretical REE concentrations versus actual (observed) values were conducted based on dilution rates. Data normalization was conducted for each sample by reducing recorded Quadrupole ppb intensities to ppm. Nb, Ta, Hf, and Zr values were originally recorded as ppm by the machine. Resulting Th, U, and Pb concentrations allow for age-correction of samples and help determine source contributions of the ore metals.

Pb isotope analyses were conducted using a Nu Plasma Multi-collector ICP-MS (England) coupled with an ESI Apex Omega Desolvating Nebulizer (Omaha, NE, USA) with the much-appreciated aid of John Samuelsen, Archeology Ph.D. candidate, University of Arkansas. Reported Pb isotope values represent an average of 60 measurements of each sample taken by the Multi-collector, with each average corrected for instrumental differences using NBS Pb Standard 981. Plotted error bars indicate instrumental repeatability versus sample homogeneity or the ability in the lab to produce isotope ratio values. Better metrics of actual error include repeat measurements of multiple samples and reporting of the standard deviation of standards (Recorded Pb isotope standard and calculated 2-sigma values: Table 5 of Appendix). Raw data were then corrected for mass and dilution using a series of Excel templates. Standardized sample bracketing was used to reduce the data and correct analyzed Pb isotopic values provided by the MC-ICP-MS for all samples. Corrected analyzed values were then normalized to the preferred average GeoRem® standard lead isotopic values for each sample, respectively.

Results produced for both concentrations and Pb isotope values were normalized to Primitive Mantle values in order to generate and interpret trends. As shown by Figure 15, a trace element concentration of subducted sediment composition and a trend of increasing

incompatibility to the left are apparent. The Pb isotope values were further manipulated in order to plot each respective sample value with those of previous studies and generate a picture of how several formations throughout Arkansas are related. The results from these plots were also age corrected to 250 my, the accepted age of the MVT ore deposits. This treatment was applied in order to make comparisons of lead and the ores possible, as the ores do not decay after deposition, as do thorium and uranium (Cains, 2019). Actual results reflect current conditions in the formations sampled and may be signatures of multiple processes and fluids acting within the resulting lithologies.

The original signatures are disguised by subsequent processes of diagenesis and alteration. Further, alteration also consists of solution thinning, silicification, dolomitization, and clay-mineral alteration (Hall and Friedman, 1969). True differentiation of the processes responsible for isotopic signatures is difficult to ascertain, based on multiple processes of boiling, cooling, meteoric waters mixing with hydrothermal fluids, and rock-water interaction (Williams-Jones and Migdisov, 2014). In addition, subsurface fluids may acquire their chemical characteristics through a variety of processes, including l) dissolution, recrystallization and ion exchange involving any number of inorganic and organic phases, 2) evaporation, 3) shale membrane filtration, 4) mixing of waters, and 5) ion diffusion (Banner *et al.*, 1989).

8. RESULTS

8.1 Elemental Concentrations

Spider diagrams (Figure 15), colloquially named from Masuda-Coryell diagrams (Masuda, 1962; Coryell *et al.*, 1963), help generate a useful overview of incompatible elemental behavior and illustrate the key components that require explanation in subduction zone magmas. Two distinct components from the slab can be identified in island arc lavas. The first is explained as a melt of the down-ramp transported sediment, whereas the second is interpreted as likely an aqueous fluid derived from altered mafic oceanic crust (Elliot *et al.*, 1997). Arc lavas can be described as representing a mix of three main components: a depleted mantle wedge, subducted sediment, and (altered) mafic oceanic crust. Both mafic crust and sediment bear much higher incompatible element concentrations than typical mantle rocks and hold the potential to impart a strong chemical signature, if added to the mantle wedge.

8.2 Lead Isotope Ratios

Lead isotope data are presented on two covariate diagrams in Figures 16 (p. 42) and 25 (p. 62). Lead isotope data are reported as ratios of a radiogenic isotope to the stable isotope. Thorogenic diagrams plot the radiogenic daughter signatures of parent Th^{232} on the y-axis as Pb^{208}/Pb^{204}. Conversely, uranogenic diagrams plot daughter isotopes from parent U^{235} as Pb^{207}/Pb^{204} on the same axis. The x-axis plots Pb^{206}/Pb^{204} ratios from U^{238}, or the most abundant versus the least isotope of Uranium. Thorium has the longest half-life (14.01 Ga) of these (Tosdal *et al.*, 1999). The least abundant Pb isotope, Pb^{204}, is inherited from the original or primeval lead of the solar system. However, the three most abundant Pb isotopes, Pb^{208}, Pb^{207}, and Pb^{206}, are partly original, partly radiogenic, and continue to increase in abundance as they are stable end-products of the radioactive decay of uranium and thorium (Cannon and Pierce, 1969).

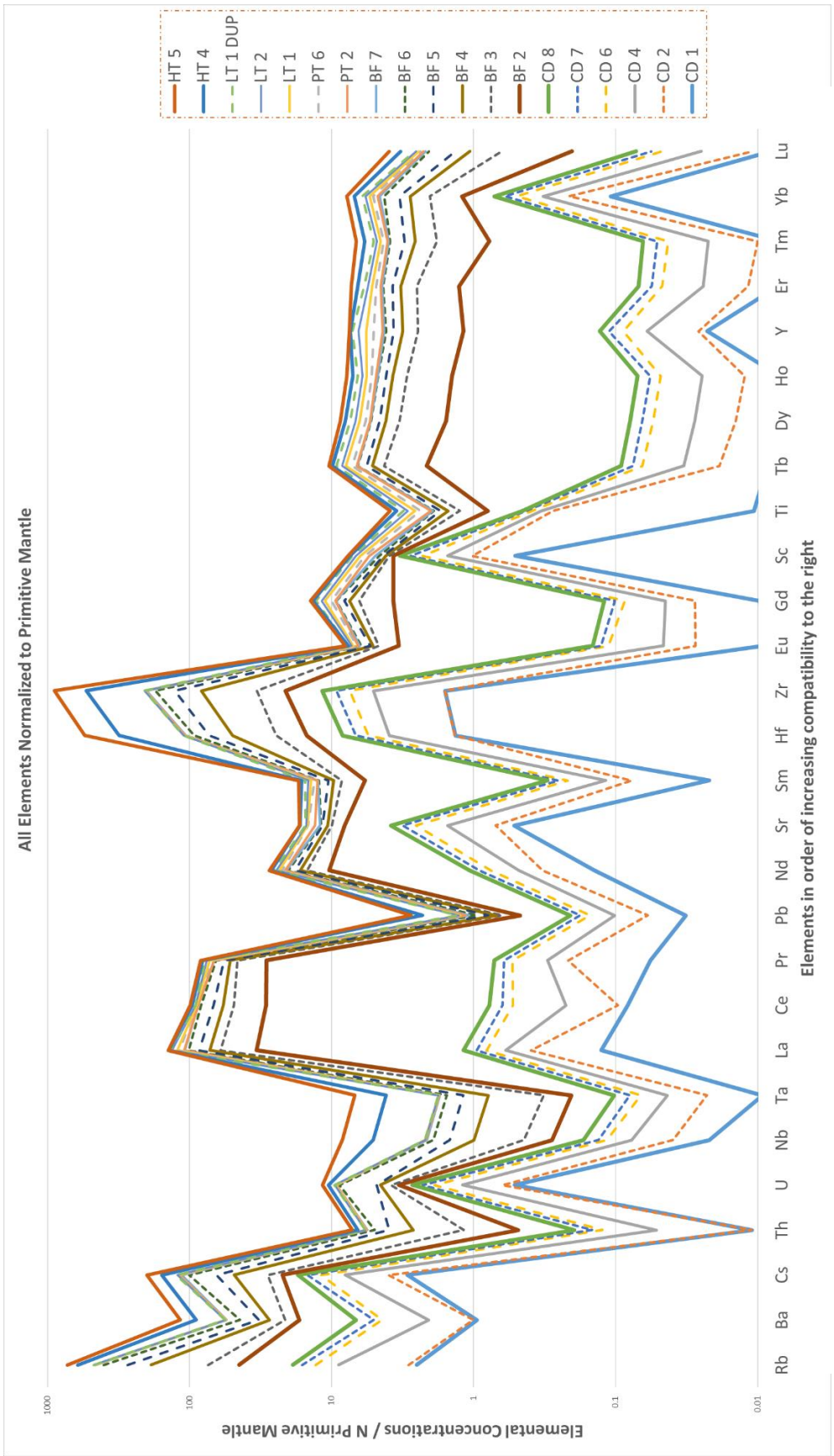

Figure 15. Trace element concentrations of samples normalized to Primitive Mantle values.

Primitive Mantle Analytes																												
	Rb	Ba	Cs	Th	U	Nb	Ta	La	Ce	Pr	Pb	Nd	Sr	Sm	Hf	Zr	Eu	Gd	Sc	Ti	Tb	Dy	Ho	Y	Er	Tm	Yb	Lu
Sample Name																												
CD 1	1.05601	4.50113	0.05889	0.050892739	0.80916	1.55168	0.04301	0.0646	0.11405	0.01226	0.25225	0.15385	8.50376	0.00802	0.34643	15.2257	0.00127	0.00482	7.95688	8.46744	0.00079	0.00481	0.00101	0.09498	0.00304	0.00047	0.04709	0.00053
CD 2	0.14583	0.2771	0.02084	9.9569E-05	0.17639	1.21794	0.06229	0.13763	0.0191	0.03429	0.21516	0.19993	2.99971	0.02046	0.00485	0.17057	0.00256	0.00902	7.97868	211.695	0.00094	0.00423	0.00076	0.0146	0.00189	0.00019	0.04528	0.0002
CD 4	2.54289	5.02746	0.08082	0.187267948	0.91247	2.68495	0.09502	0.10279	0.17542	0.01848	0.3277	0.16731	13.4145	0.01458	0.65968	33.3546	0.00262	0.00846	7.84986	47.0295	0.00134	0.00854	0.00174	0.1413	0.00531	0.00081	0.04907	0.00094
CD 6	1.68779	11.1624	0.07684	0.333925879	1.08805	2.64854	0.10616	0.11103	0.4239	0.05044	0.39386	0.29926	16.5759	0.03676	0.4166	23.0112	0.00933	0.02075	11.8384	41.6787	0.00291	0.01704	0.00337	0.11819	0.00957	0.00136	0.07407	0.00149
CD 7	1.30917	3.09459	0.05954	0.10493024	0.64113	1.20482	0.05947	0.07129	0.13432	0.01643	0.20398	0.16403	10.3603	0.01351	0.32377	17.5027	0.00196	0.00751	7.89841	30.6258	0.00104	0.00655	0.00125	0.09636	0.0037	0.00053	0.04754	0.0006
CD 8	1.10892	7.89955	0.0505	0.221946653	0.64563	2.60314	0.10769	0.11626	0.20293	0.02315	0.24104	0.17662	10.5752	0.0175	0.40721	22.5659	0.00264	0.00964	7.89015	24.2057	0.00143	0.00905	0.00187	0.07725	0.00576	0.00087	0.04947	0.00104
BF 2	10.9709	48.3345	0.09833	1.34134709	1.03911	7.79392	0.47322	16.6194	38.9822	6.07443	2.05935	10.1313	69.8494	2.03036	1.69919	91.8461	0.44955	1.7859	6.02273	270.359	0.18847	0.94173	0.19255	4.39677	0.50438	0.04702	0.21269	0.00874
BF 3	12.2404	20.699	0.11612	3.204726768	0.70802	11.3637	0.53743	13.64	27.126	3.73107	1.26385	4.85214	30.9294	0.95063	2.47745	118.704	0.1811	1.36396	3.79587	368.196	0.19711	1.12485	0.21682	5.39111	0.52743	0.06878	0.36183	0.02901
BF 4	47.2456	29.3126	0.41175	6.811644181	1.12661	39.1947	2.15357	5.96327	12.9663	1.21895	0.49217	1.84046	11.6744	0.44082	6.55226	473.577	0.06424	0.5235	3.29635	207.611	0.0816	0.51554	0.10777	2.91558	0.31201	0.05051	0.32771	0.02854
BF 5	36.4831	24.0555	0.32379	5.977764279	0.43857	33.7234	1.82496	6.99731	13.7004	1.18231	0.76863	1.63042	14.1064	0.32719	5.92949	422.588	0.03194	0.34483	3.0739	163.668	0.04852	0.2849	0.06112	2.04884	0.19205	0.03161	0.23632	0.01878
BF 6	53.8352	55.8901	0.71701	4.814766427	6.32016	30.733	1.70226	7.94378	20.4378	1.76608	1.28077	2.39102	5.86588	0.62773	5.16853	448.253	0.11866	0.55883	4.22857	148.701	0.07753	0.43174	0.08405	2.05246	0.27309	0.05333	0.40679	0.04858
BF 7	25.3383	51.3942	0.26373	2.782780677	0.65659	15.872	0.81756	3.47395	5.70776	0.44248	0.96957	0.71025	3.04248	0.06678	3.44287	275.369	0.02235	0.0465	4.98965	26.6701	0.00599	0.02904	0.00278	0.56971	0.0236	0.00661	0.13655	0.00756
PT 2	1.55683	2.05406	0.06422	0.273979714	0.08323	1.39708	0.05774	0.49768	0.38827	0.01874	0.44919	0.36398	16.6964	0.042	0.40977	19.0141	0.01872	0.04375	7.5651	40.6544	0.00574	0.01592	0.01607	0.40373	0.04298	0.00531	0.07056	0.00501
PT 6	1.61353	1.15979	0.05222	0.297189757	0.11993	1.92742	0.07513	4.49095	2.35571	0.64185	0.62121	1.14113	24.8213	0.22754	0.34275	19.5285	0.02331	0.29829	6.56089	304.992	0.04418	0.25948	0.05217	2.79187	0.13798	0.01733	0.15338	0.00739
LT 1	0.24234	0.84873	0.03054	0.110928956	0.09635	0.6801	0.02454	1.96811	0.91879	0.41314	0.21887	1.06842	2.71288	0.28109	0.14573	7.18051	0.05422	0.55144	6.88544	170.386	0.07274	0.37388	0.06473	2.8416	0.14226	0.01465	0.13616	0.00456
LT 2	0.19649	0.43353	0.01987	0.096050669	0.14538	0.22729	0.01059	5.68486	1.70818	0.71909	0.20272	1.21746	3.89116	0.23998	0.05622	2.43092	0.02518	0.3206	6.85536	249.556	0.04685	0.27692	0.05685	3.05552	0.14922	0.01802	0.15199	0.00694
LT1 DUP	0.29597	0.94309	0.03114	0.111225496	0.09915	0.72928	0.01842	2.05964	0.10201	0.43877	0.22192	1.09342	3.41802	0.28896	0.15401	7.92753	0.05823	0.57323	6.83289	178.978	0.07408	0.38797	0.06772	2.9773	0.14998	0.01606	0.13812	0.00509
HT 4	58.2375	159.294	0.66833	3.60902784	1.5048	204.378	10.985	1.37751	7.34674	0.71172	7.77243	1.2149	22.4799	0.33522	52.5684	3116.08	0.00093	0.30324	4.15296	288.987	0.05716	0.3779	0.08303	0.79619	0.27821	0.05245	0.36744	0.04333
HT 5	48.2582	123.433	0.85628	2.725450621	1.7704	230.079	12.4676	0.74815	3.79287	0.49577	3.69136	1.00341	2.21491	0.28383	59.9301	3465.97	0.04939	0.27182	4.00801	297.558	0.05856	0.41611	0.09505	0.65912	0.31611	0.05792	0.3884	0.0458
	Rb	Ba	Cs	Th	U	Nb	Ta	La	Ce	Pr	Pb	Nd	Sr	Sm	Hf	Zr	Eu	Gd	Sc	Ti	Tb	Dy	Ho	Y	Er	Tm	Yb	Lu

Table 2. Trace element compositions of analyzed formations in order of increasing compatibility.

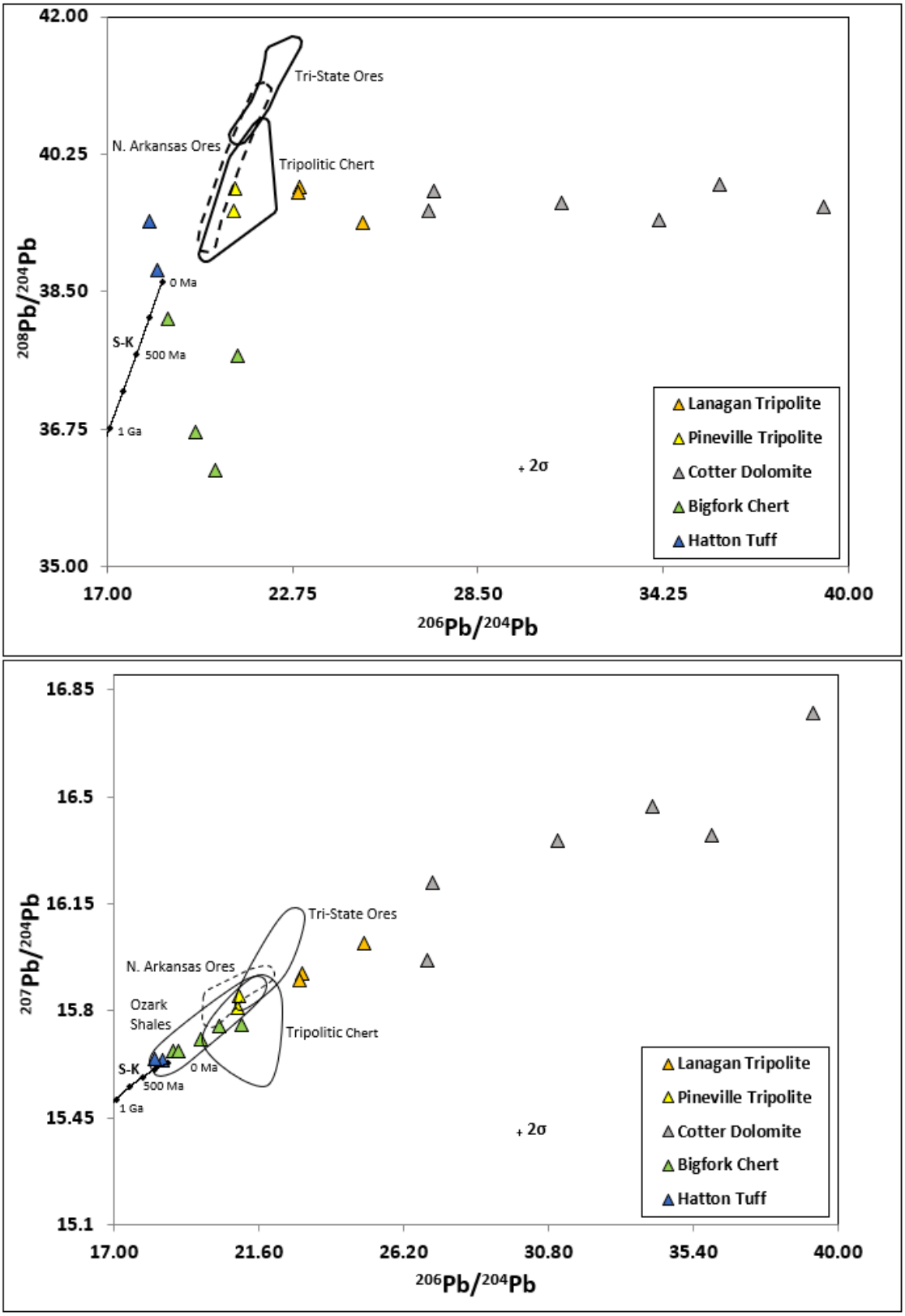

Figure 16. Covariate diagrams displaying present day Pb isotope values formations sampled in this study, in conjunction with previous work on the ores (Bottoms *et al.*, 2019) and the tripolitic chert by McKim (2018). Also plotted is Stacey and Kramers (1975) model for orogene deposits.

9. INTERPRETATIONS

Two age ranges of datasets are represented by these lead plots, the first Ordovician, while the second (tripolitic chert) is Pennsylvanian age with the presumably younger MVT ores (~250 ma).

9.1 Rare Earth Elements

Rivers are the main source of rare earth elements (REE) transported to the oceans. The relative concentrations of REE in rivers resemble those of shale and greatly influence the chemistry of continental shelf waters (Piper, 1974). REE are comprised of the lanthanide elements plus scandium and yttrium, which have similar physical properties and are often found in the same ores and deposits. Specifically, REE include the light rare earth elements (LREE), such as lanthanum, cerium, praseodymium, neodymium, samarium, europium, and the heavy rare earth elements (HREE), gadolinium, terbium, dysprosium, holmium, erbium, thulium, ytterbium, lutetium, scandium and yttrium (Weiss *et al.*, 2016).

Incompatible elements and associated isotopic systems are named as such in that they preferentially enter a melt phase relative to a solid residue (Elliott *et al.*, 1997). Incompatible elements to the left of the spider diagram favor the melt phase and are the most abundant in an enriched mantle (Eiler, 2000), as shown by the concentration trends produced from the sampled formations in this study (Figure 15). Conversely, depleted source signatures toward the right of the diagram are those that have increased concentrations greater than 1 ($\geq$1) of compatible elements that favor the solid phase (McKim, 2018). Further, depleted sources, such as MORB (Mid-Ocean Ridge Basalt) magmas exhibit low incompatible element abundances and low ratios of more to less incompatible elements. The Hatton Tuff is volcanic and the most enriched in all elemental concentrations of Figure 15, although notably depleted in Pb isotopes.

As found by McKim (2018), the tripolitic chert originated from more enriched or evolved sources. The concentrations reported for the formations sampled in this study and normalized to Primitive Mantle values generally produce a variation of REE toward an increasing negative compatibility trend and show similar negative/positive variability. An enrichment trend of the subduction sediment compositions to the left of the spider diagram (Figure 15) is attributable to the effects produced by the addition of sediment. This dynamic is also indicative of more enriched and evolved crustal contributions. These findings are supported by the fact that all formations, including the tripolitic chert sampled for this and previous studies, are noticeably enriched in the more incompatible elements (left side of the spider diagram), as compared to the more compatible elements found on the right side of the spider diagram.

Furthermore, the differences in mantle and sediment decline towards the increasingly compatible right side of the spider diagram as sediment becomes less of an influence on the amounts of these mantle elements. Highly incompatible elements found to the left of the 'spidergram' are generally the least abundant in the depleted mantle and reflect slab addition effects, whereas those on the right will predominately reflect melting and fractionation processes. In addition, the contrast between depleted mantle and subducted sediment can be up to seven orders of magnitude (Elliott *et al.*, 1997).

Positive inflections on a logarithmic scale indicate an enrichment in those particular elements compared to the elemental concentrations of the original averaged Primitive Mantle values (McKim, 2018). Rb, Cs, U, Hf, La, Pr, Zr, and Yb are shown to reflect shared positive inflections among all formations sampled in this study. For the lithologies in this study, the Cotter Dolomite is shown to be the contributing source of Sc, Ti, Y, and Yb, as indicated by positive spikes, and reflected in lesser concentrations among the Bigfork and tripolitic cherts,

respectively. The positive U anomaly may be attributed to soluble U^{6+} uranyl ions that are much more fluid mobile and indicate a reducing environment (also demonstrated by sulfur dynamics of sulfate to sulfide) than those of generally insoluble U^{4+} or Th. Transition refractory metal elements of Nb/Ta are negative spikes, while La and Hf, Zr, Sc, and Y comprise significant positive spikes toward elements of greater compatibility. Ti exhibits a negative inflection for all formations.

Sr, Sc, and Y are shown as positive differences within the Cotter Dolomite, respectively. The presence of a small spike in yttrium and negative inflection in Ce help support the presence of fluorite mineralization in the Cotter Dolomite, as shown by the tripolitic chert (Lanagan) and Boone chert analyses conducted by Cains, 2019. Elements with values less than 1 (<1) indicate depleted elemental contributions relative to those of typical Primitive Mantle, as in the case of most elements within the Cotter Dolomite, with the exceptions of increasingly compatible and enriched Rb, Ba, Cs, Hf, and Zr compared to Primitive Mantle values. Ba also shows a positive difference within all formations compared to Pb. Further, Cains, 2019 showed that the penecontemporaneous chert is enriched in Ba and Sr, while other Boone cherts are enriched in Ba, Rb, Sr, Y, La, Ni, and Zr. This study also showed that Ba-Cl ratios would have been much higher if oil-field brines had contributed. Philbrick's 2016 study of the Lower Mississippian Novaculite also indicated enriched values for Ba. Elevated Ba/Th ratios are likely the most prominent signature of the addition of elemental material from altered oceanic crust (Elliot *et al.*, 1997). The tripolitic chert was also analyzed for Be, Co, Cr, Cu, Ni, and V, and is shown to be enriched in Dy along with considerable levels of Cr, V, and Zn (McKim, 2018). Eu and Dy among the elements in this study reflect a negative difference from Tb toward more compatible REEs. In addition, a positive anomaly trend for Yb is seen in all formations and appears to be

likely sourced from a positive Yb spike within the Cotter Dolomite, commonly included in the mineral monazite, along with many other lanthanide elements (Figures 15 and 17).

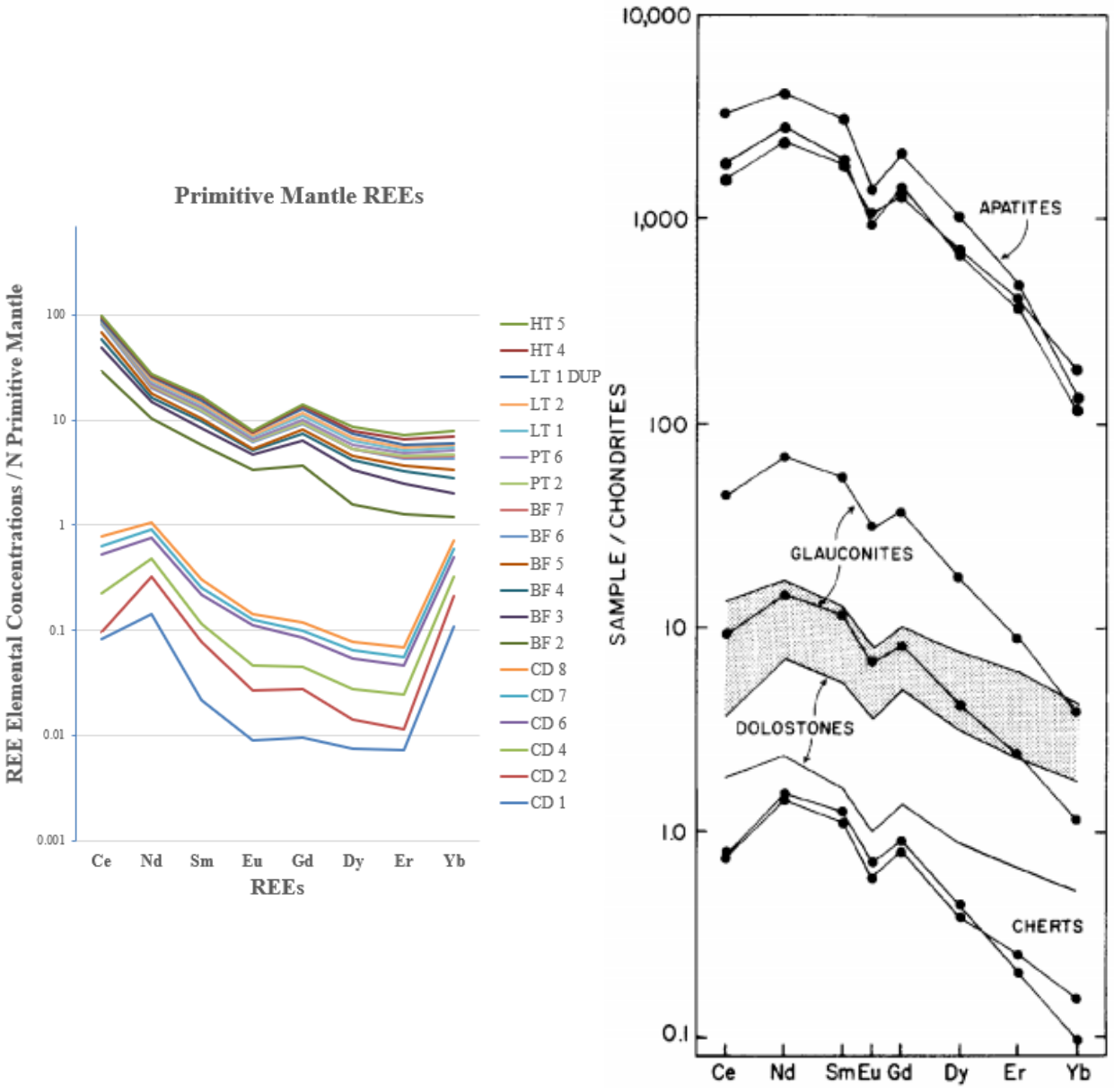

Figure 17. REE patterns for various diagenetic and depositional phases from the Burlington-Keokuk Formation, illustrating large range in REE abundances and similarity in REE patterns among the different phases (Banner, 1988a). Note the difference in REE trends of Cotter Dolomite from other formations above in graph on the left.

In oxygenated mid-ocean waters, oxidation of Ce (III) to rather insoluble Ce (IV) allows for the preferential removal of Ce from the water column. This process results in seawater with a

pronounced negative Ce anomaly linked to the subducting slab (Elderfield and Greaves, 1982). Furthermore, particulate Fe and Mn in the hydrothermal plume preferentially scavenge more Ce, producing ridge-influenced seawater with a negative Ce anomaly (Figure 17) more extreme than found elsewhere in seawater (Klinkhammer *et al.*, 1983). Ce has a strong affinity for elements like phosphorus (Weiss *et al.*, 2016), found in phosphate nodules of the Chattanooga Shale by Kesler *et al.*, 1994a (Figures 26, 28). Additionally, sediments in shale and chert deposited in a system with a high sedimentation rate, such as found along a continental margin, will retain low ΣREE abundances as rapid burial limits sediment interaction with dissolved REE in seawater (Ruhlin and Owen, 1986). Moreover, in cases where negative Ce anomalies are observed, they have been shown to correlate with light rare earth enrichment (Elliot *et al.*, 1997; Piper, 1974; and Woodhead, 1989). This statement is supported by Figure 15 in this study through enrichment of the light REE lanthanum, cerium, praseodymium, and neodymium, with an opposite and negative difference for samarium and depletion of europium, respectively. The relative and absolute concentrations of REE in authigenic and biogenic phases of deep-sea sediments vary greatly. This is due to competition between these phases for REE that results in fractionation from the parent material, primarily from terrigenous inputs, but also from marine volcanism. The strongest aspect of this fractionation is shown by a depletion of Ce relative to La in barite, $CaCO_3$, opalline silica, phillipsite, phosphorite, and montmorillonitic clays, with a Ce enrichment in Fe/Mn nodules (Piper, 1974).

In time, elemental concentrations evolve into low $^{87}Sr/^{86}Sr$ and high $^{143}Nd/^{144}Nd$ ratios (Sun and McDonough, 1989), as shown by the Bigfork Chert, tripolitic chert, and Hatton Tuff. Dissimilar Nd-Sr-Sm trends are shown as an overall negative difference with a positive Sr spike and negative Nd trend in the Cotter Dolomite, possibly a result of sub-aerial exposure during

lithification and delayed burial processes. Another dissimilar anomaly is indicated by the positive spike exhibited by heavy rare earth elements, such as scandium in the Cotter contrasted with a positive difference in Gd, negative difference in Ti, and positive difference in Tb for all other sampled formations.

The large negative spikes of Ba, Th, and Pb exhibited among all formations sampled as well as negative differences in the concentrations of Sm in the Cotter and Ti in the other formations are inferred to indicate alteration from the original lithology with flushing by aqueous fluid(s) originating from altered mafic oceanic crust. All Pb concentrations, a result of Th and U decay overtime, reflect an average of those radiogenic element values. All sample elemental concentration values are enriched in comparison to the Primitive Mantle, with exception of the Cotter Dolomite.

Further, the heavy rare earth element Gadolinium (Gd) is depleted in the Cotter, while enriched in all other sampled formations. The Ce/Pb ratios should become depleted toward continental crust due to fractionation during primary continental crust-mantle differentiation (Hofmann *et al.*, 1986), also shown by all formations sampled in this study. Arc source depletion of a prior mantle protolith can be evidenced by Nb/Ta ratios (Elliott *et al.*, 1997). As two highly incompatible elements with the same valence, and apparently identical ionic radius (Shannon, 1976), Nb and Ta are difficult to fractionate during melting. However, even highly incompatible elements are fractionated from one another in near fractional melting processes (Johnson *et al.*, 1990).

The incompatible elements associated with subduction zone magmatism are fluid mobile or fluid immobile. Interpreted in different ways, fluid mobile large ion-lithophile elements (LILE), and fluid immobile high-field strength elements (HFSE) are closely related in theory

(Elliot *et al.*, 1997). The justification is that large ions, such as K^{+} and Ba^{2+}, partition freely into an aqueous fluid phase, more easily than small, highly charged ions like Zr^{4+} or Nb^{5+}. In contrast, light rare earth elements (LREE), like La^{3+} and actinides, including Th^{4+}, have large ionic radii, but are also highly charged. HSFE elements are less prevalent in sediments relative to other elements of comparable incompatibility, and as so are least enriched by the addition of sediment (Elliot *et al.*, 1997). Furthermore, high field strength elements are not easily transported by fluids [e.g. Tatsumi *et al.*, 1986], and are thus minimally affected by possible slab-derived 'fluid' components (Th and U^{4+}).

As explained by Elliott *et al.*, 1997, it is evident that two components are required from the subducted slab. A light rare earth element enrichment component bears a full range of incompatible elements and controls the budgets of most of these elements. The second component has a major influence on only the budgets of certain incompatible elements, principally 2^{+} cations, such as Ba, Ra, Sr, and Pb and to a lesser degree other large ion lithophiles Rb, K, and U, and does not perceptibly contribute LREE, Th, Nb, and Zr. Ranging evidence from isotopic and incompatible element ratios implicates these components as a sediment melt and aqueous fluids derived from altered oceanic crust.

Further, ore-bearing fluid appears to have contained elevated Ca/Na ratios, indicating that major cation ratios can be used to identify ore fluid in Ozark Plateau MVT districts (Wenz *et al.*, 2012). Upper limits on possible metal concentrations, other than those in stage 3 dolomite fluid inclusions, are of similar magnitude to the highest measured concentrations of Pb, Zn, Cu, and Ba found in typical sedimentary brines (Leach *et al.*, 2010). According to Cains, 2019, ores were carried as chloride complexes until reaching depositional environments. Further, salinity increases with depth. The highly soluble minerals typical of evaporite sedimentary rocks include

halite: NaCl(s), sylvite: KCl(s), fluorite: CaF_2(s), gypsum: $CaSO_4 \cdot 2H_2O$(s) that precipitate from concentrated salt solutions or brines. Congruent dissolution of evaporite rock minerals is a source of dissolved chloride, sulfate, and fluoride ions, but has no notable impact on water acid-base chemistry (Bleam, 2017).

In his "A Treatise on Metamorphism," Charles Van Hise (1904) explained how metasomatic fluids advectively and aggressively move through rocks. He also conjectured that most hydrothermal solutions originate as common meteoric waters that are heated through circulation deep in the Earth's crust. Upwelling thermal waters saturated with respect to CO_2 rising from significant depth often become supersaturated. These fluids meet colder oxygen-rich and oxidized meteoric waters as well as the atmosphere, which may induce specific reactions such as H_2S oxidation as well as mixing and cooling corrosion. Further, solutional aggressiveness can also be renewed or enhanced by mixing of waters with contrasting chemistry, particularly those differing in CO_2 and H_2S content or salinity. Mixing corrosion has a similar effect and is produced by waters of different temperatures due to contrasting CO_2 contents. In addition, the conversion of H_2S to H_2SO_4 produces a sharp increase in dissolution as sulfuric waters become more aggressive with production of sulfuric acid (Dublyanksy, 2019).

In addition, leaching has a significant effect in removing REE from the noncarbonated phases (OOM differences in Figure 17 (Banner *et al.*, 1988a). Mass balance calculations suggest that both glauconite and apatite release REE into 1.25 N HCl. It was also found that 1.25 N HCl leaches Rb and Sr from the minor silicate components of the dolostones (Banner *et al.*, 1988a). The various diagenetic and depositional phases from the Mississippian Burlington-Keokuk Formation of the midcontinent (Figure 17) generate the same relative REE trend (decreasing compatibility) as the formations sampled in this study.

It is likely that most, if not all, Cambrian-Ordovician carbonate rocks in North America have undergone some level of diagenetic alteration due to contact with Mississippi Valley-type fluids (Gregg *et al.*, 2012). The presence of a strongly evaporitic Sabkha environment in the flow path (Cotter Dolomite) also appears to be necessary for the high salinities required for metal solubility and transport (Erel *et al.*, 2006). It also appears that lead, manganese, zinc, and cobalt substitute for magnesium in the structure of dolomite. Further, stabilization of early dolomite may result in increased cation and anion ordering, increased stoichiometry, Sr depletion, Mn and Fe enrichment, depletion in ^{18}O and an increase in $^{87}Sr/^{86}Sr$ values (Montañez, 1992).

9.2 Fluid Flow paths in Relation to Tripolitic Chert

The depositional setting and mixing environment presented by the Paran Fault in the Menuha Ridge area of the Dead Sea Transform margin appears to be quite relatable to those of the Ouachitas and Ozarks regions discussed in this study. Simple-zoned ferroan dolomite values plot at the non-radiogenic end of the line, whereas complex-zoned ferroan dolomites plot at the radiogenic end. Ferroan and non-ferroan dolomitization along the Paran Fault has also been shown to cause significant enrichment of several elements, including Mg, Cu, Mn, Ni, V, Zn, Pb, and U (Erel *et al.*, 2006). The enriched radiogenic Pb isotope values of the Cotter Dolomite from this study combined with the previous results of other related studies indicate a linear two end-member mixing model (Figure 25). According to several studies, one of the most robust formational mechanisms for many MVT districts is topography-driven fluid flow (Leach *et al.*, 2010), as well as density-driven groundwater and brine fluid flow regimes or systems (Erel *et al.*, 2006). In the region of the Paran fault, mixing of two metalliferous groundwater sources was involved in the dolomitization and mineralization along the structure. The first of these fluids

include the Mg-rich Dead Sea Rift brine migrating deep in the subsurface before dolomitizing the carbonate bedrock with temperatures reaching 75˚ C. The second and shallower groundwater obtained high solute concentrations from leaching igneous rocks and clastic sediments in the subsurface and migrated at lower temperatures (T ≤ 50˚ C) (Erel *et al.*, 2006). The latter of the two hydrothermal fluid pulses that produced the tripolitic chert within the Mississippian basal Upper Boone in the Ozarks has a history quite similar to that of the Paran Fault. Dolomitization occurred initially from meteoric or connate waters, while a second fluid pulse produced euhedral quartz druse within the tripolitic chert (Figure 3).

The unconformable contact between the base of the Stanley Shale and the "tripolitic upper Novaculite" in the Shell International Paper Well 1-21 (Godo *et al.*, 2014), is stratigraphically shown to correlate with the basal Upper Boone Formation, where the tripolitic chert is found (Figure 18). Unconformities often produce conduits with porous structure and permeability through erosion and further groundwater interaction. These unique flow paths and capping aquitards in the Stanley produce a very likely flow path for the initial pulse of MVT brines in route to their final deposition, leaching fine-grained Lower Boone limestone as part of the tripolite formation process and leaving significant dissolution channels within their interaction path (McKim *et al.*, 2017).

The younger, Morrowan Jackfork Sandstone consists of a deep marine arenaceous flysch sequence characterized by an alternation of well sorted, medium to fine-grained, sandstone with either shale or silty shale. Jackfork sedimentological characteristics illustrate turbidite deposition (Simbo *et al.*, 2019). The upper Jackfork is partially coeval to the upper Prairie Grove Member of the Morrowan Hale Formation, and overlain by the Johns Valley Shale, itself coeval to the Brentwood Limestone of the Morrowan Bloyd Formation.

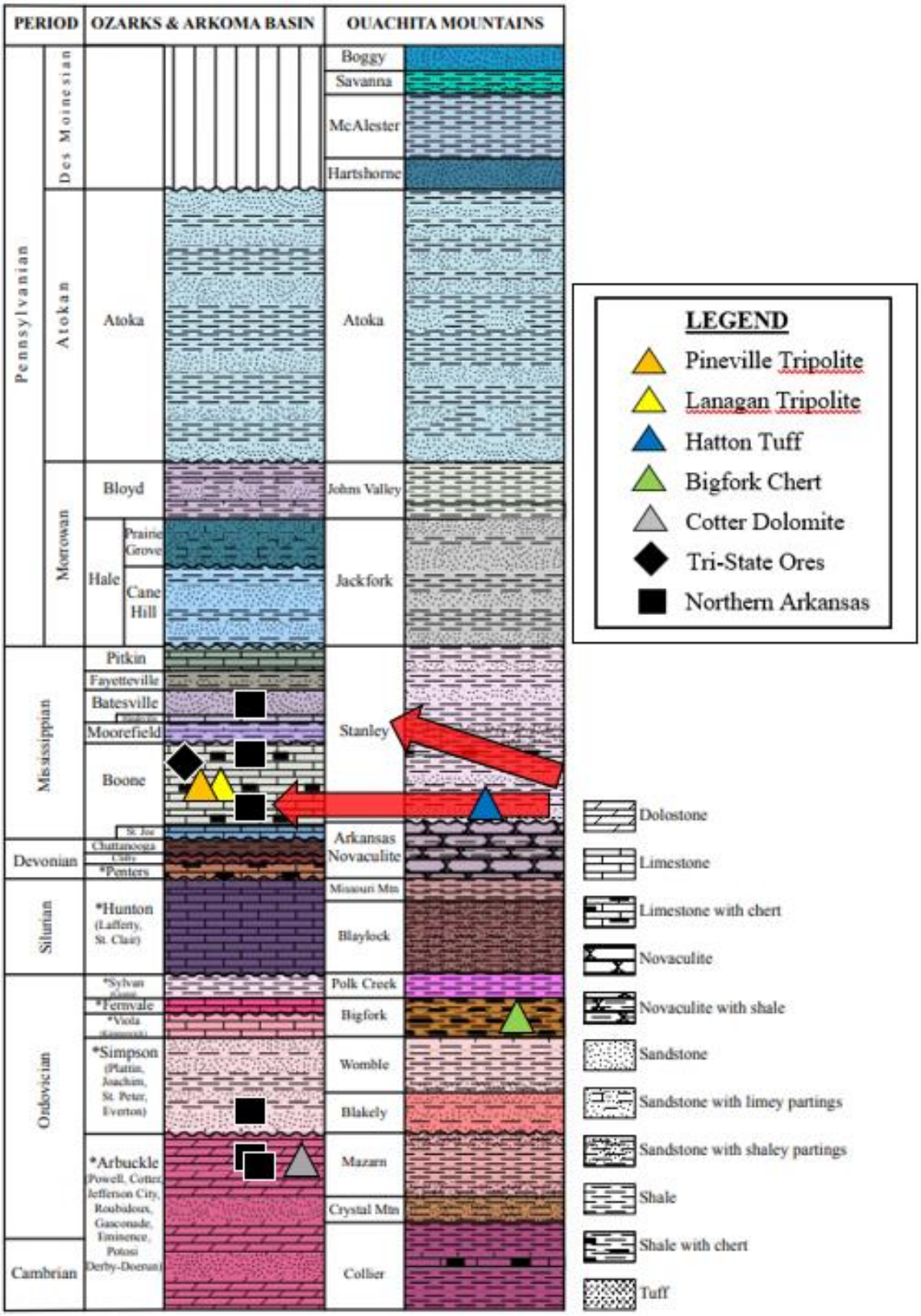

Figure 18: Interpreted stratigraphic column with sampled formations from this study; red arrows hypothesize flow paths. Modified from (Fig. 1, Godo *et al.*, 2014), AGS Info. Circ. 39C, p. 42.

A second round of hydrothermal fluids has been evidenced by silica overgrowths on quartz oolith nuclei in the Brentwood Limestone, Bloyd Formation of Morrowan, early Pennsylvanian age (Figure 19 from Henbest, 1968).

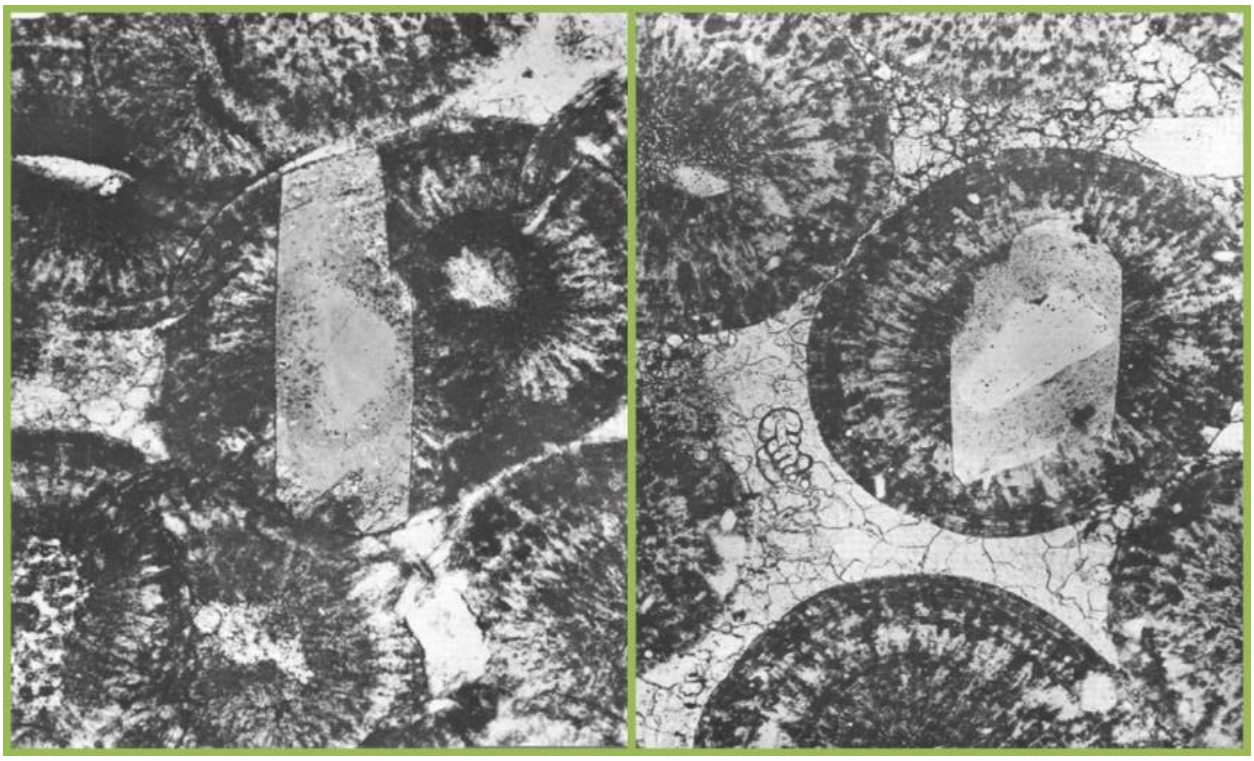

Figure 19: Quartz sand oolith nuclei (small detrital grains) within the Brentwood Limestone of the Bloyd Formation, Morrowan-Pennsylvanian in age (Henbest, 1968, p. 43) and coeval with the Johns Valley Shale, underlain by the Jackfork Sandstone. Nuclei have undergone a secondary diagenetic sequence of euhedral quartz overgrowths due to a hydrothermal event. The Brentwood is of Pennsylvanian age. These ooliths had to be deposited and lithified before the quartz overgrowths could form. We are unable to date quartz, but it has to be post-Lower Morrowan (Lower Pennsylvanian).

9.3 Quartz in Arkansas

Until recently, the tripolitic chert has only been noted as part of the highstand-regressive diagenetic limestone-chert sequence. Later, a hydrothermal event confined to the basal Upper Boone/Elsey Formations bounded by unconformities produced fine-grained white chert. Through decalcitization, the remaining carbonate was removed, producing micro-porous tripolite. A second hydrothermal event later produced euhedral quartz druse within the micro-porosity of the tripolitic chert (Figure 3).

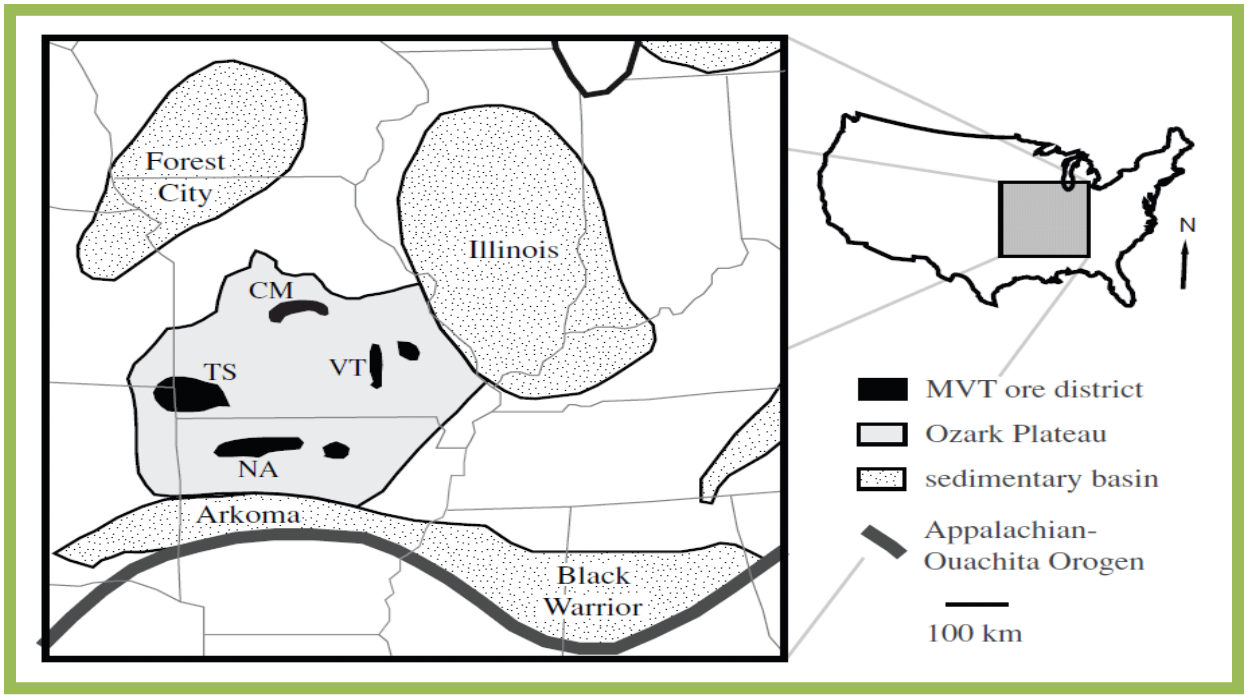

CM—Central Missouri district, NA—Northern Arkansas district, TS—Tri-State district, VT—Viburnum Trend

Figure 20. Regional overview of MVT deposits located within the Ozark Plateau. The Appalachian – Ouachita Orogeny, late Paleozoic – late Carboniferous (Pennsylvanian to early Permian noted by the dark gray line is hypothesized to have produced a laterally accreted hydrothermal fluid movement northward through the Arkoma sedimentary basin and emplaced the euhedral quartz within the tripolite in the Lower Mississippian section exposed on the Ozark Dome. MVT deposits may have been emplaced at the terminous of these hydrothermal fluid pulses. (Wenz *et al.*, 2012).

The available evidence, already recorded in large part by Miser (1943, p. 98-100) and shown in Figures 20 and 21, indicates that the quartz crystals and associated mineralization took place between the early Pennsylvanian and early Cretaceous, but that it is not related to the Cretaceous igneous activity in Arkansas (Engel *et al.*, 1951). Further, the quartz deposits are believed to have formed during the final stages of the Ouachita Orogeny, as suggested by the control of the quartz crystallization within fractures produced by folding of the Paleozoic rocks, the recurrent deformation during quartz formation, and the localization of the major quartz deposits in zones of greatest metamorphism (Miser, 1943, p. 102-107) in the orogeny, although very little metamorphism is present. The conclusion of most recent workers (Honess, 1923, p. 259; Morgan, 1924, p. 19-21; Powers, 1928, p. 1047-1049; Miser, 1934, p. 1007-1009; Harlton, 1938, p. 861-864), who have studied the geology of the Arkansas-Oklahoma area is that the Ouachita deformation occurred in middle Pennsylvanian time (Engel, 1951, p. 243). Therefore, a late-middle Pennsylvanian age seems to be indicated for the quartz crystal deposits.

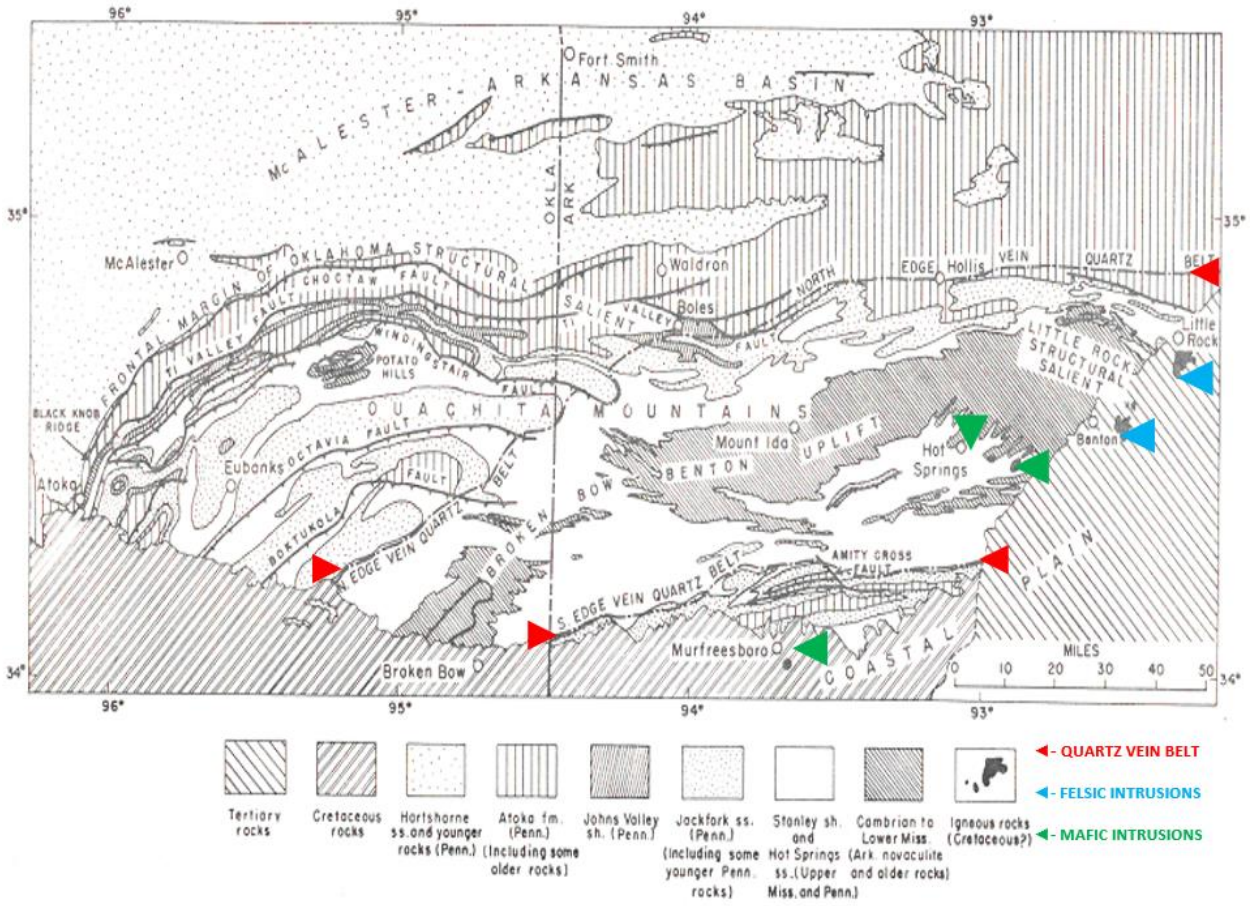

Figure 21. Modified from Hugh D. Miser (1959), showing delineation of quartz belt within the Ouachita Mountains. Felsic (blue) and ultramafic (green) Cretaceous igneous intrusions are also shown.

While estimates of quartz age have been made, the chemical make-up of the elements silicon and oxygen precludes any tangible evidence for accurate age dating. The age estimates of quartz are at best most reliably made from cross-cutting relationships, as quartz formations will be younger than any rock they are found in (Figure 19). Quartz intrusions are an anomaly in the Ouachitas (Figure 21); an anticlinorium produced by the collision of Laurasia and Gondwana, and later separation followed by subduction and formation of a decollement (basal detachment fault) during the Ouachita Orogeny, a middle-Pennsylvanian orogenic event. Quartz belt crystals may be the same age as the tripolite, late Paleozoic, and cut across all Paleozoic strata in the Ouachitas between the two lines shown between the red arrows. Large crystals are found close

to the source of hydrothermal fluids (Miser, 1959). Green and blue arrows are mafic and felsic intrusions, neither of which contain quartz. Alkaline rocks are undersaturated with respect to quartz and contain high levels of potassium (K). Bowen's Reaction Series states that quartz will precipitate if, and only if, silicon and oxygen are left over after all other cation-anion relationships are filled and satisfied.

9.4 Sulphur and Related Minerals

Negative $\delta^{34}S$ values are typical of diagenetic environments where reduced sulphur compounds are formed (Krouse, 1980, Figure 22). Pyrite is the most common reaction product, present in many shales or other organic-rich sedimentary lithologies and formed by bacteria reducing seawater sulfate in marine sediments. Gypsum and its dehydrated polymorph anhydrite are principal constituents of marine evaporates in sedimentary strata and can be major contributors to groundwater sulfate. Gypsum is also common in the soil of arid regions and sabhka environments. Gypsum and anhydrite are not restricted to major evaporite sequences in the geological record; minor sulfate nodules and laminations on bedding planes can occur throughout limestone and dolomite sequences. Further, the dissolution of sulfate minerals increases permeability, and thus, can enhance sulfate concentrations in groundwater (Clark and Fritz, 1997).

The primary controls for the extraction, transportation, and deposition of Pb and Zn under MVT ore forming conditions are related to the redox state and concentration of sulfur species sulfate and hydrogen-sulfide (SO_4 and H_2S). Sulfate is produced in heavier, anoxic conditions. While most MVT ore fluids are believed to have been in equilibrium with carbonate-bearing lithologies limiting pH values greater than ~ 4.5 to 5, lower pH values resulting in more reduced

sulfur and higher metal contents are possible through cooling and change in pH (Leach *et al.*, 2010). Thus, the Ozark MVT deposits formed from sedimentary brines in crystalline basement rocks ascending into carbonate cover rocks in order to precipitate metals in sufficient quantities. Evaporites are generally highly enriched in sulfur. Topography-driven fluid flow is credited as the most robust fluid-drive mechanism for many MVT districts (Garven *et al.*, 1993; Leach *et al.*, 2010). Tectonic setting is not a first-order control on MVT forming processes (Bradley and Leach, 2003). Three versions of the main genetic models by the same author exist for sulfide ore precipitation (Leach *et al.*, 2010): a mixing model (Anderson, 1975), reduced sulfur model (Anderson, 1973), and finally, a sulfate reduction model (Anderson, 1987).

According to Clark and Fritz, (1997): While the sulfate content of modern seawater has a very homogenous and well-defined isotopic composition (Figure 23), that composition has not been constant in the past. Pronounced variations are found in all major evaporite deposits throughout geologic time. These variations were most likely controlled by major inputs or removal of sulfate from oceanic reservoirs during changes in tectonic activity and weathering rates. Further, sulphur isotopes can be used to trace plate tectonic activity. Calcite precipitation also affects the Ca^{2+}/SO_4^{2-}ratio. Groundwaters typically move towards calcite saturation within the soil or along the flow path; dissolution of sulfate in turn forces calcite precipitation according to the common ion effect, resulting in a disproportionate increase in sulfate (SO_4^{2-}).

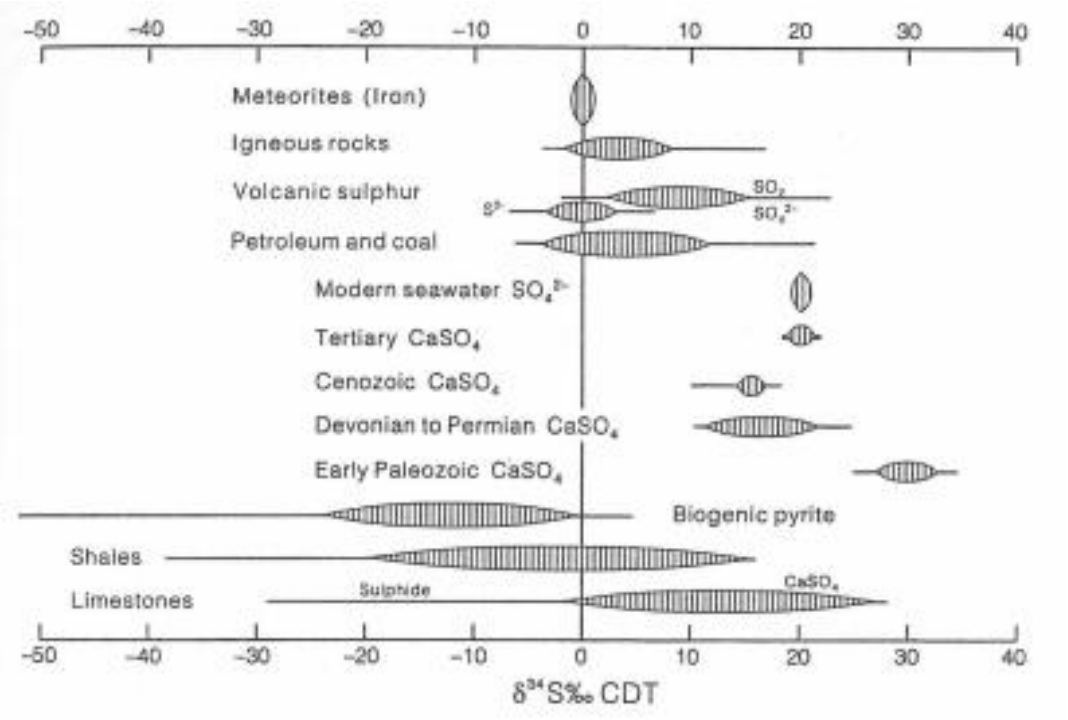

Figure 22. Ranges in contents of $\delta^{34}S$ Sulphur and Sulphur compounds in different materials and environments (Clark and Fritz, 1997, p. 139).

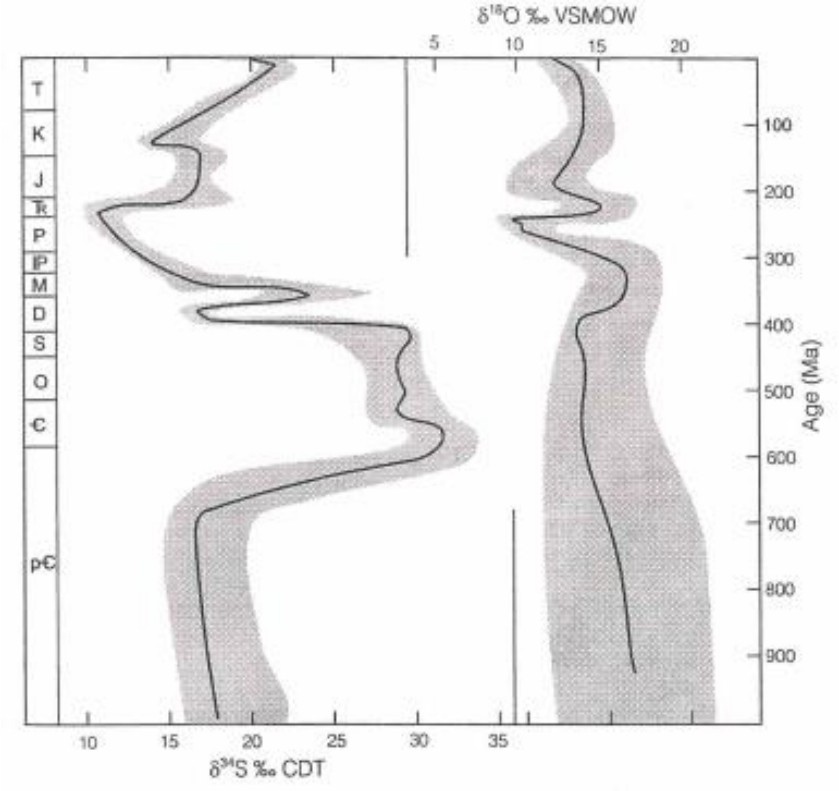

Figure 23. The ^{34}S and ^{18}O composition of marine sulfate through geologic time (Clark and Fritz, 1997, p. 141).

Quartz found throughout the Ouachitas and northward onto the Ozark Dome, although in lesser amounts, was driven by the Ouachita Orogeny, and likely originated from multiple igneous intrusions during the Cretaceous. These intrusions would have conducted the heat needed to produce high-silica groundwaters, and precipitate associated hydrothermal minerals, as these sulfide-rich basinal brines flowed northward along bedding planes, faults, and micro-fractures. A combination of shallowing Pre-Cambrian basement topography along with surficial cooling may explain the emplacement of ores where they are presently located within the Tri-State region and elsewhere. The formation temperature of MVTs is between 75˚ to 200˚ C.

Both calcite and quartz can form when two solutions of different temperatures are mixed at constant pressure. Quartz deposition should predominate over calcite above 300 degrees Celsius while calcite should predominate at temperatures below 150 degrees C, when pressure and temperature changes in rising solutions cause precipitation. In addition, replacement of either quartz by calcite or calcite by quartz can result from transport of $CaCO_3$ and SiO_2 along thermal gradients (Sharp, 1965). Calcite is the most common mineral found in hydrothermal caves in carbonate rocks. Quartz, barite, fluorite and sulfides are also regularly reported within deep-seated hydrothermal caves, which cover a range of depths from roughly 0.3 to 4.0 km. This brief list does not consider ore-related hydrothermal karst in which the list of associated minerals can be quite lengthy (Dublyansky, 2019).

9.5 Lead Isotopes and Potential Source Contributions

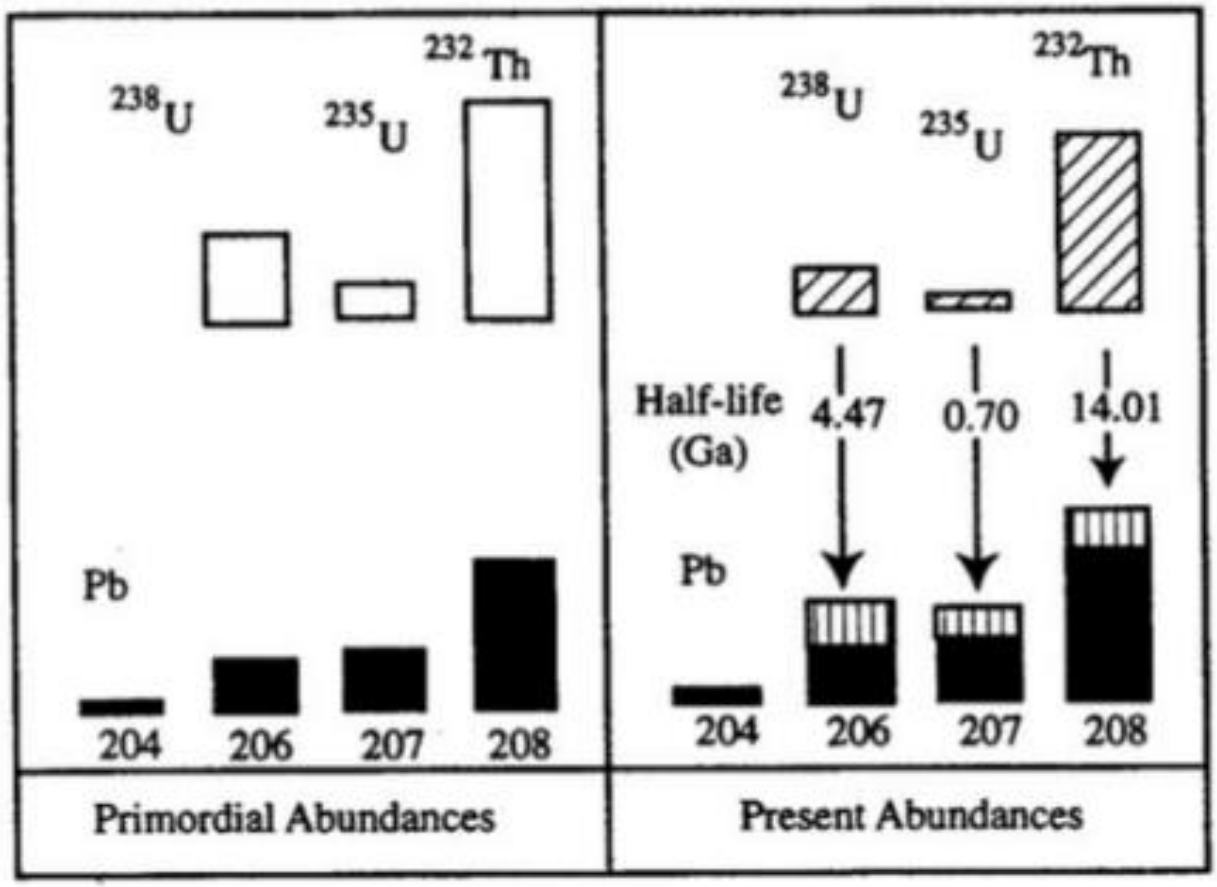

Figure 24. Relative primeval and present-day abundance of the isotopes of uranium (U), thorium (Th), and lead (Pb) showing half-lives in billions of years (Ga) (From Tosdal *et al.*, 1999).

As explained by Cannon and Pierce, (1969), "the isotopic composition of lead (Figure 24) varies in lead ores in significant ways. The least abundant isotope, Pb^{204}, is inherited from the original or primeval lead of the solar system; whereas the three most abundant isotopes, Pb^{208}, Pb^{207}, and Pb^{206}, are partly original, partly radiogenic. These three continue to increase in abundance because they are stable end-products of the radioactive decay of uranium and thorium." Figure 24 shows how the average composition of lead in earth materials may have changed during earth history by decay of U^{238} to Pb^{206}, U^{235} to Pb^{207}, and Th^{232} to Pb^{208}. Thorium is insoluble, while Uranium dissociates into uranyl ions (U^{6+}) in aqueous solutions (Tosdal *et al.*, 1999). Further, this idealized model implies that about two-thirds of earth-lead is original, and about one-third is radiogenic. Such isotopic evolution of lead is the primary cause of the variation of isotopic composition that we find in lead of ore deposits.

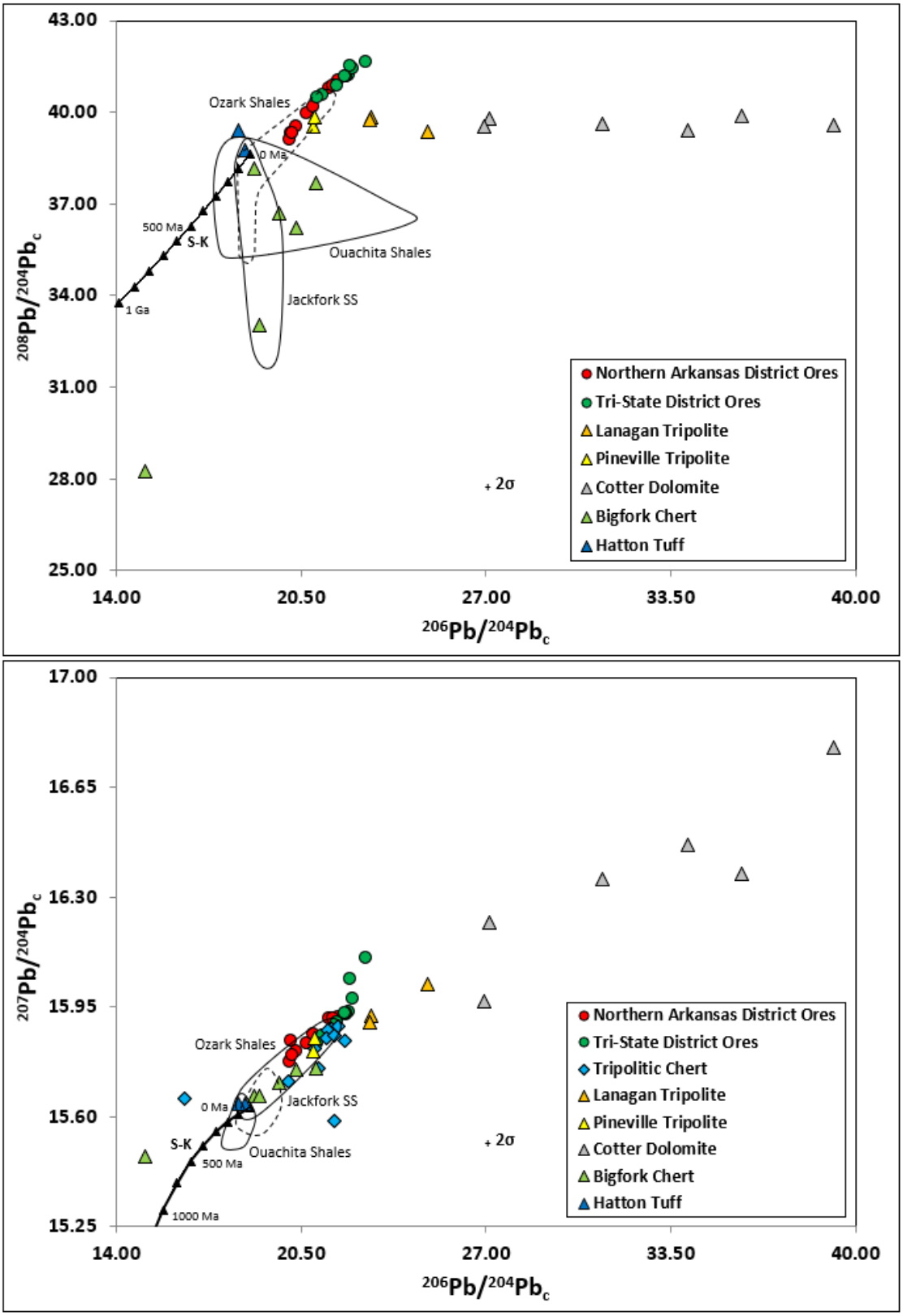

Figure 25. Age corrected Pb isotope data, corrected to 250 million years. Data plotted in conjunction with Ouachita and Ozark clastics Pb isotope values analyzed by Bottoms *et al.*, 2019 and Simbo *et al.*, 2019. Also plotted is Stacey and Kramers (1975) model for orogene deposits.

The values plotted for the ores and formations sampled within this study have produced a vast range of Pb isotope values. Clumping in a field or region signifies source, while a linear distribution indicates that lead is emplaced from different sources. Genetically related components plot along very tight and linear regression-line trends (Cains, 2019). Exploration samples that plot on mantle mixing lines and have high $^{206}Pb/^{204}Pb$ ratios are considered to hold the best chance of representing a large metallogenic event (Carr, 1995). The spatial distribution of Pb isotope compositions found within this and previous studies indicates that there were at least two pulses of mineralizing solutions involved in the precipitation of the Tri-State and Northern Arkansas MVT ores. The Cotter Dolomite greatly extends this MVT mixing trend and causes it to turn from a broad and principally linear trend to that of a linear two end-member mixing model. As explained by Kesler *et al.*, 1994b, Pb isotope values associated with sphalerite, fluorite, barite and sparry dolomite in Mississippi Valley-type deposits of the southern Appalachians fall into four distinct isotopic groups, each characteristic of a single district. Most sphalerite signatures form two small clusters, whereas barite, fluorite, and sparry dolomite compositions are notably more scattered. These Pb isotope signatures reflect the distribution of the deposits, which are hosted by two main paleoaquifers; Arkansas has 14 different aquifers within its geographical boundaries. As stated by Simbo *et al.*, 2019, "Of particular interest is to identify the source rock that contributed the more radiogenic component of Pb to the MVT ores".

The enriched Pb isotopic compositions have been interpreted as representing a shallow crustal source likely resulting from heated basinal saline brines flowing through paleoaquifers (Anderson, 1991; Kesler, 1994b), such as the tripolitic chert of the basal Upper Boone. Pre-Cambrian basement as well as carbonate cements in sandstone aquifers are recognized as likely sources of Pb (Heyl *et al.*, 1974), while other research designates shales as a likely low-sulfide

source of ore Pb (Bottoms *et al.*, 2019). According to Simbo *et al.*, (2019), his thorogenic diagram trends indicate that many of the previous samples could not have supplied lead to the ores. However, the uranogenic plots depict sandstone members of the upper and middle Jackfork Sandstone and the lowermost section of the Chattanooga Shale, as the best candidates for contribution of less-radiogenic Pb to the ores.

The high U/Th values shown by the Cotter Dolomite seem to suggest an input of fluorite lead and other minerals into the mixing dynamic of hydrothermal MVT ore brines. This is likely a result of a variety of hydrothermal interaction processes of the ore fluids with wall rock within the dolomite. From Kesler *et al*., 1994a; another possible source for this type of lead is shale containing organic matter that would concentrate uranium. Further, the Devonian Chattanooga Shale phosphorite displays a high Pb/Pb ratio similar to that of the radiogenic fluorites as shown in Figure 28. Phosphorite contains 20 to 50 percent CaO and 1 to 3 percent F, (Howard and Hough, 1979), making it a plausible source for fluorite formation. From Wedepohl (1969), phosphorite around the world is reported to have average Th/U ratios of less than 0.1. Phosphorite from Tennessee contains as much as 3.8 % F (Cathcart, 1989).

Fluorite, also called fluorspar, is a common halide mineral with the chemical formula CaF_2 and is the principal fluorine mineral. Although typically quite pure, as much as 20 percent yttrium or cerium may replace calcium. Mostly occurring as a glassy, multi-colored, vein mineral, fluorite is often associated with lead and silver ores in low temperature hydrothermal deposits. Fluorite is less often an accessory mineral in pegmatites and granites, as well as in hot-spring deposits. Fluorite primarily occurs as a pore-filling mineral in carbonate rocks, as is the case of the doubly terminated euhedral quartz druse found within the tripolitic chert (Figure 3, Minor, 2013). When fluorite occurs as a cavity fill in carbonate rocks, it can usually be

associated with calcite, dolomite, anhydrite, gypsum and sulfur. In hydrothermal vein deposits, fluorite may be found with calcite, dolomite, barite, galena, sphalerite, as well as silver ores.

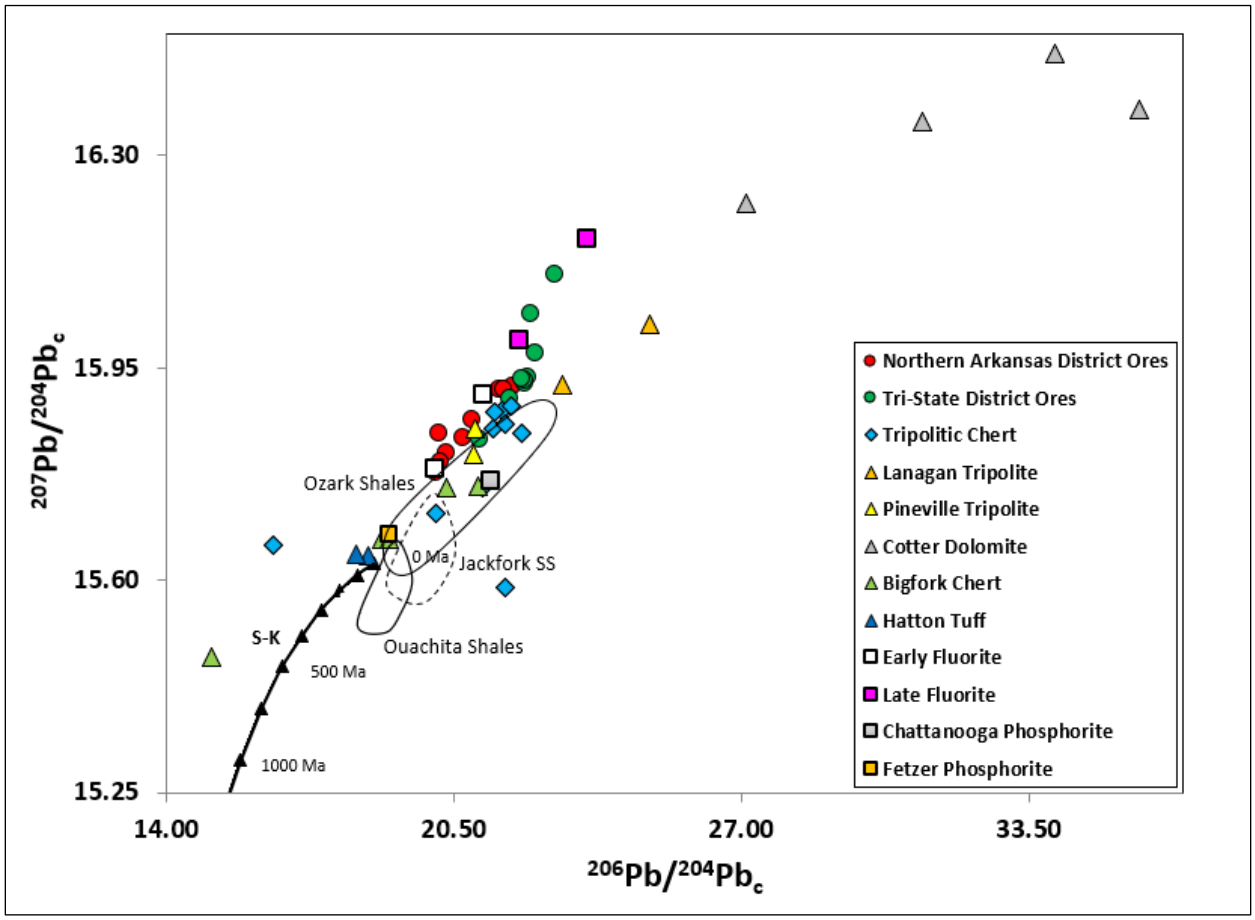

Figure 26. Age-corrected Pb isotope data from this study and other previous work on Ouachita and Ozark clastics Pb isotope values analyzed by Bottoms *et al.*, (2019) and Simbo *et al.*, (2019) and Tripolitic Chert by McKim, (2018). Also plotted is Stacey and Kramers (1975) model for orogene deposits. Note fluorite and phosphorite values compiled by Kesler *et al.*, 1994a.

The formation of precipitated fluorite deposits is either a result of temperature (cooling) and pressure changes along the hydrothermal fluid flow-path, fluid mixing, or as a product of the metasomatic fluid interaction with host rocks. Among these processes, those which increase the pH of initially rather acidic (pH $\leq$ 3) hydrothermal fluids are likely to be principally important. Mixing can produce hydrothermal solutions that vary between either unsaturation or supersaturation with respect to fluorite crystallization. The most influential parameters are the

temperature, salinity, calcium, and fluoride concentrations of fluids before mixing (Richardson and Holland, 1979). Based on observations from southeastern Missouri and northeastern Arkansas, stylolites and fractures acted as fluid-flow conduits throughout the subsurface (Montañez, 1992), and mineralization accompanied deformation events as recorded in those microstructures as well as evidence of fluid flow control, in addition to intergranular flow through pore space (Diehl *et al.*, 1992). A decrease in the temperature in the flow direction is the most plausible mechanism of fluorite precipitation in Mississippi Valley fluorite deposits and related flow paths, such as faults and fractures (Richardson and Holland, 1979). Where present in the Cambrian Mt. Simon Sandstone aquifer of Illinois and Indiana, anhydrite, barite and fluorite occur as poikilotopic cements all formed as authigenic phases postdating quartz precipitation but preceding formation of non-ferroan dolomite. Figure 27 below from Fishman, 1997 shows the relative age relationships of several minerals found within the Cambrian Mt. Simon Sandstone; which appear to correlate with the accepted formation age of the Tri-State MVT ore district (250 Ma). This is evidenced by the partial to extensive dissolution and/or replacement of all three minerals by dolomite. The scarcity of these cements make their former regional extent difficult to ascertain (Fishman, 1997). Further, in the Illinois-Kentucky Fluorspar District, an increasing abundance of radiogenic isotopes is found to the southeast (Heyl *et al.*, 1966). Plausible evidence appears to exist for contributing fluids from formations in this region and further South (Missouri and Tennessee) mixing to precipitate the MVT ores of the Tri-State and Northern Arkansas ore districts. The Cotter Dolomite sampled in this study is also highly radiogenic as shown by the trends in Figures 16, 25, and 26.

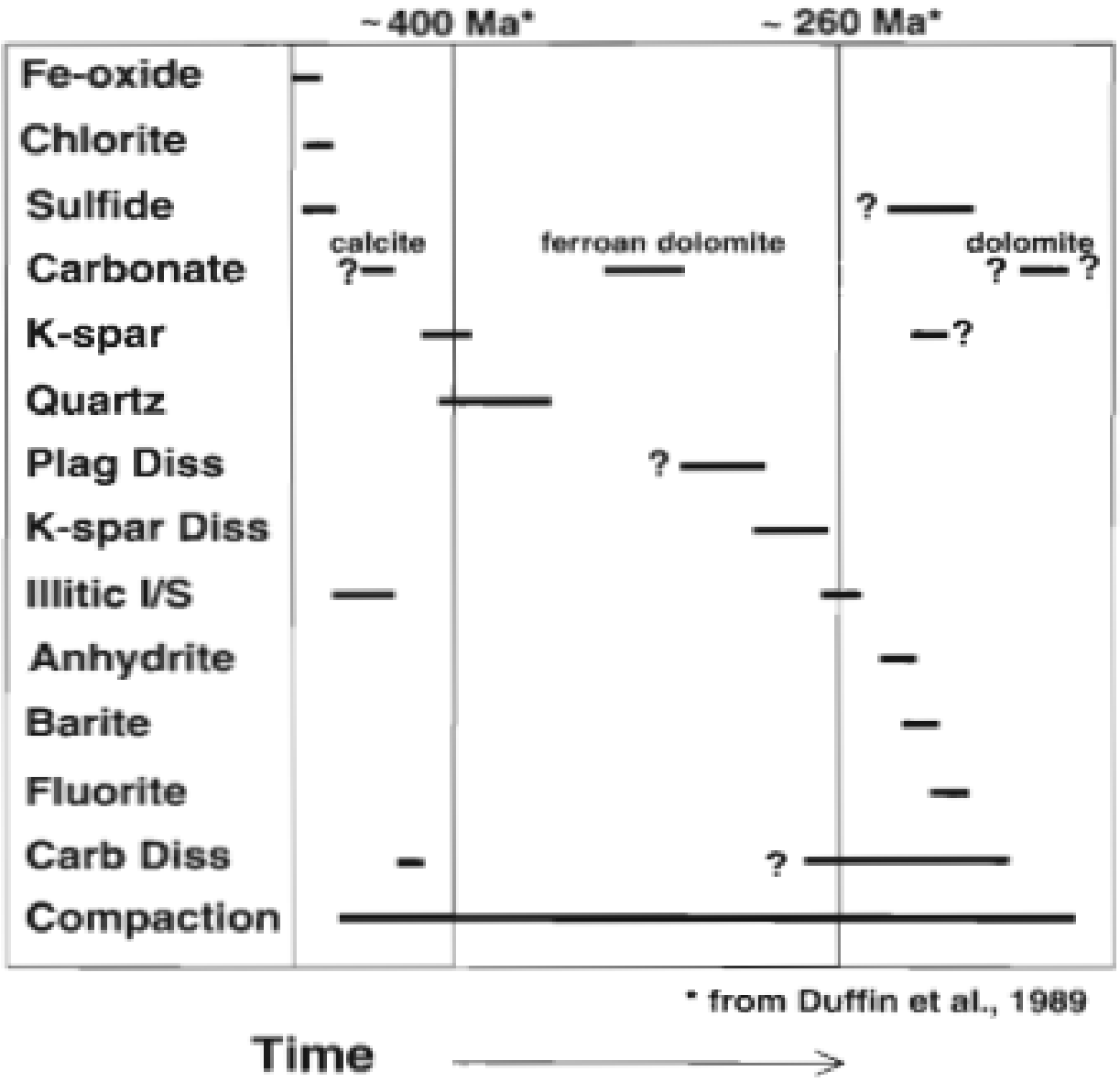

Figure 27. Diagram showing the nature and relative timing of alterations in the Cambrian Mt. Simon Sandstone aquifer of Illinois and Indiana. Diagenetic events are largely precipitation of the mineral mentioned unless otherwise noted (Plag - plagioclase, Diss - dissolution). Dates on formation of authigenic K-spar and Illite/Smectite (I/S) clays are from data published in Duffin *et al.*, 1989. From Fishman, 1997.

9.6 Dolomite and Proximal Aquifers

As stated by Lumsden and Caudle, 2001, the Lower Ordovician Upper Knox Dolomite is similar in mineralogy, texture and geochemistry over an area stretching from the Southern Appalachians, to the Ozarks and Texas-Oklahoma. Previous studies have concluded that there are at least three generations of dolomite in the Upper Knox, and multiple episodes of exposure to the atmosphere related to fluctuation in sea level are the dominant mechanisms of dolomite formation rather than burial or a single event of massive karst formation. Mass-balance calculations propose that a volume of water equal to that of the modern oceans would be required to dolomitize and cement the entire Knox. Further, vug, fracture, and cavity-fill dolomite, chert, and calcite precipitated from fluids migrating through the Upper Knox after the formation of replacive dolomite (Lumsden and Caudle, 2001).

Late diagenetic dolomites of the Lower Ordovician Knox Group in the southern Appalachian Basin record the spatial and temporal evolution of large-scale subsurface fluid migration systems that developed in response to different burial and tectonic stages of late Paleozoic Alleghenian tectonism in the southern Appalachian basin (Kesler *et al.*, 1994b; Montañez, 1989; Montañez, 1994). Zoned dolomite cements in tectonic fractures and breccias combined with fluid inclusion data indicate that the late diagenetic dolomites were precipitated from hot, saline basinal brines that underwent extensive fluid-rock interaction with clastic lithologies. Non-porous to sucrosic, late diagenetic dolomites exhibit porosities and permeabilities significantly greater than those of early diagenetic replacement dolomites and host limestones (Montañez, 1994). Further, late diagenetic dolomitization of the Knox was related to secondary porosity development, hydrocarbon migration, and local MVT mineralization. "Late"

dolomite cements occur in secondary solution voids and fractures ‘paragenetically’ associated with authigenic pyrite, fluorite, calcite, quartz, anhydrite and MVT minerals (Montañez, 1994).

Marine carbonates of the Burlington-Keokuk Fm. (Mississippian) of the midcontinent region have been subject to major episodes of regionally extensive (100,000 km²) dolomitization. Various previous studies of Burlington-Keokuk dolostones outline a diagenetic history in which lime mud was pervasively dolomitized by a seawater-dominated fluid. Dolomite geochemistry methods indicate markedly different sources of diagenetic fluid constituents for the two major dolomite generations (Banner, 1986, 1988b). Dolomite I is constrained to be of Mississippian age, while Dolomite II and II' may have formed as late as Pennsylvanian time. Based on petrographic constraints, the major episodes of dolomitization probably occurred prior to Pennsylvanian time. An age of 342 Ma was used to calculate the εNd (T) for these dolostones (Banner, 1988a).

Fluorite-lead plots far into the high U/Th region of both thorogenic and uranogenic diagrams, as shown by Figure 28 and possibly the Cotter Dolomite in this study.

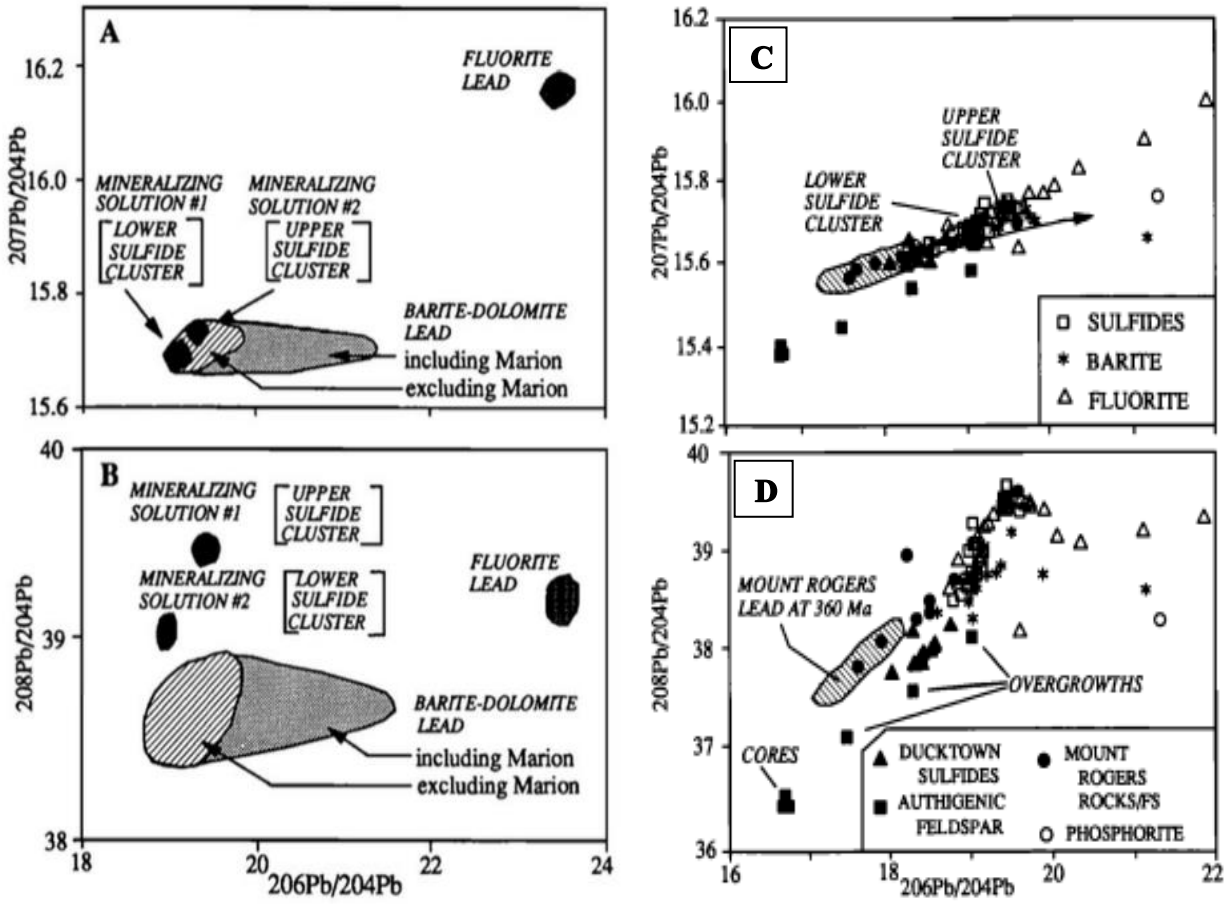

Figure 28. Approximate ranges of elemental compositional groups that account for Pb isotope compositions of MVT deposits in the southern Appalachians (Kesler *et al.*, 1994a: from LeHuray, 1982, 1984; Aleinikoff *et al.*, 1993). Late Cretaceous and closely age-related plutonic rock signatures also plot high on U/Th end of the thorogenic (^{235}U) scale (Kesler, 1994a, modified figures (A, B) from Bouse, 1995), as do (C, D) sulfides and associated minerals in peripheral deposits (modified Figure 9B, Bouse, 1999), largely attributed to a dynamic of increasing contribution of Proterozoic Pb from country rocks.

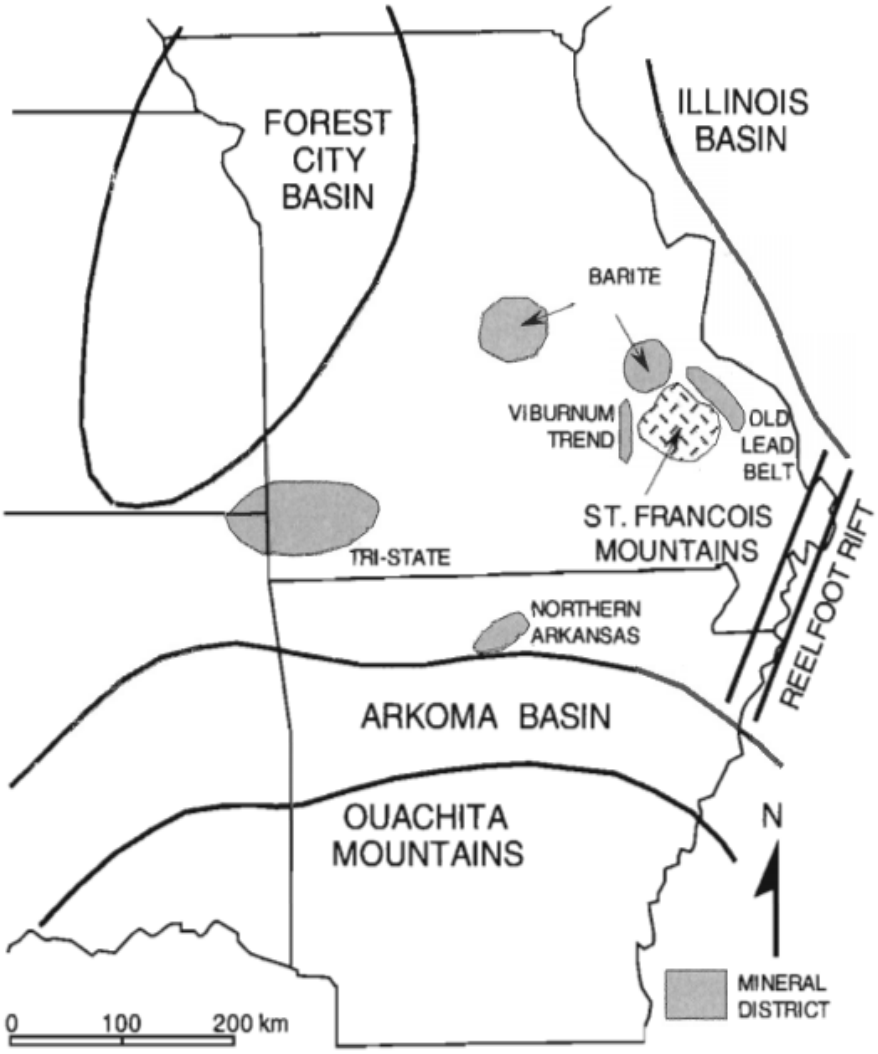

Figure 29. Map of major tectonic features and their relationship of MVT districts and surrounding sedimentary basins (He, Z. *et al.,* 1997).

9.7 Precipitation of Sulfide Minerals

As explained by Anderson (1975), precipitation of sulfide minerals results from the mixing of two end-member fluids, a metal rich-sulfide poor fluid and a metal poor-sulfide rich fluid. Many of the sample values are far more radiogenic than the average crustal lead growth curve for the upper crust, lower crust, and orogene compositions determined by Stacey and Kramers (1975). The average crustal lead growth curve is a compilation of geochemical Pb data

relating mountain-building events through time, and is incorporated into the Pb isotope plots in this study (Figures 16, 25, and 26). From Cains, 2019, most upper crust rocks plot around 0 Ma. Therefore, these sample plots appear to confirm an upper crustal source of Pb for the Tri-State and Northern Arkansas MVTs, in accord with their close association with sedimentary basins (Leach *et al.*, 2010). High gamma μ ($^{238}U/^{204}Pb$) values also indicate a supracrustal origin for Pb (Goldhaber *et al.*, 1995).

While all three aquifer systems are composed of dolostone, limestone, and sandstone, the Western Interior Plains aquifer system is briny compared to the Ozark and St. Francois aquifers. The Ozark and St. Francois aquifers are composed of several dolomite and other potential source and/or transport formations, as shown by Figure 30 from He, Z. *et al.*, 1997. The combined Ozark and St. Francois aquifers of the Ozark Plateaus aquifer system are considered to be equivalent to the unnamed lower aquifer units of the Western Interior Plains aquifer system (Figure 31, Pope *et al.*, 2009). The Ozark confining unit and the Springfield Plateau aquifer of the Ozark Plateaus aquifer system are equivalent to the confining unit and upper aquifer unit (both unnamed) of the Western Interior Plains aquifer system, respectively. Regional groundwater movement in the aquifer system is southeastward to eastward (Miller and Appel, 1997). Further, the Western Interior Plains aquifer system extends westward into Kansas and Oklahoma and groundwater flow is generally toward the east (Figure 31, Pope *et al.*, 2009). Other potential source contributions may also be found in large basins northwest of the Ozark Uplift, in the Forest City Basin (Eastern Kansas, Western Missouri), to the northeast in the Illinois Basin (Eastern Missouri) (Wenz *et al.*, 2012), and towards the Reelfoot Rift to the southeast as shown by Figures 29, 32, and 33 (He, Z. *et al.*, 1997; Diehl *et al.*, 1992; Braile, 1986). Furthermore, a lack of temporal overlap between gangue and metal sulfide deposition

indicates that different fluid contributions to gangue and sulfide mineral deposition within discrete intervals is possible and likely (Appold *et al.*, 2004).

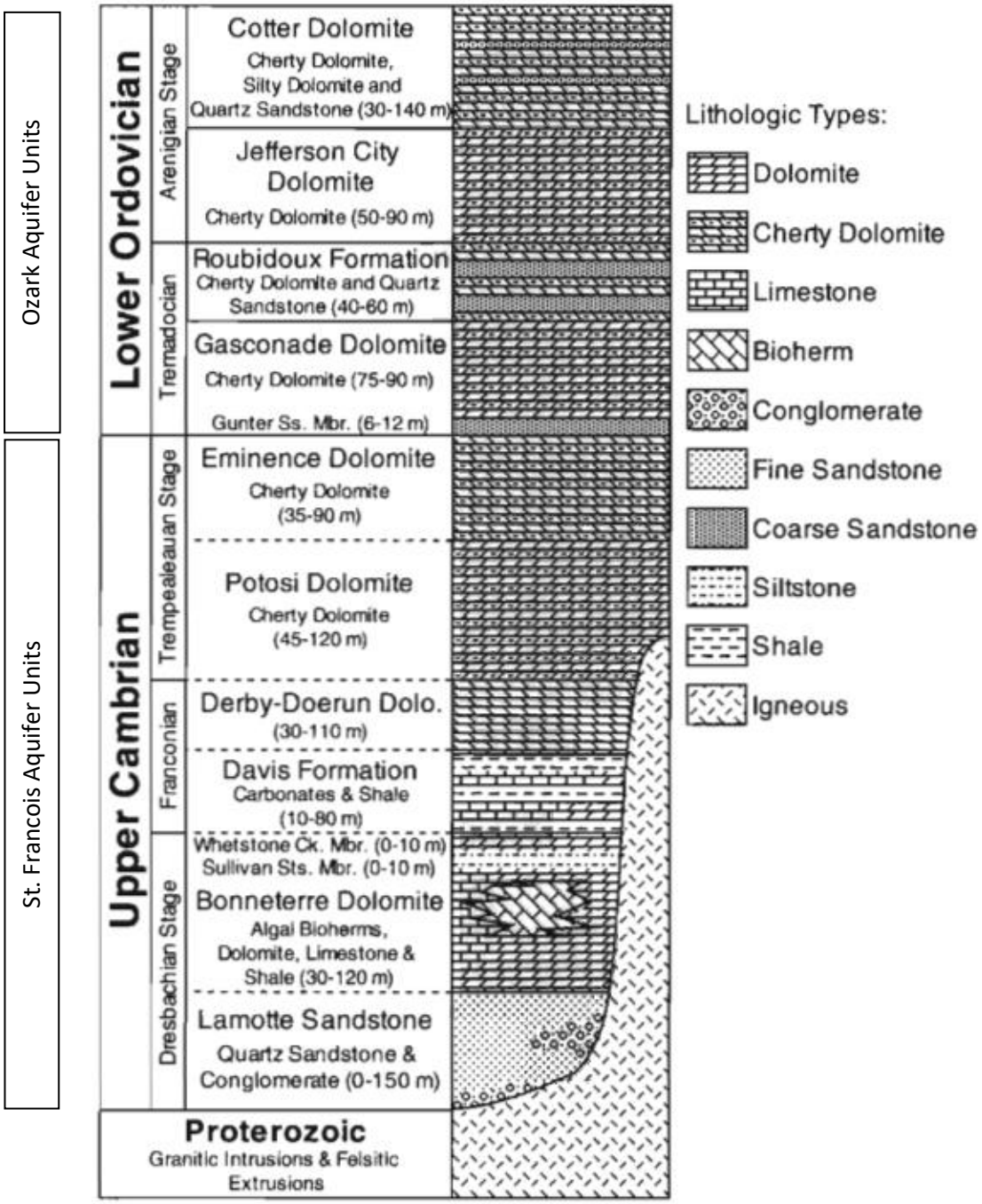

Figure 30. Cambro-Ordovician section in southern Missouri. Lower Ordovician strata represent the Ozark Aquifer units, with the Upper Cambrian St. Francois aquifer below. The Eminence and Potosi Dolomites are the most permeable, while the Derby-Doerun and Davis Formations compose the St. Francois Confining Unit. Thicknesses for units are approximate ranges measured in this study by He, Z. *et al.*, 1997.

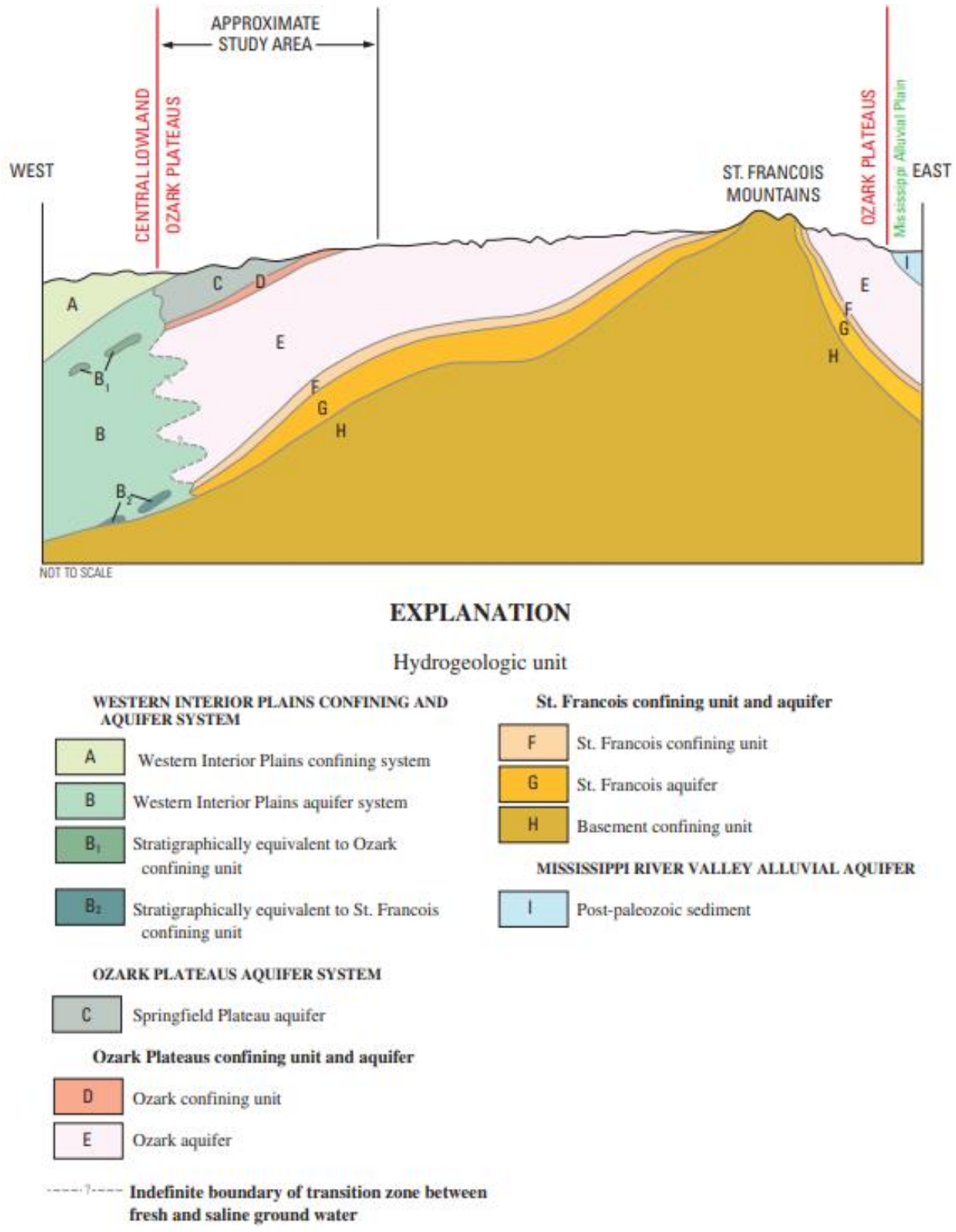

Figure 31. Generalized geohydrologic section showing Ozark Plateaus aquifer system and adjacent hydrologic units (from Imes and Emmett, 1994). Approximate study area represents region including Tri-State MVT mining district (Pope *et al.*, 2009).

9.8 New Madrid Seismic Zone (NMSZ) and Reelfoot Rift

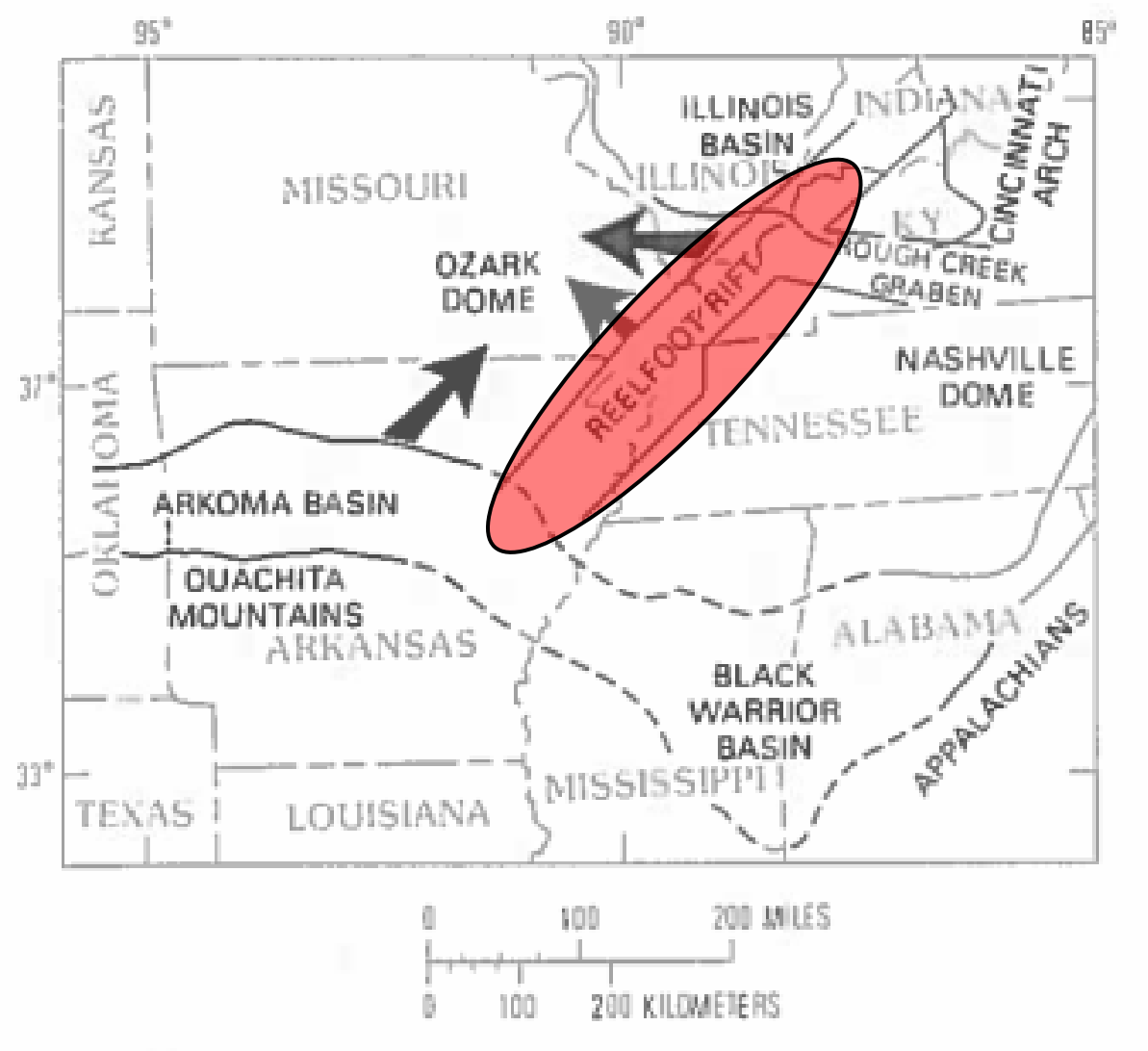

Figure 32. The Appalachian and Ouachita fold belts may have created a hydraulic head through topographic relief in the Late Pennsylvanian to early Permian that influenced the flow of hot brines north and northwest (bold arrows) to form the Mississippi Valley-type deposits (Leach and Rowan, 1986). Dates for mineralization in the lead-zinc districts overlap with the timing of Ouachita tectonism. Heavy lines are province boundaries, while dashed lines indicate projections of boundaries underneath Mississippi Embayment (Diehl *et al.*, 1992). The New Madrid Seismic Zone (NMSZ) is indicated by outlined red oval.

The New Madrid Seismic Zone (NMSZ), shown by the red oval above in Figure 32 and below in Figure 33, is a major seismic region driven by compressional and tensional stress (Braile *et al.*, 1984), produced by motion of the North American plate. The NMSZ is the most active east of the Rockies in the contiguous United States, experiencing an average of

approximately 200 earthquakes (greater than M1.5) per year (Williams, 2011). The NMSZ is a 150-mile (240 km) long fault system oriented N24°E (Guccione, 2005). The NMSZ is located southwest of the Wabash Valley seismic zone (Pratt, 2012).

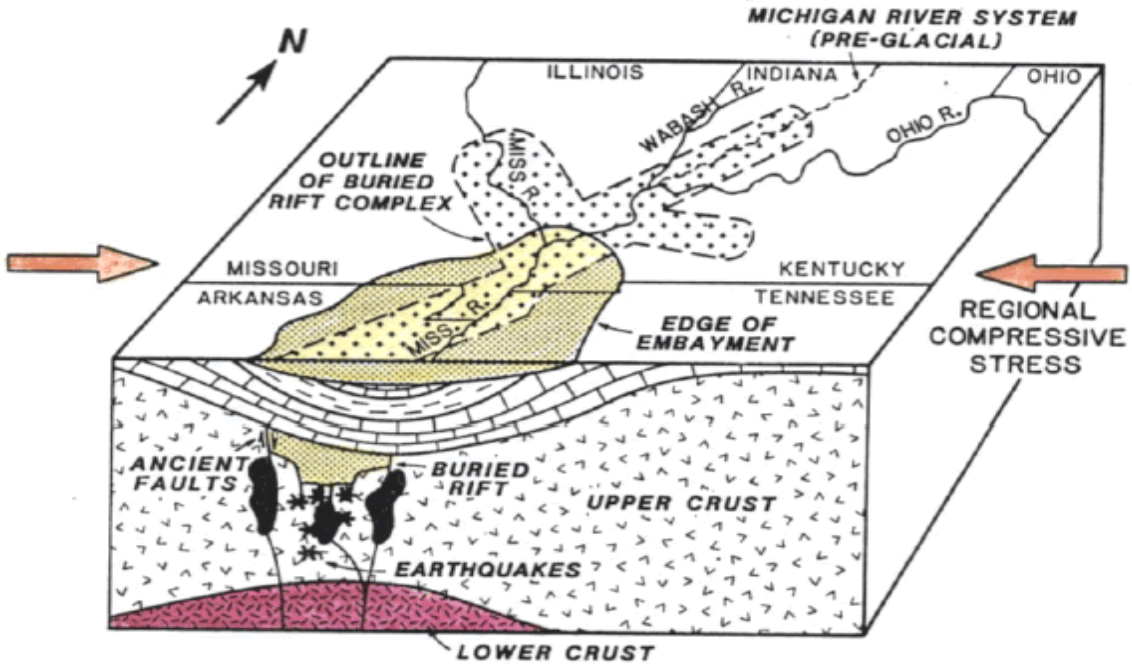

Figure 33. Block diagram illustrating the present configuration of the buried New Madrid Rift Complex. The structurally controlled rivers, Paleozoic rocks in cratonic sedimentary basins, and the Mississippi Embayment, all associated with the buried rift complex, are also shown. Dark areas indicate intrusions near the edge of the buried rift. An uplifted and possibly anomalously dense lower crust is suggested as the cause of the linear positive gravity anomaly associated with the upper Mississippi Embayment (Braile, 1986).

Seismicity in the New Madrid seismic zone, shown above in Figure 33, forms four distinct arms, three of which radiate outward from the town of New Madrid, Missouri (Pratt, 2012). The contiguous northern and southern dextral strike-slip New Madrid faults (Guccione, 2005) that make up the New Madrid seismic zone are seated in the central arm and subterranean geological feature known as the Reelfoot Rift. This Reelfoot thrust fault extends 60 km south from New Madrid, Missouri, with hypocenters and focal mechanisms defining fault planes

dipping 32° – 55° to the southwest (Pratt, 2012). Isostatic rebound caused by de-glaciation of North America is also proposed as a source of the intraplate seismicity occurring in the New Madrid seismic zone (Grollimund *et al.*, 2001). Downwelling mantle flow viscously coupled to the ancient Farallon slab, which actively subducted under the western margin of North America during the Cretaceous, may serve as the driving mechanism for these unique mid-plate events (Forte *et al.*, 2007). The Reelfoot Rift may have an influence on the formation of the MVTs (Figure 32) as it is believed to be of 750 my age, originating during the break-up of supercontinent Rodinia in the Neoproterozoic Era (Diehl *et al.*, 1992). Similarly, the host rocks of the Central Tennessee MVT district, and the Tri-State MVT ore district are Paleozoic carbonates (Ordovician to Lower Mississippian), both of which support epigenetic mineralization of the ores (Moyers, 2015).

Furthermore, as stated by Clendenin and Duane (1990),

"Field relations confirm that a tectonic link exists between the Appalachian-Ouachita Orogeny and the Mississippi Valley-type Pb-Zn deposits of the Ozarks. Fluids were expelled from both the Reelfoot rift and the Arkoma basin into structurally controlled hydrologic domains. These two source areas fed different fluids into at least six domains and account for regional differences in the ore deposits. Movement of fluids out of the Reelfoot rift also indicates that a foreland basin is not a prerequisite for the migration of fluids. Seismic pumping and distal fluid focusing along faults appears to be the most plausible mechanism to move hot, reactive fluids through a carbonate terrane to a site of ore deposition."

9.9 Authigenic Feldspars

Lead isotope analyses of widespread authigenic potassium feldspar, or mixed-layer illite-smectite clays, produced by potassic diagenesis in the Lamotte Sandstone of southeastern Missouri were conducted by Aleinikoff *et al.*, 1993. As stated by Aleinikoff *et al.*, this study indicates that the potassium feldspar formed from fluids that carried lead closely related to the $^{208}Pb/^{204}Pb$ of one end-member of the lead that formed main-stage (cube-octohedral) mineralization of ores of the Viburnum Trend of southeastern Missouri. Trace element studies indicate that ~2 ppm Pb can easily be removed from the Lamotte Sandstone, suggesting a source area for the old lead belt in southeast Missouri possibly covering 11,000 square miles with an assumed thickness of 200 feet (Doe and Delevaux, 1972). This similarity is important because the $^{208}Pb/^{204}Pb$ ratios of the Viburnum Trend of southeastern Missouri are unique compared to all other MVT ores of the southern mid-continent (Diehl and Goldhaber, 1989).

Similarly, the Cotter Dolomite Pb isotope values in this study remain highly radiogenic in comparison to the recorded values of other formations in this study. Moreover, in comparison with other global SEDEX (sedimentary exhalative) sediment-hosted Pb-Zn deposits via a compilation of Pb isotope data by Leach and others, 2005, the MVT deposits in the Midcontinent region of the United States contain very high abundances of radiogenic Pb. Basement-derived lead has been interpreted as a significant component of the Tri-State district as well as many others, related to their close association with sedimentary basins (Leach *et al.*, 2010). In addition, the propensity of potassium feldspar to incorporate Pb into its crystal structure, while excluding U and Th, allows it to record Pb isotopic compositions that are effectively time invariant (Patterson and Tatsumoto, 1964).

Alfred Otto Carl Neir, a physics professor at the University of Minnesota, (1938) designated J-type or “Joplin type” lead ores (Figure 34) that are highly radiogenic galena discovered in three samples from Joplin, Missouri. “*J-leads*” are considered exceptional because of their enriched abundances of radiogenic isotopes in contrast to common or *ordinary lead* and found in the Tri-State and Southeast Missouri districts (Moyers *et al.*, 2015). These Pb deposits are exceptionally enriched in 206, 207, and 208 Pb (Cannon and Pierce, 1969) and seem to imply “impossible” Pb ratios, since they do not follow hypothetical models for lead evolution.

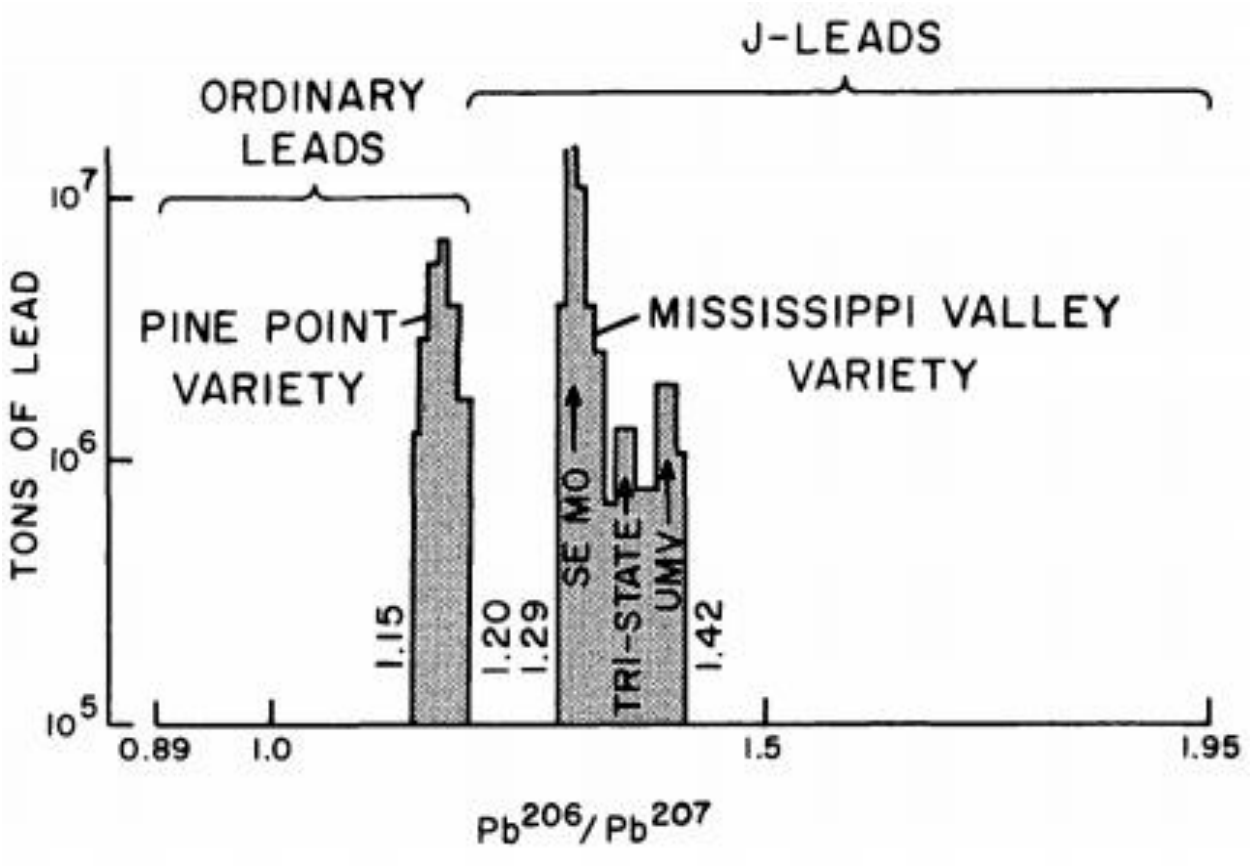

Figure 34. Isotopic composition versus tons of lead produced in worldwide Phanerozoic Stratiform lead-zinc deposits. SE MO: Southeast Missouri district. Tri-State: Tri-State mining region (Mo.-Kans.-Okla.). UMV: Upper Mississippi Valley district (Wis.-Ill.-Iowa). (Cannon and Pierce, 1969, p. G9).

Another type of exceptional lead with some similarity to J-lead comprises five percent of the analyses. These are designated "U-leads", because they are abnormally enriched in the decay

products of uranium, ^{206}Pb and ^{207}Pb. Figure 34 with Figure 2 (not shown) from Cannon and Pierce (1969), shows the gross relationships between the field of U-leads, the field of J-leads, and, within the smaller triangle, the field of ordinary leads. The analyses plotted within the U-lead field by Cannon and Pierce, 1969 have unique significance for uranium exploration, because they represent analyses of galenas from uranium ore deposits.

Pb isotopes yield valuable insights into the origin of Pb within a sample, typically allowing for reliable fingerprinting of their source (Longman *et al.*, 2018). Traditionally, interpretation of Pb isotopic ratios is performed through 3-isotope or 4-isotope plots and comparing the location of the sink mixture data (archived isotope signals recorded) to known source isotopic signatures. Model-Pb ages in SEDEX deposits that are generally older than their host rock ages. In contrast, Mississippi Valley-type model ages show little or no correlation with mineralization age determinations. Some MVT deposits express future model ages, while others suggest models significantly older than their host rocks (Leach *et al.*, 2010). While these approaches allow for identification of general source inputs, such as anthropogenic or lithogenic Pb, these models are limited to n+1 sources. Likely oversimplification, with only limited conclusions possible, results from these approaches due to the complexity of Pb inputs, particularly in an anthropogenically polluted world. While these models may be useful in a general overview, Bayesian mixing models help quantitatively assess source proportions and 'fingerprint' analyzed Pb in isotopic mixtures (Longman *et al.*, 2018).

10. CONCLUSIONS

A broad and linear two end-member mixing trend was produced when plotting uranogenic MVT ore age-corrected (250 Ma) Cotter Dolomite values in this study against Christophe Simbo's plots of whole rock values of Ouachita shales and the Jackfork Sandstone. These age-corrected isotope plots show a genetically related trend among the formations sampled within the Ouachita and Ozarks Mountains and associated Tri-State MVT ores. The Cotter Dolomite and Lanagan and Pineville Tripolites present an upper end-member of the Ozark MVT mixing trend.

High light Pb (^{204}Pb) isotope values found within the Cotter Formation may be attributed to a large amount of volcanic ash accumulating in a short period of time; Ordovician formations also accumulated in a short period of geologic time. Two ashfalls within close proximity to the study area are known as the Hatton and Beavers Bend Tuffs. This light lead signature may be credited to these two periods of pyroclastic ashfall preserved within the Stanley Formation of the Ouachita Basin or from other, more distant sources. Two samples of the Hatton Tuff were analyzed for this study and yielded 208/207/206 Pb isotope values of (HT 4 (J 22): 39.112430, 15.65551, 19.03556; HT 5 (J 23): 39.979120, 15.69791, and 19.53898), respectively.

The elemental concentrations shown in Figure 15 appear to support input from a volcanic sediment source among formations within the Ouachita Mountains as well as the tripolitic chert, evidenced by related trends of the Bigfork Chert, Hatton Tuff, and tripolitic chert. A positive shift of Nd in these formations may also indicate a volcanic contribution of Nd. A negative Ce anomaly coupled with a positive Y anomaly is a signature of seawater, as seen in the Cotter Dolomite and also found in the Boone limestone, which may indicate that they retain seawater signatures from the time of their deposition (Cains, 2019).

Hydrothermal fluids produced by the Ouachita Orogeny interacted with effected Phanerozoic carbonate and clastic formations as they moved northward to sites of deposition. Pb isotope analyses from this study indicate that some portion of the lead emplaced within the MVT ore deposits of the Tri-State District may have originated within the tripolitic chert of the basal Upper Boone. It is difficult to ascertain whether the lead in the tripolite was original or emplaced from hydrothermal fluids, as the measured Pb values reflect original signatures with overprinting by diagenetic processes. The occurrence of Pb within the tripolitic chert is an anomaly and additional study of the interval is needed to explain its presence (McKim, 2018). The tripolitic chert samples from Pineville and Lanagan, Missouri roadcuts analyzed in this study confirm a Pb isotope enrichment pattern as hydrothermal fluids responsible for mineralization moved north through the Ozark Dome toward the emplacement of the Tri-State District MVT ores.

The enriched Pb isotope signatures exhibited by the Cotter Dolomite appear to indicate some input of fluorite and other associated halide/evaporite minerals, such as barite, possibly phosphoritic in origin. An anomaly of elemental yttrium within the Cotter supports the presence of fluorite and other evaporite mineral precipitations, possibly from a minimum of two hydrothermal fluids interacting within this dolomite formation. Additionally, the early Ordovician Upper Knox and Cotter Dolomites exhibit widespread distribution over a large geographic area, indicating early deposition. The ages of formation of associated hydrothermal mineral deposits of anhydrite, barite, calcite, fluorite, and quartz shown by Fishman, 1997 (Figure 27) closely correlate with the proposed age of the MVT ore deposits (250 Ma).

Early Ordovician age and position near Cambrian basement rocks may have contributed to geochemical influx in the depositional makeup of the Cotter and related formations, as in the

case of potassium feldspar dissolution within the Lamotte, Mt. Simon, and Reagan Sandstones, or possibly others. Faults near or in between Lanagan and Pineville, Missouri, may have produced any of a number of pathways for the highly radiogenic end-member of the Ozark MVT ore deposits from the east/southeast as demonstrated by the Cotter Dolomite. To the north and east, MVT brine fluids may have also interacted with freshwater fluids in the Ozark or underlying St. Francois Aquifers after the Ouachita Orogeny and related faulting. The briny Western Interior Plains aquifer is located just west of the Tri-State MVT ore district.

As shown in this thesis, many potential sources are present in the geographic area surrounding the Tri-State MVT district. Further work and analysis of any of the formations named herein, or associated with the study region, are needed to further constrain the dynamics of the MVT ore emplacement of the Northern Arkansas, Tri-State, and related lead-zinc deposits. Samples from formations plotting in the enriched Pb isotope region of the Cotter in this study would help further support the findings here within.

11. FUTURE WORK

Extensive ferruginous mineralization and dolomitization in shear faults in the Upper Cretaceous limestones of the Central Negev Desert adjacent to the Dead Sea Transform margin are related to topographically driven flow of metalliferous groundwaters through an underlying clastic aquifer (Nubian Sandstone) and flow of the fluids up the fault zones (Erel, 2006). The reported isotopic values of the Jackfork Sandstone (Simbo *et al.*, 2019) and Chattanooga Shale (Bottoms *et al.*, 2019) do seem to be related to the sampled formations in both the Ouachitas and Ozarks in this study.

Other similar clastic lithologies within the Ouachitas and Ozarks could be analyzed for Pb isotopes for comparison to the data found herein and other previous studies as cited in this study. Other work, as mentioned above, supports the theory that sedimentary basinal brines flowed along a south-north flow path through sandstone and other lithologies in route to the depositional environments of the MVT ore deposits. The Cason and Sylvan Shales and other similar clastic lithologies such as the Davis Formation are found within the Ozark Dome. Such formations within the Ouachita Mountains include the Blaylock and Hartshorne Sandstones, both of which are stratigraphically younger than the Bigfork Chert and other associated Ouachita sandstones and shales. The Blakely and Crystal Mountain Sandstones are stratigraphically older than the Bigfork, but may also hold isotopic signatures relating the MVTs to the basinal brines that originated from within this deep sedimentary basin. Increased abundance of organic matter in carbonate rocks or thermally altered organic matter may also indicate effects of the passage of heated sedimentary brines (Leach *et al.*, 2010).

The Devonian Penters Chert is stratigraphically equivalent to the Lower Novaculite and found in Northwest and North-Central Arkansas, while the Mississippian Grand Falls Chert

Member of the Boone Formation is ~100 feet below the Short Creek oolite member and located in the Shoal Creek section of southwestern Missouri (Smith and Siebenthal, 1907). These three occurrences of chert could also be analyzed for their genetic relation to the ores and formations mentioned and studied in this and previous works considering their proximal relation to the study area and situation within the flow path.

The quartz found throughout the Ouachitas and Arkoma Basin is younger than the Ouachita Orogeny. Due to the nature of silicon and oxygen, we are currently unable to accurately date such samples. Any improvement or progress toward this endeavor would greatly improve the understanding of the timing of these dynamic geologic processes.

Sulphur isotopes of included sulfates/sulfides and sulphur compounds of formations discussed in these studies and related to the MVT ore deposits could also be analyzed in order to help distinguish source contributions. The dissolution of gypsum and anhydrite occurs without measurable isotope effects, thus, isotope contents of SO_4^{2-} can be used as a tracer of sulfate origin (Clark and Fritz, 1997). Comparison of sulfate isotope signatures in groundwater with their coeval geological period in Figure 23 (Fig. 6-2 from Clark and Fritz, 1997) can help discern a lithogenic source from others of sulfate salinity.

Clumped isotopic analyses of the formations studied for this project, as well as any of the others named herein and otherwise, could be conducted in order to constrain the temperature of formation water(s) ($\delta^{18}O$ and $\delta^{13}C$) for paleoclimate reconstruction. The residence time of groundwater in an aquifer and the groundwater age are an important parameter in any palaeohydrologic and geohydraulic study.

Other tools and approaches include analysis of ionic ratios, mineral saturation indices, carbonate isotope geochemistry, and ^{37}Cl isotopes in order to trace chloride salinity (Clark and

Fritz, 1997). The radiogenic isotopes of hydrogen (^{3}H – tritium, carbon (^{14}C radiocarbon), and in special cases krypton (^{81}Kr, ^{85}Kr), argon (^{39}Ar), chlorine (^{36}Cl), and iodine (^{129}I) with very different half-lives are being used to evaluate relative or absolute groundwater ages (Geyh, 2000, p. 95-96). $^{234}U/^{238}U$ analysis provides information on hydrodynamic mixing processes from rock joints and flow regimes. This process also yields information on the hydrogeological history of the aquifer (Geyh, 2000).

REFERENCES CITED

Aber, J. S. (2003). *Ouachita Mountains*. Retrieved November 24, 2018, from http://academic.emporia.edu/aberjame/struc_geo/ouachita/ouachita.htm

Anderson, G. M. (1973). The hydrothermal transport and deposition of galena and sphalerite near 100°C. *Economic Geology, 68*, 480-492. https://doi.org/10.2113/gsecongeo.68.4.480

Anderson, G. M. (1975). Precipitation of Mississippi Valley-type ores. *Economic Geology, 70*, 937–942. https://doi.org/10.2113/gsecongeo.70.5.937

Anderson, G. M. (1983). Some geochemical aspects of sulfide precipitation in carbonate rocks, in G. Kisvarsanyi, S. K. Grant, W. P. Pratt, and J. W. Koenig, eds., International Conference on Mississippi Valley-Type Lead-Zinc Deposits: Proceedings Volume: Rolla, Missouri, University of Missouri-Rolla Press, p. 61–76.

Anderson, G. M. and Garven, G. (1987). Sulfate-sulfide-carbonate associations in Mississippi Valley-Type lead-zinc deposits. *Economic Geology, 82*, 482-488. https://doi.org/10.2113/gsecongeo.82.2.482

Anderson, W. H. (1991). Mineralization and hydrocarbon emplacement in the Cambrian-Ordovician Mascot Dolomite of the Knox Group in South-Central Kentucky. *Kentucky Geological Survey Report of Investigations, 44*. University of Kentucky. https://uknowledge.uky.edu/kgs_ri/44

Appold, M. S., Numelin, T. J., Shepherd, T. J., and Chenery, S. R. (2004). Limits on the metal content of fluid inclusions in gangue minerals from the Viburnum Trend, Southeast Missouri, determined by Laser Ablation ICP-MS, *Economic Geology*, *99*(1), 185-198. http://dx.doi.org/10.2113/gsecongeo.99.1.185

Arizona Board of Regents (2005). Lead. *Sustainability of semi-Arid Hydrology and Riparian Areas.* http://web.sahra.arizona.edu/programs/isotopes/lead.html

Arkansas Geological Survey (2018). Bigfork Chert/Formation. Retrieved November 23, 2018 from https://www.geology.arkansas.gov/geology/stratigraphic-summary-of-the-arkansas-river-valley-and-ouachita-mountains.html

Avildsen, C., Bie, J., Patel, C., and Sarvis, B. (2011, July 6). *The Ordovician Period*. Retrieved from www.ucmp.berekely.edu/ordovician/ordovician.php.

Banner, J. L., Hanson, G. N., and Meyers, W. J. (1988a). Rare earth element and Nd isotopic variations in regionally extensive dolomites from the Burlington-Keokuk Formation (Mississippian): Implications for REE mobility during carbonate diagenesis. *Journal of Sedimentary Petrology, 58*(3), 415-432.

Banner, J. L., Hanson, G. N., and Meyers, W. J. (1988b). Determination of initial Sr-isotopic compositions of dolostones from the Burlington–Keokuk Formation (Mississippian): Constraints from cathodoluminescence, glauconite paragenesis, and analytical methods. *Journal of Sedimentary Petrology, 58*, 673-687. http://www.jsg.utexas.edu/banner/files/Determination-of-initial-Sr-Journal-of-Sed.-Pet.-1988.pdf

Banner, J. L., Wasserburg, G. J., Dobson, P. F., Carpenter, A. B., and Moore, C. H. (1989). Isotopic and trace element constraints on the origin and evolution of saline groundwaters from Central Missouri. *Geochemica et Cosmochimica Acta, 53*(2), 383-398. https://doi.org/10.1016/0016-7037(89)90390-6

Bastin, E. S. (1939). Theories of formation of ore deposits: *Scientific American, 49*(6), 538–547.

Bleam, William (2017). Ch. 6.3.1.4 Evaporite Rocks, Soil and Environmental Chemistry, Academic Press, 2nd Edition, 586 p.

Bottoms, B. M., Potra, A., Samuelsen, J. R., and Schutter, S. R. (2019). Geochemical investigations of the Woodford–Chattanooga and Fayetteville Shales: Implications for genesis of the Mississippi Valley–type zinc–lead ores in the southern Ozark Region and hydrocarbon exploration. AAPG Bulletin 7-2019. https://doi.org/10.1306/12171818101

Bradley, D. C. and Leach, D. L. (2003). Tectonic controls of Mississippi Valley-type lead-zinc mineralization in orogenic forelands. *Mineralium Deposita, 38*(6), 652-667. https://link.springer.com/article/10.1007/s00126-003-0355-2

Braile, L., Hinze, W. J., Sexton, J., Keller, R., and Lidiak, E. (1984). Tectonic development of the New Madrid seismic zone. U.S. Geological Survey Open-File Report 84-770, 204-233.

Braile, L.W., Hinze, W. J., Keller, G. R., Lidiak, E.G., and Sexton, J. L. (1986). Tectonic Development of the New Madrid Rift Complex, Mississippi Embayment, North America. *Tectonophysics, 131*(1-2), 21 p. https://doi.org/10.1016/0040-1951(86)90265-9

Cains, J. M., Potra, A., and Pollock, E. D. (2016). Lower Mississippian chert development, Southern Midcontinent Region. *Journal of the Arkansas Academy of Science, 70(*12). Retrieved May 22, 2019 from http://scholarworks.uark.edu/jaas/vol70/iss1/12

Cains, J. M. (2019). *Geochemical Analysis of Mississippian Cherts and Devonian-Mississippian Novaculites, Southern Midcontinent Region.* [Masters Thesis, University of Arkansas]. Retrieved November 14, 2019 from https://scholarworks.uark.edu/etd/3248

Cannon, R. S. Jr. and Pierce, A. P. (1969). Lead isotope guides for Mississippi Valley lead-zinc exploration. US Geological Survey Bulletin 1312-G: p. 20.

Caplan, W. M. (1957). Plate IX. Post-Boone Mississippian Isopach. Subsurface Geology of Northwestern Arkansas. Arkansas Geological and Conservation Commission, Information Circular 19. 14 p.

Carr, G. R., Dean, J. A., Suppel, D. W., and Heithersay, P. S. (1995). Precise lead isotope fingerprinting of hydrothermal activity associated with Ordovician to Carboniferous metallogenic events in the Lachlan fold belt of New South Wales. *Economic Geology, 90*(6), 1467-1505. https://doi.org/10.2113/gsecongeo.90.6.1467

Cathcart, J. B. (1989). The phosphate deposits of Tennessee, U.S.A., in Notholt, A.J.G., ed., Phosphate deposits of the world: Cambridge, U.K., *Cambridge University Press, 2*, 6-13.

Chinn, A. A. and Konig, R. H. (1973). Stress inferred from calcite twin lamellae in relation to regional structure of northwestern Arkansas. *Geological Society of America Bulletin, 84*(11), p. 3731-3736. https://doi.org/10.1130/0016-7606(1973)84%3C3731:SIFCTL%3E2.0.CO;2

Clark, I. D. and Fritz, P. (1997). Environmental Isotopes in Hydrogeology, Taylor & Francis: Boca Raton, FL: CRC Press, (2nd Edition) p. 1-328.

Clendenin, C. W. and Duane, M. J. (1990). Focused fluid flow and Ozark Mississippi Valley-type deposits. *Geology, 18*(2), 116-119. Retrieved February 4, 2020 from https://pubs.geoscienceworld.org/gsa/geology/article/18/2/116-119/190851

Conley, D. J., Frings, P. J., Fontorbe, G., Clymans, W., Stadmark, J., Hendry, K. R., Marron, A. O., and De La Rocha, C. L. (2017, December 11). Biosilicification Drives a Decline of Dissolved Si in the Oceans through Geologic Time. *Frontiers in Marine Science, 4*(397). https://doi.org/10.3389/fmars.2017.00397. 17 p.

Corbella, M., Ayora, C. and Cardellach, E. (2004). Hydrothermal mixing, carbonate dissolution and sulfide precipitation in Mississippi Valley-type deposits. *Mineralium Deposita, 39*, 344-357. https://link.springer.com/article/10.1007%2Fs00126-004-0412-5

Coryell, C. D., Chase, J. W. and Winchester, J. W. (1963). A procedure for geochemical interpretation of terrestrial rare earth abundance patterns. *Journal of Geophysical Research, 68*, 559-566. https://doi.org/10.1029/JZ068i002p00559

Denison, R. E. (1989). Foreland structure adjacent to the Ouachita foldbelt, *in* Hatcher, R. D., Jr., Thomas, W. A., and Viele, G. W., eds., The Appalachian-Ouachita Orogen in the United States: Geological Society of America, *The Geology of North America, (F-2)*, 681-694.

Diehl, S. F., Goldhaber, M. B., Taylor, C. D., Swolfs, H. S., and Gent, C. A. (1992). Microstructures in the Cambrian Bonneterrre Formation, Lamotte Sandstone, and Basal Clastic Rocks of Southeast Missouri and Northeast Arkansas--Implications of Regional Sulfide Occurrence in Stylolites and Extensional Veinlets for Ore Genesis. Chapter A in: Thorman, C. H. editor. Application of Structural Geology to Mineral and Energy Resources of the United States, USGS Bulletin 2012, p. A1-A13.

Doe, B. R. and Delevaux, M. H. (1972). Source of Lead in Southeast Missouri Galena Ores. *Economic Geology, 67*(4), 409-425. https://doi.org/10.2113/gsecongeo.67.4.409

Dublyansky, Y. (2019). Hydrothermal Caves, Innsbruck University, Encyclopaedia of Caves, Third Edition. p. 391-397. Retrieved January 24, 2020 from https://www.sciencedirect.com/topics/earth-and-planetary-sciences/fluorite

Duffin, M. E., Lee, M. C., Klein, G. D., and Hay, R. L. (1989). Potassic diagenesis of Cambrian sandstones and Precambrian granitic basement in UPH-3 deep hole, Upper Mississippi Valley, U.S.A. *Journal of Sedimentary Petrology, 59*, 848–861. https://doi.org/10.1306/212F908E-2B24-11D7-8648000102C1865D

Eiler, J. M., Crawford, A., Elliott, T., Farley, K. A., Valley, J. W., and Stolper, E. M. (2000). Oxygen isotope geochemistry of oceanic-arc lavas. *Journal of Petrology*, *41*(2), 229-256. https://doi.org/10.1093/petrology/41.2.229

Elderfield, H., and Greaves, M. J. (1982). The rare earth elements in seawater. *Nature, 296*, 214-219. Retrieved March 17, 2020 from https://www.nature.com/articles/296214a0

Elliott, T. (1997). Inside the Subduction Factory. Geophysical Monograph 138. © 2003 by American Geophysical Union. https://doi.org/10.1029/138GM03. Editor: Eiler, John. p. 23-45.

Erel, Y., Listovsky, N., Matthews, A., Ilani, S., and Avni, Y. (2006, November). NASA/ADS: Tracing end-member fluid sources in sub-surface iron mineralization and dolomitization along a proximal fault to the dead sea transform. *Geochimica et Cosmochimica Acta, 70*(22), 5552-5570. Retrieved October 9, 2019 from http://citeseerx.ist.psu.edu/viewdoc/download?doi=10.1.1.572.6747&rep=rep1&type=pdf

Fishman, N. S. (1997). Basin-wide fluid movement in a Cambrian paleoaquifer: Evidence from the Mount Simon Sandstone, Illinois and Indiana, *in* Montañez, I.P., *et al.*, eds., Basin-wide diagenetic patterns: Integrated petrologic, geochemical, and hydrologic considerations: *SEPM (Society for Sedimentary Geology) Special Publication 57*, 221-234.

Forte, A. M., Mitrovica, J. X., Moucha, R., Simmons, N. A., and Grand, S. P. (2007). Descent of the ancient Farallon slab drives localized mantle flow below the New Madrid seismic zone. Geophysical Research Letters – Wiley Online Library (February 23, 2007), p. 1-13.

Garven, G., Ge, S., Person, M. A., and Sverjensky, D. A. (1993). Genesis of stratabound ore deposits in the Midcontinent basins of North America: 1. The role of regional groundwater flow. *American Journal of Science, 293*, 497-568. https://doi.org/10.2475/ajs.293.6.497

Geyh, M. (2000). Environmental isotopes in the hydrological cycle. *UNESCO IHP-V Technical Documents in Hydrology, 4*(39). Edited by W. G. Mook. 196 p. Retrieved August 28, 2019 from https://unesdoc.unesco.org/ark:/48223/pf0000121542

Godo, T., Li, P., and Ratchford, M. E. (2014). Structural and Stratigraphic Analysis of the Shell International Paper No. 1-21 Well, Southern Ouachita Fold and Thrust Belt, Pike County, Arkansas. Arkansas Geological Survey. Retrieved December 7, 2019 from https://www.geology.arkansas.gov/docs/pdf/publication/information-circulars/IC-39C-International-Paper-No.-1-21.pdf

Goldhaber, M. B., Church, S. E., Doe, B. R., Aleinikoff, J. N., Brannon, J. C., Podosek, F. A., Mosier, E. L., Taylor, C. D., and Gent, C. A. (1995). Lead and sulfur isotope investigation of Paleozoic sedimentary rocks from the southern Midcontinent of the United States: implications for paleohydrology and ore genesis of the Southeast Missouri lead belts: *Economic Geology*, *90*, 1875–1910. https://doi.org/10.2113/gsecongeo.90.7.1875

Goldstein, A. Jr. and Hendricks, T. A. (1953). Siliceous sediments of Ouachita facies in Oklahoma. *Geological Society of America Bulletin, 64*(4), 421-442. https://doi.org/10.1130/0016-7606(1953)64[421:SSOOFI]2.0.CO;2

Gregg, J. M. and Shelton, K. L. (2012, January 1). Mississippi Valley-type Mineralization and Ore Deposits in the Cambrian-Ordovician Great American Carbonate Bank. GeoScience World Books. Retrieved September 30, 2018 from https://pubs.geoscienceworld.org/books/book/1267/chapter/107094655/Mississippi-Valley-type-Mineralization-and-Ore

Grollimund, B. and Zoback, M. D. (2001). Did deglaciation trigger intraplate seismicity in the New Madrid seismic zone? *Geology*, *29*(2), 175–178. Retrieved August 28, 2019 from https://pangea.stanford.edu/departments/geophysics/dropbox/STRESS/publications/MDZ%20PDF's/2001/GrollimunZobackGeology%202001PDF.pdf

Grotzinger, J. P. and James, N. P. (2000). Carbonate Sedimentation and Diagenesis in the Evolving Precambrian World. *SEPM (Society for Sedimentary Geology), Special Publication 67*. Retrieved September 7, 2019 from https://pubs.geoscienceworld.org/books/book/1880/Carbonate-Sedimentation-and-Diagenesis-in-the

Guccione, M. J., Marple, R., and Autin, W. J. (2005). Evidence for Holocene displacements on the Bootheel fault (lineament) in southeastern Missouri: Seismotectonic implications for the New Madrid region. *Geological Society of America Bulletin*, *117*(3-4), 319-333. https://doi.org/10.1130/B25435.1

Hall, W. E. and Friedman, I. (1969). Oxygen and carbon isotopic composition of ore and host rock of selected Mississippi Valley deposits. *USGS Professional Paper, 650-C*, C140-C148. Retrieved May 12, 2017 from https://pubs.usgs.gov/pp/0650c/report.pdf

He, Z. (1995). Sedimentary facies and variations of stable isotope composition of Upper Cambrian to Lower Ordovician strata in southern Missouri: implications for the origin of MVT deposits, and the geochemical and hydrological features of regional ore-forming fluids [Unpublished Ph.D. dissertation, University of Missouri–Rolla]. Missouri Institute of Science and Technology Scholars' Mine, 124 p.

He, Z., Gregg, J. M., Shelton, K. L., and Palmer, J. R. (1997). Sedimentary facies control of fluid flow and Mineralization in Cambro-Ordovician Strata, Southern Missouri. Basin-Wide Diagenetic Patterns: Integrated Petrologic, Geochemical, and Hydrologic Considerations, *SEPM (Society for Sedimentary Geology) Special Publication 57*. Retrieved June 8, 2018 from https://pubs.geoscienceworld.org/books/book/1106/chapter/10551281/Sedimentary-Facies-Control-of-Fluid-Flow-and

Henbest, L. G. (1968). Diagenesis in oolitic limestones of Morrow (Early Pennsylvanian) age in northwestern Arkansas and adjacent Oklahoma: U.S. Geological Survey Professional Paper 594-H, p. H1-H22.

Heyl, A. V., Delevaux, M. H., Zartman, R. E., and Brock, M. R. (1966). Isotopic study of galenas from the Upper Mississippi Valley, the Illinois-Kentucky, and some Appalachian Valley mineral districts. *Economic Geology, 61*(5), 933-961.

Heyl, A. V., Landis, G. P., and Zartman, R. E. (1974). Isotopic evidence for the origin of Mississippi Valley-type mineral deposits: A review. *Economic Geology, 69*(6), 992-1006.

Hofmann, A. W., Jochum, K. P., Seufert, M., and White, W. M. (1986). Nb and Pb in oceanic basalts: new constraints on mantle evolution. *Earth and Planetary Science Letters, 79*, 33-45.

Holland, S. M., (2018, May 17). Ordovician Period Geochronology, Encyclopedia Britannica, Inc. Published. Retrieved from https://www.britannica.com/science/Ordovician-Period

Honess, C. W. (1923). Geology of the southern Ouachita Mountains of Oklahoma: Oklahoma Geological Survey Bulletin 32, part 1: 278 p., part 2: 76 p.

Howard, P. F., and Hough, M. J. (1979). On the geochemistry and origin of the D Tree, Wonarah, and Sherrin Creek phosphorite deposits of the Georgina basin, northern Australia: *Economic Geology, 74*(2), 260-284. https://doi.org/10.2113/gsecongeo.74.2.260

Hudson, M. (2000). Coordinated strike-slip and normal faulting in the southern Ozark dome of northern Arkansas: Deformation in a late Paleozoic foreland. *Geology, 28*(6), 511-514. https://doi.org/10.1130/0091-7613(2000)28<511:CSANFI>2.0.CO;2

Imes, J. L. and Emmett, L. F. (1994). Geohydrology of the Ozark Plateaus aquifer system in parts of Missouri, Arkansas, Oklahoma, and Kansas: U.S. Geological Survey Professional Paper 1414–D, 127 p.

Johnson, K. T., Dick, H. J., and Shimizu, N. (1990). Melting in the oceanic upper mantle: an ion microprobe study of diopsides in abyssal peridotites, *Journal of Geophysical Research, 95*(B3), 2661-2678. https://doi.org/10.1029/JB095iB03p02661

Kesler, S. E., Cumming, G. L., Krstic, D., and Appold, M. S. (1994a). Lead isotope geochemistry of Mississippi Valley-type deposits of the southern Appalachians. *Economic Geology, 89*(2), 307-321. https://doi.org/10.2113/gsecongeo.89.2.307

Kesler, S. E., Appold, M. S., Cumming, G. L., and Krstic, D. (1994b). Lead isotope geochemistry of Mississippi Valley-type mineralization in the central Appalachians. *Economic Geology, 89*(7), 1492-1500. https://doi.org/10.2113/gsecongeo.89.7.1492

Kidder, D. L. and Tomescu, I. (2016, September 15) Biogenic chert and the Ordovician silica cycle. *Palaeogeography, Palaeoclimatology, Palaeoecology, 458*, 29-38. https://doi.org/10.1016/j.palaeo.2015.10.013

Klinkhammer, G., Elderfield, H., and Hudson, A. (1983). Rare earth elements in seawater near hydrothermal vents. *Nature, 305*, 185-188. https://doi.org/10.1038/305185a0

Lane, H. R. (1978). The Burlington Shelf (Mississippian, north-central United States). *Geologica et Palaeontologica, 12*, 165-176.

Leach, D. L. and Rowan, E. L. (1986). Genetic link between Ouachita foldbelt tectonism and the Mississippi Valley–type lead-zinc deposits of the Ozarks. *Geology, 14*(11), 931-935. https://doi.org/10.1130/0091-7613(1986)14<931:GLBOFT>2.0.CO;2

Leach, D. L., Taylor, R. D., Fey, D. L., Diehl, S. F., and Saltus, R. W. (2010). A Deposit Model for Mississippi Valley-Type Lead-Zinc Ores: Chapter A in mineral deposit models for resource assessment. *U. S. Geological Survey Scientific Investigations Report 2010-5070*, 1-8. Retrieved May 29, 2018 from https://pubs.er.usgs.gov/publication/sir20105070A

Leach, D. L. and Sangster, D. F. (1993). Mississippi valley-type lead-zinc deposits: Geological association of Canada special paper 40, p. 289-314.

Lee, R. C. (2000). The effect of Mississippi Valley-type mineralization on the natural background chemistry of groundwater in the Ozark Plateaus region of the United States. [Masters Thesis: Colorado School of Mines]. 210 p.

Liu, Y. (2016, December). How to explain Si isotopes of chert? American Geophysical Union, Fall Meeting 2016, abstract #V51A-3033. Retrieved November 14, 2018 from http://adsabs.harvard.edu/abs/2016AGUEM_V51A3033I

Longman, J., Veres, D., Ersek, V., Phillips, D. L., Chauvel, C., and Tamas, C. G. (2018). Quantitative assessment of Pb sources in isotopic mixtures using a Bayesian mixing model. *Scientific Reports 2018, 8*(6154), 1-32. Retrieved February 8, 2020 from https://www.ncbi.nlm.nih.gov/pmc/articles/PMC5906678/

Lumsden, D. N. and Caudle, C. G. (2001, May). Origin of massive dolostone: the Upper Knox model. *SEPM (Society for Sedimentary Geology) Journal of Sedimentary Research, 71*(3), 400-409.

Maliva, R. G., Knoll, A. H., and Siever, R. (1989). Secular Change in Chert Distribution: A Reflection of Evolving Biological Participation in the Silica Cycle. *Palaios, 4*(6), 519-532. https://doi.org/10.2307/3514743

Manger, W. L. and Thompson, T. L. (1982). Regional depositional setting of lower Mississippian Waulsortian mound facies, southern midcontinent, Arkansas, Missouri and Oklahoma. *In* Bolton, K., Lane, H. R., and LeMone, D. V., (eds.), Symposium on the paleoenvironmental setting and distribution of the Waulsortian facies, El Paso Geological Society and University of Texas at El Paso. p. 43-50.

Manger, W. L., Zachry, D. L., and Garrigan, M. L. (1988). An introduction to the geology of northwestern Arkansas: Field trips. The Compass, Sigma Gamm Epsilon *65*(4), 242-257.

Manger, W. L. and Shelby, P. R. (2000). Natural-Gas Production from the Boone Formation (Lower Mississippian), Northwestern Arkansas. *Oklahoma Geological Survey Circular, 101*, 163-169.

Masuda, A. (1962). Regularities in variation of relative abundances of lanthanide elements and an attempt to analyze separation-index patterns of some minerals. *Journal of Earth Sciences, Nagoya University, 10*(2), 173-187.

McFarland, J. D. (1998, revised 2004). Stratigraphic Summary of Arkansas, Arkansas Geological Commission, Information Circular 36, 39 p.

McKim, S., Cains, J., Chick, J., McFarlin, F., and Potra, A. (2017). Lithologic Stratigraphic Position, Sequence and Diagenetic History, Lower Mississippian Tripolitic Chert, Northern Arkansas and Missouri. *Journal of the Arkansas Academy of Science, 71*(28), 165-168.

McKim, S. (2018). The Origin of Tripolitic Chert and its Isotopic and Elemental Relationship to the Lead-Zinc Deposits in the Southern Ozark Region, Arkansas, Missouri and Oklahoma. [Undergraduate Honors Thesis, University of Arkansas]. 36 p.

McKnight, E. T. and Fischer, R. P. (1970). Geology and Ore Deposits of the Picher Field Oklahoma and Kansas. U.S. DOI, Geological Survey Professional Paper 588. U.S. Government Printing Office, Washington, D.C. 20402. 163 p.

Miller, J. A. and Appel, C. L. (1997). U.S. Geological Survey, Hydrologic atlas 730-D. https://pubs.usgs.gov/ha/ha730/ch_d/D-text5.html

Minor, P. M. (2013). Analysis of Tripolitic Chert in the Boone Formation (Lower Mississippian, Osagean), Northwest Arkansas and Southwestern Missouri. [Masters Thesis, University of Arkansas]. 80 p.

Miser, H. D. and Purdue, A. H. (1929). Geology of the DeQueen and Caddo Gap Quadrangles, Arkansas: USGS Bulletin 808.

Miser, H. D. (1959). Structure and Vein Quartz of the Ouachita Mountains of Oklahoma and Arkansas: The Geology of the Ouachita Mountains – A Symposium, Published by Dallas Geological Society and the Ardmore Geological Society, Dallas, Texas.

Montañez, I. P. (1989). Regional dolomitization of Early Ordovician, Upper Knox Group, Appalachians. [Doctoral Dissertation, Virginia Tech University]. 321 p.

Montañez, I. P. and Read, J. F. (1992). Fluid-rock interaction history during stabilization of early dolomites, Upper Knox Group (Lower Ordovician), U.S. Appalachians. *Journal of Sedimentary Petrology, 62*(5), 753-778. https://doi.org/10.1306/D42679D3-2B26-11D7-8648000102C1865D

Montañez, I. P. (1994). Late Diagenetic Dolomitization of Lower Ordovician, Upper Knox Carbonates: A Record of the Hydrodynamic Evolution of the Southern Appalachian Basin. *American Association of Petroleum Geologists Bulletin, 78*(8), 1210-1239. https://doi.org/10.1306/A25FEAB3-171B-11D7-8645000102C1865D

Morris, N. (2017). Lost Names in the Paleozoic Lithostratigraphy of Arkansas. [Masters Thesis, University of Arkansas]. Retrieved May 29, 2019 from http://scholarworks.uark.edu/etd/1913

Mose, D. (1969). The age of the Hatton Tuff of the Ouachita Mountains, Southeastern Oklahoma. *Geological Society of America Bulletin, 80*(11), 2373-2378. https://doi.org/10.1130/0016-7606(1969)80[2373:TAOTHT]2.0.CO;2

Moyers, A. (2015). Source Constraints of Ore Metals in Mississippi Valley-type Deposits in Central and Eastern Tennessee using Pb Isotopes. [Masters Thesis, University of Arkansas]. Retrieved September 30, 2019 from http://scholarworks.uark.edu/etd/39

Murray, R. W., Buchholtz ten Brink, M. R., Jones, D. L., Gerlach, D. C., and Price, R. G. III (1990). Rare earth elements as indicators of different marine depositional environments in chert and shale. *Geology, 18*, 268-271.

Niem, A. R. (1977). Mississippian pyroclastic flow and ash-fall deposits in the deep-marine Ouachita flysch basin, Oklahoma and Arkansas. *Geological Society of America Bulletin, 88*: 49-61. Retrieved November 14, 2019 from https://pubs.geoscienceworld.org/gsa/gsabulletin/article-pdf/88/1/49/3444185/i0016-7606-88-1-49.pdf

Nottmeier, A. M. (2015). Regional potentiometric surface of the Ozark aquifer in Arkansas, Kansas, Missouri, and Oklahoma, November 2014-January 2015: U.S. Geological Survey Scientific Investigations Map 3348, 1 sheet. http://dx.doi.org/10.3133/sim3348.

Overstreet, R. B., Oboh-Ikuenobe, F., and Gregg, J. M. (2003, May 1). Sequence Stratigraphy and Depositional Facies of Lower Ordovician Cyclic Carbonate Rocks, Southern Missouri, U.S.A. *Journal of Sedimentary Research, 73*(3), 421-433.

Paradis, S., Hannigan, P., and Dewing, K. (2007, January). Mississippi Valley-type lead-zinc Deposits (MVT). Retrieved on May 29, 2018 from https://www.researchgate.net/publication/228477629_Mississippi_Valley-type_lead-zinc_deposits_MVT

Patterson, C. and Tatsumoto, M. (1964). The significance of lead isotopes in detrital feldspar with respect to chemical differentiation within the earth's mantle. *Geochemica et Cosmochimica Acta, 28,* 1-22. https://doi.org/10.1016/0016-7037(64)90052-3.

Philbrick, J., Pollock, E., and Potra, A. (2016). Comparison of the Elemental Geochemistry of the Arkansas Novaculite and the Boone Chert in their Type Regions, Arkansas. *Journal of the Arkansas Academy of Science, 70*. 184-189.

Piper, D. Z. (1974). Rare earth elements in the sedimentary cycle: A summary: Chemical *Geology, 14*, 285-304.

Pope, L. M., Mehl, H. E., and Coiner, R. L. (2009). Quality Characteristics of Ground Water in the Ozark Aquifer of Northwestern Arkansas, Southeastern Kansas, Southwestern Missouri, and Northeastern Oklahoma, 2006–07. *Scientific Investigations Report 2009–5093*. 62 p. https://pubs.usgs.gov/sir/2009/5093/pdf/SIR2009-5093.pdf

Purdue, A. H. (1909). Lexicon of Geologic Names of the United States, Part 1, A-L. U.S. D.O.I.: Geological Survey Bulletin 896, United States Government Printing Office, Washington, 1957, p. 184, 529.

Rasbury, T. E. and Cole, J. M. (2009, July 10). Directly dating geologic events: U-Pb dating of carbonates. https://doi.org/10.1029/2007RG000246. 2 p.

Richardson, C. K. and Holland, H. D. (1979). Fluorite Deposition in hydrothermal Systems, *Geochemica et Cosmochimica Acta, 43*(8), 1327-1335. http://doi.org/10.1016/0016-7037(79)90122-4

Ross, R. J., Hintze, L. F., Ethington, R. L., Miller, J. F., Taylor, M. E., Repetski, J. E., Sprinkle, J. E., and Guensburg, T. E. (1993). The Ibexian Series (Lower Ordovician), a replacement for "Canadian Series" in North American chronostratigraphy. United States Geological Survey Open-File Report 93-598, 75 p.

Ruhlin, D. E., and Owen, R. M. (1986). The rare earth element geochemistry of hydrothermal sediments from the East Pacific Rise: Examination of a seawater scavenging mechanism: *Geochimica et Cosmochimica Acta, 50,* 393-400.

Scholle, P. A. (1978). A Color Illustrated Guide to carbonate Rock Constituents, Textures, Cements, and Porosities: *American Association of Petroleum Geologists, Memoir 27*, p. 129-168. Accessed June 8, 2018 from Diagenesis: https://www.sepmstrata.org/page.aspx?pageid=92

Shannon, R. D. (1976, September). Revised effective ionic radii and systematic studies of interatomic distances in halides and chalcogenides, *Acta Crystallographica, 32*, 751-767. https://doi.org/10.1107/S0567739476001551

Scotese, C. R. (2001). Paleogeography, PALEOMAP Project, Arlington, Texas, *Atlas of Earth History, 1*, 52 p. Retrieved April 16, 2020 from http://www.scotese.com/

Siever, R. (1991). Silica in the oceans: biological-geochemical interplay, in *Scientists on Gaia*, eds S. H. Schneider and P. J. Boston (Cambridge, MA: MIT Press), 287–295.

Sharp, W. E. (1965). Deposition of hydrothermal quartz and calcite. *Economic Geology, 60*(8). 1635-1644. https://doi.org/10.2113/gsecongeo.60.8.1635

Shelby, P. R. (1986). Depositional history of the St. Joe and Boone Formations in northern Arkansas: *Arkansas Academy of Science Proceedings, 40*, 67-71.

Simbo, C. W., Potra, A., and Samelusen, J. R. (2019). A geochemical evaluation of the genetic relationship between Ouachita Mountains Paleozoic rocks and the Mississippi Valley-type mineralization in the southern Ozark Region, USA. *Ore Geology Reviews, 112*, 103029. https://doi.org/10.1016/j.oregeorev.2019.103029

Smith, W. S. and Siebenthal, C. E. (1907). Description of the Joplin district [Joplin District folio, Missouri-Kansas]: U.S. Geological Survey Geologic Atlas of the United States GF-148, p. 1-20. https://doi.org/10.3133/gf148

Stacey, J. S. and Kramer, J. D. (1975). Approximation of terrestrial lead isotope evolution by a two-stage model. *Earth and Planetary Science Letters, 26*(2), 207-221. https://doi.org/10.1016/0012-821X(75)90088-6

Stefurak, E. J., Woodward, W. F., and Lowe, D. R. (2014, April 29). Texture-specific Si isotope variations in Barberton Greenstone Belt cherts record low temperature fractionations in early Archean seawater. *Geochemica et Cosmochimica Acta, 150*, 26-52.

Sun, S.-s. and McDonough, W. F. (1989). Chemical and isotopic systematics of oceanic basalts: implications for mantle composition and processes. *Geological Society, London, Special Publications, 42*, 313 - 345.

Suneson, N. H. (2012). Arkoma Basin Petroleum - Past, Present, and Future. Shale Shaker, *Journal of the Oklahoma Geological Society*, originally published in *63*(1), July-August 2012 Issue, Oklahoma Geological Survey | (405) 325-7315 | nsuneson@ou.edu. p. 40, 60.

Swain, R. and Rout, G. R. (2017). Ch. 8: Silicon in Agriculture © Springer International Publishing AG 2017. E. Lichtfouse (ed.), *Sustainable Agriculture Reviews,* Sustainable Agriculture Reviews 25, DOI 10.1007/978-3-319-58679-3_8, p. 233-260.

Tatsumi, Y., Hamilton, D. L., and Nesbitt, R. W. (1986, September). Chemical characteristics of fluid phase released from a subducted lithosphere and origin of arc magmas: evidence from high pressure experiments and natural rocks, *Journal of Volcanology and Geothermal Research, 29*(1-4), 293-309. https://doi.org/10.1016/0377-0273(86)90049-1

Tosdal, R. M., Wooden, J. L., and Bouse, R. M. (1999). Pb Isotopes, ore deposits, and metallogenic terranes. *Applications of radiogenic isotopes to ore deposit research and exploration: Reviews in Economic Geology, 12*, 28 p.

Ulrich, E. O. (1911). Revision of the Paleozoic Systems. GSA Bulletin (Jan 1, 1911) 22 (1): p. 281-680. https://doi.org/10.1130/GSAB-22-281.

Van-Hise, C. R. (1904). A Treatise on Metamorphism. 1286 p.

Wedepohl, K. H. (1969). Handbook of geochemistry: Berlin, Springer-Verlag, 2415 p.

Weiss, B. (2016). *Rare Earth Elements: Overview.* Massachusetts Institute of Technology. http://web.mit.edu/12.000/www/m2016/finalwebsite/elements/ree.html

Wenz, Z. J., Appold, M. S., Shelton, K. L. and Tesfaye, S. (2012, January). Geochemistry of Mississippi Valley-type mineralizing fluids of the Ozark Plateau: A regional synthesis. *American Journal of Science, 312*(1), 22-80. https://doi.org/10.2475/01.2012.02

Williams, R. A., McCallister, N. S., and Dart, R. L. (2011). *20 Cool Facts about the New Madrid Seismic Zone*. United States Geological Survey. https://pubs.usgs.gov/gip/134/

Williams-Jones, A. E. and Migdisov, A. A. (2014, January). Experimental Constraints on the Transport and Deposition of Metals in Ore-Forming Hydrothermal Systems. *Society of Economic Geologists, Inc. Special Publication 18*, 77-95. Retrieved May 22, 2019 from https://www.segweb.org/SEG/_Events/Conference_Archive/2014/Conference_Proceedings/data/papers/invited/Williams-Jones-Abstract.pdf

Woodhead, J. D. (1989). Geochemistry of the Mariana arc (western Pacific): source composition and processes, *Chemical Geology, 76*(1-2), 24 p. https://doi.org/10.1016/0009-2541(89)90124-1

Young, S. A. (2009). *Isotope stratigraphy: Applications for Ordovician paleoceanography & paleoclimatology*. Department of Geological Sciences, Indiana University. Retrieved October 10, 2019 from http://www.indiana.edu/~paleoind/Lectures/Lecture%2010%20-%20Hirnantian%20extinction%20Young.pdf

FIGURES

1. Pope, L. M., Mehl, H. E., and Coiner, R. L. (2009). Quality Characteristics of Ground Water in the Ozark Aquifer of Northwestern Arkansas, Southeastern Kansas, Southwestern Missouri, and Northeastern Oklahoma, 2006–07. *Scientific Investigations Report 2009–5093*. 62 p. https://pubs.usgs.gov/sir/2009/5093/pdf/SIR2009-5093.pdf

2. Constructed Stratigraphic column of the Ozark and Ouachita Mountain regions, Arkansas, USA. Modified from Godo, T., Li, P., and Ratchford, M. E. (2014). Structural and Stratigraphic Analysis of the Shell International Paper No. 1-21 Well, Southern Ouachita Fold and Thrust Belt, Pike County, Arkansas. Arkansas Geological Survey. Retrieved December 7, 2019 from https://www.geology.arkansas.gov/docs/pdf/publication/information-circulars/IC-39C-International-Paper-No.-1-21.pdf

3. Minor, P. M. (2013). Analysis of Tripolitic Chert in the Boone Formation (Lower Mississippian, Osagean), Northwest Arkansas and Southwestern Missouri. [Masters Thesis, University of Arkansas]. 80 p.

4. Scotese, C. R. (2001). Paleogeography, PALEOMAP Project, Arlington, Texas, *Atlas of Earth History, 1*, 52 p. Retrieved April 16, 2020 from http://www.scotese.com/

5. Suneson, N. H. (2012). Arkoma Basin Petroleum - Past, Present, and Future. Shale Shaker, *Journal of the Oklahoma Geological Society*, originally published in *63*(1), July-August 2012 Issue, Oklahoma Geological Survey | (405) 325-7315 | nsuneson@ou.edu. p. 40, 60.

6. Kidder, D. L. and Tomescu, I. (2016, September 15) Biogenic chert and the Ordovician silica cycle. *Palaeogeography, Palaeoclimatology, Palaeoecology, 458*, 29-38. https://doi.org/10.1016/j.palaeo.2015.10.013

7. Manger, W. L., Zachry, D. L., and Garrigan, M. L. (1988). An introduction to the geology of northwestern Arkansas: Field trips. The Compass, Sigma Gamm Epsilon *65*(4), 242-257.

8. Caplan, W. M. (1957). Plate IX. Post-Boone Mississippian Isopach. Subsurface Geology of Northwestern Arkansas. Arkansas Geological and Conservation Commission, Information Circular 19. 14 p.

9. Overstreet, R. B., Oboh-Ikuenobe, F., and Gregg, J. M. (2003, May 1). Sequence Stratigraphy and Depositional Facies of Lower Ordovician Cyclic Carbonate Rocks, Southern Missouri, U.S.A. *Journal of Sedimentary Research, 73*(3), 421-433.

10. Gregg, J. M. and Shelton, K. L. (2012, January 1). Mississippi Valley-type Mineralization and Ore Deposits in the Cambrian-Ordovician Great American Carbonate Bank. GeoScience World Books. Retrieved September 30, 2018 from https://pubs.geoscienceworld.org/books/book/1267/chapter/107094655/Mississippi-Valley-type-Mineralization-and-Ore

11. Modified from Lee, R. C. (2000). The effect of Mississippi Valley-type mineralization on the natural background chemistry of groundwater in the Ozark Plateaus region of the United States. [Masters Thesis: Colorado School of Mines]. 210 p.

12. Conley, D. J., Frings, P. J., Fontorbe, G., Clymans, W., Stadmark, J., Hendry, K. R., Marron, A. O., and De La Rocha, C. L. (2017, December 11). Biosilicification Drives a Decline of Dissolved Si in the Oceans through Geologic Time. *Frontiers in Marine Science, 4*(397). https://doi.org/10.3389/fmars.2017.00397. 17 p.

13. Scholle, P. A. (1978). A Color Illustrated Guide to carbonate Rock Constituents, Textures, Cements, and Porosities: *American Association of Petroleum Geologists, Memoir 27*, Tulsa, p. 129-168. Accessed June 8, 2018 from Diagenesis: https://www.sepmstrata.org/page.aspx?pageid=92

14. Sample Map generated by John Samuelsen 2019, complied sample locations from Bottoms *et al.*, (2019), Cains, (2019), and McKim, (2018) , and Simbo *et al.*, (2019) in addition to values from this study.

15. Compiled trace element concentration values from this study

16. Covariate Pb isotope plots from this study

17. Banner, J. L., Hanson, G. N., and Meyers, W. J. (1988a). Rare earth element and Nd isotopic variations in regionally extensive dolomites from the Burlington-Keokuk Formation (Mississippian): Implications for REE mobility during carbonate diagenesis. *Journal of Sedimentary Petrology, 58*(3), 415-432.

18. Modified from Godo *et al.*, 2014

19. Henbest, L. G. (1968). Diagenesis in oolitic limestones of Morrow (Early Pennsylvanian) age in northwestern Arkansas and adjacent Oklahoma: U.S. Geological Survey Professional Paper 594-H, 22 p., p. H5.

20. Wenz, Z. J., Appold, M. S., Shelton, K. L. and Tesfaye, S. (2012, January). Geochemistry of Mississippi Valley-type mineralizing fluids of the Ozark Plateau: A regional synthesis. *American Journal of Science, 312*(1), 22-80. https://doi.org/10.2475/01.2012.02

21. Miser, H. D. (1959). Structure and Vein Quartz of the Ouachita Mountains of Oklahoma and Arkansas: The Geology of the Ouachita Mountains – A Symposium, Published by Dallas Geological Society and the Ardmore Geological Society, Dallas, Texas.

22. From Clark and Fritz 1997; Modified from Krouse, 1980

23. From Clark and Fritz, 1997; modified from Claypool, 1980

24. From Tosdal *et al.*, 1999; modified from Cannon *et al.*, (1961) and Gulson (1986)

25. Age-corrected covariate Pb isotope plots

26. Age-corrected Pb isotope plot with values from works by McKim (2018), Bottoms *et al.*, (2019) and Simbo *et al.*, (2019). Fluorite and Phosphorite values from Kesler *et al.*, 1994a.

27. Fishman, N. S. (1997). Basin-wide fluid movement in a Cambrian paleoaquifer: Evidence from the Mount Simon Sandstone, Illinois and Indiana, *in* Montañez, I.P., *et al.*, eds., Basin-wide diagenetic patterns: Integrated petrologic, geochemical, and hydrologic considerations: *SEPM (Society for Sedimentary Geology) Special Publication 57*, 221-234.

28. From Kesler, 1994a, A, B) modified from Bouse, 1995; C, D) modified from Bouse, 1999

29. He, Z., Gregg, J. M., Shelton, K. L., and Palmer, J. R. (1997). Sedimentary facies control of fluid flow and Mineralization in Cambro-Ordovician Strata, Southern Missouri. Basin-Wide Diagenetic Patterns: Integrated Petrologic, Geochemical, and Hydrologic Considerations, *SEPM (Society for Sedimentary Geology) Special Publication 57*. Retrieved June 8, 2018 from https://pubs.geoscienceworld.org/books/book/1106/chapter/10551281/Sedimentary-Facies-Control-of-Fluid-Flow-and

30. He, Z., Gregg, J. M., Shelton, K. L., and Palmer, J. R. (1997).

31. Pope, L. M., Mehl, H. E., and Coiner, R. L. (2009). Quality Characteristics of Ground Water in the Ozark Aquifer of Northwestern Arkansas, Southeastern Kansas, Southwestern Missouri, and Northeastern Oklahoma, 2006–07. *Scientific Investigations Report 2009–5093*. 62 p. https://pubs.usgs.gov/sir/2009/5093/pdf/SIR2009-5093.pdf

32. Diehl, S. F., Goldhaber, M. B., Taylor, C. D., Swolfs, H. S., and Gent, C. A. (1992). Microstructures in the Cambrian Bonneterrre Formation, Lamotte Sandstone, and Basal Clastic Rocks of Southeast Missouri and Northeast Arkansas--Implications of Regional Sulfide Occurrence in Stylolites and Extensional Veinlets for Ore Genesis. Chapter A in: Thorman, C. H. editor. Application of Structural Geology to Mineral and Energy Resources of the United States, USGS Bulletin 2012, p. A1-A13.

33. Braile, L.W., Hinze, W. J., Keller, G. R., Lidiak, E.G., and Sexton, J. L. (1986). Tectonic Development of the New Madrid Rift Complex, Mississippi Embayment, North America. *Tectonophysics, 131*(1-2), 21 p. https://doi.org/10.1016/0040-1951(86)90265-9

34. Cannon, R. S. Jr. and Pierce, A. P. (1969). Lead isotope guides for Mississippi Valley lead-zinc exploration. US Geological Survey Bulletin 1312-G: p. 20.

APPENDIX

Detailed Chemical Processing

1. 6 ml 7N HNO_3 and 4 mL HF was added, samples heated to 200º C (120º C) for 12+ hours, allowed to cool, opened, and dried down at 90º C (120º C)
2. 1 ml 6N HCl and 1 ml 7N HNO_3 added, samples heated to 200º C for 12+ hours, allowed to cool, opened and dried down at 90º C (100º C)
3. 2 mL concentrated HNO_3, samples heated to 200º C for 1 hour, allowed to cool and dried down at 90º C
4. 2 mL 7N HNO_3 added, samples heated until back into solution in preparation for Concentration Analysis
5. 0.6 mL of sample were drawn by pipette from the 23 mL Teflon sample vials and added to large centrifuge tubes with 4.4 mL of triple-distilled Savillex water in order to dilute them for Concentration analysis on the Quadrupole Inductive Plasma Mass-Spectrometer
6. 04/26/2019: 15 samples were deemed to have too much precipitate in them and run in a centrifuge for two 10-minute intervals at 3900 rpm and rotated 180º in between to remove residue from the liquid and then pipette 4-mL of each sample into clean centrifuge tubes. The original isotope samples were placed on the hot plate at 90º C to dry them down in preparation for addition of 2 mL 1 N HBr and heating to 175º C until dissolved.
7. 04/28/2019: 2 mL of 1 N HBr were added to isotope samples in order to prepare them for column chemistry and heated with the caps on until the sample was dissolved. Samples were allowed to cool and then opened and dried down at 90º C (~12 hours) in each sequence. This step was repeated 3 times.

8. 1 mL of 1 N HBr was added to the beakers which were again capped and placed on the hotplate 175º C until dissolved.
9. Samples were cooled down and transferred to 1.5 mL centrifuge tubes, centrifuged for 10 minutes, rotated 180º, and centrifuged again for 10 minutes.
10. Trace element compositions for all samples were collected using a Thermo Scientific iCAP Quadrupole ICP-MS (single-collector mass spectrometer). Table 2 shows the overall elemental whole-rock concentration data in ppm. Data are shown in conjunction with analyzed standards.

5/3/2019: Isotope Column Chemistry led by John Samuelsen, Archeology Ph.D. candidate, using his Teflon heat shrink tube columns and expertise:

a. Columns were thoroughly rinsed in DI three times to remove previous Strontium resin residue, boiled in 50% Nitric acid to leach any remaining residue and impurities, and then triple rinsed in double-distilled and Savillex water, respectively.
b. Cleaning consisted of a round of 2 mL 0.5 N HNO_3 followed by a rinse with 2 mL 4xH2O Savillex (3DI) water.
c. Columns were conditioned using an initial round of 2 mL 6N HCl.
d. Samples were previously dissolved in mL 1 N HBr and collected from isotope centrifuge tubes after 7 minutes at 3900 rpm in Dr. Suarez's lab centrifuge. 0.8 mL of 1 N HBr were added to the blanks, while 0.8 mL of all samples were pipetted from the isotope centrifuge tubes, loaded into the columns, and allowed

to completely run through the Pb resin. 3 individual rounds of 1 mL 1 N HBr followed in order to rinse the samples through the columns.

e. Samples were then collected by using clean Savillex beakers to catch the run-through remnants produced by the addition of 1 mL 20% HNO_3, which was allowed to run through to completion. Samples were then capped in a timely fashion afterwards to prevent evaporation.

f. 0.2 mL of each collected sample were pipetted from the Savillex column collection beakers and added to 2.98 mL of 2% HNO3 in new 15 mL centrifuge tubes in preparation for Pb isotope concentration analysis in order to calculate dilution rates for Pb isotope analysis on the Nu Plasma MC ICP-MS. .9 mL of each blank was withdrawn and added to 2.1 mL of 2% HNO_3 for this step so that all sample tubes contained 3 mL of sample for Pb isotopic concentration analysis on the Mass Spectrometer in order to calculate final concentrations for analysis on the Multi-Collector in order to avoid over-volting caused by excessive Pb ions in inadequately diluted samples.

g. 05/10/2019: Samples were then dried down for 8 hours at 90 C for 5 hours and then at 60 C for the remaining 3 hours and then capped.

h. Samples were then again dissolved/hydrated with appropriate volume of Thallium-spiked 2% HNO3 as needed in order to safely and accurately “run them” on the Multi-Collector without over-volting due to excessive concentrations of Pb in the samples.

Table 3. Trace Element Concentration Standards (ppm)

Element	Standards					
	BIR-1	DNC-1	W-2	BHVO-2	AGV-2	QLO-1
Rb	-3.8885	13.2657	20.2758	13.8948	56.7046	73.4196
Ba	6.37155	104.207	188.203	132.609	1083.44	1410.25
Cs	0.0851	0.19483	0.10632	0.08708	0.46488	1.78752
Th	0.01567	0.04786	2.84298	2.02189	5.94954	3.45841
U	0.07653	0.11068	0.4485	0.33726	1.89889	1.93545
Nb	3.30913	129.945	154.871	105.931	9.78229	71.8787
Ta	0.13424	3.30222	3.74281	3.64498	0.29871	1.73407
La	0.28495	6.98685	41.5992	55.672	44.3199	17.9098
Ce	-5.9044	18.0777	99.4238	151.022	74.0333	44.5416
Pr	0.12641	2.08396	8.73727	18.0848	9.48562	4.0412
Pb	2.89781	5.4182	7.89801	1.74399	13.1202	13.7508
Nd	2.8102	4.82361	12.6365	24.5162	12.978	6.98822
Sr	109.772	216.372	304.006	620.067	696.916	312.268
Sm	1.0331	1.3569	3.52563	5.92535	3.07304	1.70976
Hf	2.43777	25.1064	17.7976	24.8345	4.27377	11.1364
Zr	125.994	3086.02	2060.75	2648.04	468.12	1243.41
Eu	0.35464	0.44235	1.12452	2.04758	0.74338	0.38606
Gd	1.76264	1.94903	3.97118	6.10116	2.93067	1.91753
Sc	39.9986	43.2197	37.2949	34.9474	-10.284	7.55867
Ti	5850.77	2582.27	7017.75	16122.9	6109.7	3431.97
Tb	0.3554	0.38755	0.66124	0.9243	0.43848	0.3403
Dy	2.49631	2.78189	4.0068	5.19499	2.51467	2.21891
Ho	0.54757	0.63594	0.8162	0.967	0.48824	0.47639
Y	17.6031	17.1867	18.0798	28.3122	14.9531	11.0289
Er	1.61649	2.00341	2.2521	2.46197	1.39434	1.53941
Tm	0.25611	0.32534	0.33095	0.33979	0.21996	0.26818
Yb	1.68926	2.06893	1.93025	1.91975	1.59005	1.90305
Lu	0.17461	0.23451	0.2051	0.19892	0.16435	0.2197

Table 4. Normalized Pb isotope data of formations sampled by author (Figures 16, 25, 26).

***** Note: Error values taken from initial Mass Spec recorded values *****

Normalized Pb isotope measurement data and errors of ore sample analyzes of this study						
Sample	$^{208}Pb/^{204}Pb$	% error	$^{207}Pb/^{204}Pb$	% error	$^{206}Pb/^{204}Pb$	% error
CD 1	39.87182092	{ 1.56E-03 }	16.37521412	{ 6.45E-04 }	35.99267572	{ 4.11E-03 }
CD 2	39.78297094	{ 1.78E-03 }	16.22070662	{ 6.49E-04 }	27.11648913	{ 9.61E-04 }
CD 4	39.52827488	{ 1.03E-03 }	15.96671349	{ 3.44E-04 }	26.96464716	{ 7.58E-04 }
CD 6	39.63116341	{ 9.59E-04 }	16.35547307	{ 3.20E-04 }	31.10255978	{ 1.01E-03 }
CD 7	39.5833216	{ 1.74E-03 }	16.77517402	{ 7.23E-04 }	39.21032172	{ 5.49E-03 }
CD 8	39.42017067	{ 1.60E-03 }	16.46708402	{ 6.25E-04 }	34.10520337	{ 1.39E-03 }
BF 1	37.69218132	{ 1.64E-03 }	15.75557315	{ 7.72E-04 }	21.04775167	{ 3.08E-03 }
BF 2	38.15932593	{ 5.22E-04 }	15.66796794	{ 1.92E-04 }	18.86955866	{ 2.37E-04 }
BF 3	36.71075853	{ 1.01E-03 }	15.70664587	{ 3.47E-04 }	19.7576161	{ 3.77E-04 }
BF 4	28.25191839	{ 1.08E-03 }	15.4739438	{ 3.44E-04 }	15.02582733	{ 3.98E-04 }
BF 5	33.04731113	{ 8.18E-04 }	15.66807127	{ 2.72E-04 }	19.04027487	{ 3.27E-04 }
BF 6	35.73137311	{ 1.08E-03 }	15.25104571	{ 3.56E-04 }	10.35111691	{ 4.91E-04 }
BF 7	36.23597426	{ 8.03E-04 }	15.75192694	{ 2.98E-04 }	20.34683282	{ 4.43E-04 }
PT 2	39.53174153	{ 9.56E-04 }	15.80812422	{ 3.19E-04 }	20.93786251	{ 3.78E-04 }
PT 6	39.81564668	{ 1.06E-03 }	15.8491539	{ 3.40E-04 }	20.97492131	{ 3.72E-04 }
LT 1	39.82769934	{ 1.28E-03 }	15.92208828	{ 4.60E-04 }	22.96430153	{ 6.96E-04 }
LT 2	39.38412127	{ 1.87E-03 }	16.02084001	{ 7.40E-04 }	24.94351316	{ 1.36E-03 }
LT1 DUP	39.76400487	{ 2.01E-03 }	15.89983334	{ 4.21E-04 }	22.91189699	{ 6.93E-04 }
HT 4	38.77432759	{ 6.40E-04 }	15.64001102	{ 2.54E-04 }	18.55400277	{ 2.87E-04 }
HT 5	39.39754615	{ 1.51E-03 }	15.64242388	{ 4.40E-04 }	18.3007314	{ 4.10E-04 }

Table 5. Pb Standard Analyses

Standard	208/204	Error	207/204	Error	206/204	Error
NBS 981	36.6552	{ 7.61E-04 }	15.4790	{ 3.07E-04 }	16.9240	{ 3.64E-04 }
NBS 981	36.6569	{ 8.06E-04 }	15.4787	{ 3.33E-04 }	16.9138	{ 5.99E-04 }
NBS 981	36.6589	{ 8.90E-04 }	15.4793	{ 3.55E-04 }	16.9258	{ 3.97E-04 }
NBS 981	36.6563	{ 8.96E-04 }	15.4794	{ 3.35E-04 }	16.9241	{ 4.00E-04 }
NBS 981	36.6563	{ 8.91E-04 }	15.4796	{ 3.55E-04 }	16.9230	{ 3.96E-04 }
NBS 981	36.6543	{ 9.20E-04 }	15.4790	{ 3.66E-04 }	16.9236	{ 4.33E-04 }
NBS 981	36.6655	{ 1.00E-03 }	15.4823	{ 3.76E-04 }	16.9268	{ 4.36E-04 }
Average	36.65768		15.4797		16.92305	
Todt *et al.*, 1996	36.7006		15.4891		16.9356	
Correction Factor	*1.000168*		*0.999874*		*0.999823*	
Sigma (σ)		0.00376527		0.00123476		0.00428541
2 σ St. Dev.		0.00753054		0.00246951		0.00857082

Table 6. Pb isotope ratios of tripolitic chert age corrected to 250 Ma. Analyzed and compiled by McKim, 2018 and age-corrected for comparison to the Tri-State MVT ores.

Sample Name	Location	$^{206}Pb/^{204}Pb$	$^{207}Pb/^{204}Pb$	$^{208}Pb/^{204}Pb$
T1	36.412-94.213	21.664	15.587	40.272
T2	36.41294.213	21.604	15.879	40.343
T3	36.412-94.213	20.994	15.818	40.173
T5	36.566-94.371	16.411	15.658	39.559
T6	36.566-94.371	21.423	15.876	40.35
T8	36.632.418	21.386	15.849	40.266
T9	36.632.419	21.662	15.857	40.269
T10	36.632.420	22.047	15.842	39.577
T11	36.632.421	21.807	15.888	40.611
T13	36.676-94.419	20.078	15.711	38.969
T1D	36.412-94.213	21.138	15.752	39.666

Table 7. Figure 26: Kesler *et al.*, 1994a Fluorite and Phosphorite Pb Isotope Values as shown

Sample	206/204	207/204	208/204	Mineral	Location (mine)	Age of Host Rock
SB-22EF	20.037	15.787	39.136	Early fluorite	Ballard, downdip	Lower Ordovician
SW-89EF	21.114	15.909	39.207	Early fluorite	Ballard	Lower Ordovician
SW-66LF	23.472	16.166	39.221	Late fluorite	Wilson (Lee)	Lower Ordovician
SW-68LF	21.933	15.997	33.313	Late fluorite	Thompson	Lower Ordovician
Chattanooga Phosphorite	21.305	15.765	38.343	Phosphate Nodule	Clinch Mountain	Devonian
Fetzer Phosphorite	19.003	15.677	38.737	Phosphate Nodule	Central Tennessee	Middle Ordovician